The Cooperation of Condensin, Histone Methylation, and Nuclear Lamina Tethering Maintains X Chromosome Repression after the Establishment of Dosage Compensation

by

Jessica Trombley

A dissertation submitted in partial fulfillment
of the requirements for the degree of
Doctor of Philosophy
(Molecular, Cellular, and Developmental Biology)
in the University of Michigan
2024

Doctoral Committee:

       Professor Györgyi Csankovszki, Chair
       Professor Laura Buttitta
       Professor Kenneth M. Cadigan
       Professor Sundeep Kalantry

Jessica Trombley

jtromb@umich.edu

ORCID iD: 0000-0001-7213-8381

Dedication

Dedicated to Toulouse (2013-2023).

guidance you both gave me when I first came to the University of Michigan. Additionally, I am thankful to the Buttitta and Cadigan lab members for being friendly cohabitators of the 5C lab space. I appreciated all the advice, reagents, and bagel updates. Most of all, I would like to extend my deepest gratitude to Audry Rakozy, my outstanding undergraduate trainee, whose dedication and self-motivation significantly contributed to the success of my PhD project. Audry's exemplary work ethic and commitment to academics are truly commendable. I am honored to be a part of her research journey.

I am incredibly fortunate to have entered the MDCB PhD program alongside an exceptional cohort of individuals. Lotte, Bahaar, TJ, Ritvija, Rishav, Varsha, Jessy, Maria, Shilpa, Rich, and Hannah, your camaraderie and support have greatly enriched my PhD experience. I look forward to maintaining our connections as lifelong colleagues and friends.

Finally, I am grateful to my friends and family for their support. My mother inspired my interest in science and higher education. Growing up alongside her as she completed her self-supported master's degree left an indelible impression on me, serving as an enduring source of admiration. Her hard work and determination continue to motivate me, and I aspire to follow in her footsteps. My gratitude extends to my siblings for consistently bringing smiles and laughter into my life. I am deeply thankful for the unwavering support and the comfort of knowing I can confide in each of you. Thanks to my dad, whose encouragement, attentive ear, and advice have been invaluable. Your handwritten cards on every holiday were a comforting reminder of connection and inclusion, bridging the distance between us. To my grandmother, Mamatis, and Bill, your support of my academic pursuits has meant the world to me,

and I am grateful for the role you've played in my graduate education. Imogen has been my friend for nearly two decades, and I am confident our friendship will endure regardless of our physical distance. Your unwavering companionship is something I can always count on, and for that, I am sincerely grateful. Lotte, I am so glad we were able to overlap during our first-year rotations so that we would have the opportunity to become friends. I am so thankful for every coffee and snack we shared.

Lastly, I thank Toulouse for always being by me throughout my undergraduate and graduate education. Your cute Pomeranian smile and wagging tail were a daily source of joy and comfort. I will always cherish the memories of our time together

Table of Contents

List of Tables

List of Figures

Chapter 1 Introduction

***1.1* Nuclear Arrangement and Compaction of Chromosomes Have a Crucial Role in Gene Regulation**

Multicellular organisms have specialized cells with distinct functions despite containing identical genetic instructions. For example, in most tissues within the human body, there are exact copies of 23 chromosomes that must be deciphered with fidelity for tissues to operate successfully. An additional layer of complexity occurs when considering the amount of information contained within each chromosome. When placed end to end, the chromosomes in a human cell extend past 2 meters [1]. This is an incredibly vast amount of information to manage while delicately achieving the appropriate cellular processes. Consequently, chromosomes are organized in hierarchical structures and sub-nuclear territories that contribute significantly to controlling gene expression by distinct organization throughout an organism's lifetime.

1.1.1 *Chromatin Assembly by the Interaction of Chromosomes with Histones*

In eukaryotic cells, the storage of DNA is a multi-level process regulating the accessibility of DNA throughout the cell cycle by wrapping DNA around histone proteins to form structures called nucleosomes. This structure is further organized by coiling into chromatin fibers. The correct development of an organism depends on the higher-order architecture of chromatin, the formation of chromosome territories, and the arrangement of chromosomes within the nucleus [2]. The nucleosome contains an octamer of histone
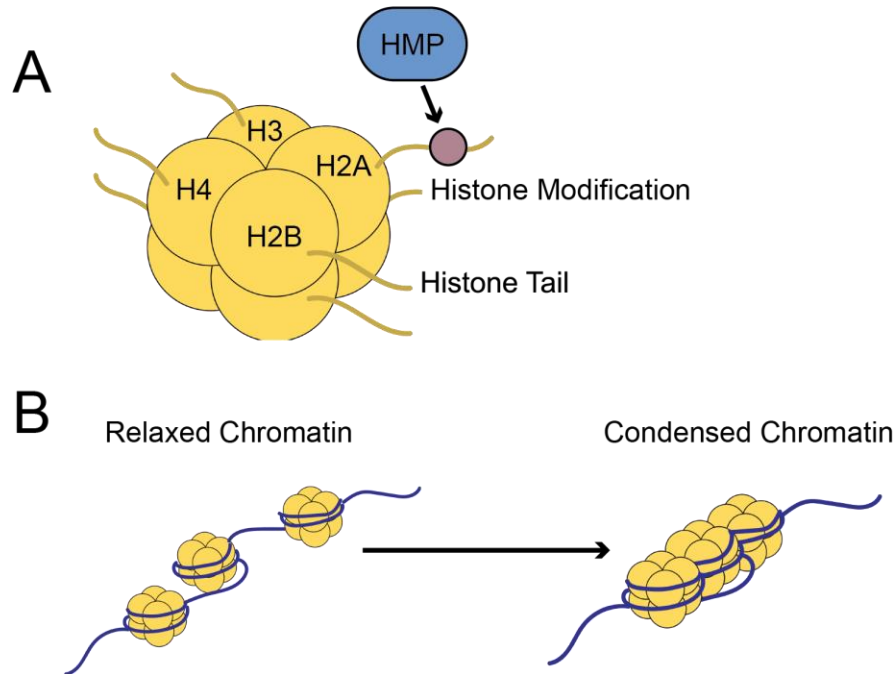
Figure 1.1 Chromosomes are organized and compacted by various histone modifications. (A) The histone octamer is standardly composed of four histone proteins in C. elegans: H2A, H2B, H3, and H4. Histone-modifying proteins (HMPs) interact with the tail domains of the histones to add or remove modifying marks such as methylation and acetylation. **(B)** The histone modifications placed on the tail domains influence a chromatin region's compaction level. Marks that repress genes bring chromosome regions closer together, while other marks allow transcription by relaxing the chromosome's coiling around histones, permitting access to the transcriptional machinery.

proteins **(Figure 1.1A)** [3]. The standard histone octamer in eukaryotes contains H2A, H2B, H3, and H4 [4]. In addition to the canonical histone proteins, several histone variants add another layer of gene expression regulation. These variants include H2A.X, H2A.Z, and H2A.B [5]. The histone proteins feature N- and C-terminal "tail" domains that can be post-translationally modified [6]. The changes made to the histone tail result in a difference in the charge, which, in turn, changes the shape of the nucleosome [7]. Based on the histone type, the amino acid of the tail, and the number and type of modifications to a tail, the relaxation or condensation of the nucleosome will vary [8] **(Fig 1.1B)**. Post-translation modifications to the histone tails include acetylation,

methylation, and phosphorylation [9]. These modified states are essential for modifying gene expression without changing the base DNA sequence. Depending on their

context, the modification has distinct functions in either transcriptional activation or repression. These various modifications work together to form a complex set of instructions that regulate transcriptional activity.

1.1.2 *Chromosomes Inhabit Specific Territories Within the Nucleus*

In addition to the level of compaction, the gene-regulatory process is affected by the sub-nuclear positioning of chromatin [10]. Since the late 1880s, scientists such as Carl Rabl have reported distinct organization within interphase cells [11,12]. It was evident that the chromosomes occupied a distinct space within the nucleus. This organization was termed chromosomal territories by Theodor Boveri in the late 19th century [13,14]. Chromosome territories refer to the nonrandom compartments within the nucleus where each chromosome is located during interphase. Visualization of the territories within the nucleus is possible through fluorescent *in situ* hybridization (FISH) of the chromosomes [15]. 3D imaging of chromosomes hybridized to fluorescent probes can be reconstructed to study nuclear organization in many species [16]. Advances in FISH probe specificity and microscopy have expanded chromosome territory research.

The definition of nuclear territories emphasizes the intentional organization of chromosomes within their compartment. Within the chromosomal territory, transcription can be regulated by allowing or preventing access to transcriptional machinery [17]. In the past, it was hypothesized that transcriptionally silent regions are purely located at the core of a chromosome territory [18]. However, transcription can occur within the compartment. Yet, it is still true that regions with high transcriptional activity are more

frequently located on the periphery of the chromosome territory [19]. In summary, the chromosomes within a nucleus form distinct territories that provide yet another level of transcriptional regulation.

1.1.3 *Chromosomal Regions Interact in cis to Form Topologically Associating Domains*

In the last ten years, topologically associating domains (TADs) have become a nuclear arrangement of interest in gene regulation research. TADs are described as areas of high *cis-interacting* chromosomal sub-domains seen in interphase [20]. By their definition, TAD domains do not interact with other genomic regions as often as in *cis* with regions within the domain. These self-interacting domains were visualized initially via chromosome conformation capture (3C) and Hi-C in the X inactivation center (XIC) of the X chromosome in the embryonic stem cells of mice [20]. Gene regulatory sequences are notably flanked by areas known as TAD boundaries that reinforce interactions within domains. A zinc finger transcription factor forms TAD boundaries called the CCTC-binding factor (CTCF) that insulates the chromosomal regions— known CTCF binding sites must have the opposite polarity to come together and insulate regions of chromatin looping [21]. Deleting TAD boundaries has been shown to cause developmental deformities and embryonic lethality in mice [22,23].

Despite TADs being found in various mammals, including humans, the role of TADs in gene regulation has become unclear [24]. Interestingly, despite TADs being observed forming on the chromosomes of various mammals, in *Caenorhabditis elegans*, only the dosage-compensated X chromosomes (see section on *C. elegans* dosage compensation) form strong TADs with strong boundaries at the sites where dosage

4

compensation machinery is recruited along the X chromosomes [25]. Furthermore, a CTCF homolog has not been identified in *C. elegans* [26]. The evolutionary loss of CTCF in *C. elegans* is the proposed reason for the lack of autosomal TAD formation [27].

1.1.4 *Chromosome Interactions With the Nuclear Lamina Contribute to Gene Repression*

As previously mentioned, the length of a singular strand of DNA far exceeds the dimensions of a cell. The management of how tightly compact chromatin does not only contribute to fitting the DNA within the cell but also organizes it in a manner that permits crucial genes' accessibility to transcription factors while "archiving" the rest of the genetic information in the form of heterochromatin. As a result, tightly compacted heterochromatic chromosome regions are often located peripherally within the nucleus. At the same time, euchromatic regions extended into the center of the nucleus [10].

Lamina-associating domains (LADs) are largely heterochromatic regions of chromosomes that localize near the nuclear periphery [28]. LADs have been observed to form in *C. elegans* and D. melanogaster, as well as in mammalian cells [28–30]. LADs are often enriched for modifications such as H3K9me2 and H3K9me3 [28]. In mammals, the lamina-associating domains (LADs) were initially identified using DamID (Dam identification). In this technique, the bacterial protein DNA adenine methyltransferase (Dam) was fused to a lamin protein that would adenine-methylate associated chromatin. From this data, it was discovered that there are regions of the chromatin that are specifically tethered to the nuclear lamina [29]. The domains that most frequently interact with the nuclear lamina are enriched at the distal ends of

chromosomes [30]. Notably, in *C. elegans*, the peripheral localization of the heterochromatic portions of chromosomes coincides with the differentiation of a cell [31]. As cells undergo differentiation, promoters needed for that tissue migrate toward the central regions of the nucleus. In contrast, promoters associated with inactive genes tend to bind to the nuclear lamina [32].

The associations of chromosomes to the nuclear lamina provide an additional layer of gene regulation. As described, the activity of regulatory proteins with DNA to alter *cis* and *trans* interactions to regulate transcription is needed throughout an organism's life. The precise organization of chromosomes within the nucleus is a process that contributes significantly to the fidelity of cellular processes, including the determination of an organism's sex and regulation of sex-associated genes [33,34]. In the upcoming sections of this introduction chapter, the spatiotemporal alteration of chromosomes regarding sex chromosome dosage compensation as a model for gene regulation is further described.

1.2 The Evolution of Sexes and Sex Determination

The evolution of separate sexes has convergently evolved multiple times throughout plants, animals, and fungi kingdoms [35]. Leading hypotheses for the development of different sexes include the conjecture that there is a desire to avoid the propagation of harmful genes by outcrossing, which would not be possible in purely hermaphroditic species [36,37]. Commonly, organisms are thought of as existing in a dioecy, in which there are distinct females and males. However, some organisms, such as *Caenorhabditis elegans*, live as an androdioecy - they have hermaphrodites and males [38,39]. In androdioecious organisms, hermaphrodites can self-fertilize and

sexually reproduce with males. Outcrossing in dioecy and androdioecy is proposed to prevent inbreeding depression that reduces offspring viability [40].

The inheritance of heterogametic sex chromosome combinations requires a refined process to distinguish between sexes. Sex determination is how an organism decides the fate of gonadal development. Gonadal development is often set to develop as female, male, or hermaphrodite [41]. Interest in the driving factors for sexual differentiation has existed throughout history, with diverse proposed determining factors typically involving nutrition and temperature. Building upon his predecessors' work, in 335 B.C.E., Aristotle believed that the environment's temperature determines the sex of offspring. The philosopher proposed that high temperatures were required to produce a male offspring [42,43]. Although this would be disproven in humans, the importance of environmental factors in sex determination is true in many organisms. For example, turtles' and alligators' sex is environmentally determined. Thus, Aristotle's proposal was not wholly incorrect. However, contrary to Aristotle's beliefs about heat being necessary for male offspring, these reptiles develop as females in warmer and males in cooler temperatures [44,45].

The true nature of human sex determination was exposed once cytologists began staining chromosomes. In 1891, Hermann Henking spotted 'X Element' while studying the firefly, *Pyrrhocoris apterus*, fixed and stained spermatocytes undergoing various stages of cell division [46]. This 'element' behaved differently than all the other chromosomes in the stained spermatocytes. During metaphase, the X Element would be in line with all other chromosomes, but by metaphase II, it was seen aligning with the metaphase plate alone [47]. In 1901, Clarence McClung proposed that 'X Element' is an

accessory chromosome associated with sex determination [48]. These observations

would eventually lead to the discovery of sex determination in many organisms,

including humans. The 'X Element' or 'accessory chromosome' was then named the X

chromosome [49]. Following these discoveries, Nettie M. Stevens' studies of mealworm

spermatogenesis in 1905 demonstrated that the Y chromosome was the factor that

decided male sexual development [50]. Thus, the proper mechanism of sex

determination was unveiled as genotypic in humans; In other words, sex is determined

chromosomally [51,52].

In chromosome-based sex determination, one or many genes often determine

sex. This system splits into two mechanistic categories: dose-dependent and dominant

sex determination. Dose-dependent sex determination functions by the presence of two

copies of the gene or genes needed for sex determination. In dominant sex

determination, only one copy of the gene or genes is needed. In organisms where the

female is the homogametic sex, sex chromosomes are delineated as XX (female) or XY

(male); this is seen in mammals and some insects. In organisms where females are

heterogametic, such as birds, females are ZW, and males are ZZ [53]. In the study of

sex determination, the best-studied model organisms are mammals (mouse and human

cell culture), *Drosophila melanogaster,* and *C. elegans*.

1.2.1 *Mammalian Sex Determination*

Mammalian sex is established early in development by the presence or absence

of the Y chromosome (XX females and XY males). The Y chromosome encodes the

sex-determining region Y (*SRY*) gene—the expression of the SRY protein results in

male sexual differentiation by promoting the growth of the testis [54]. The expression of

Sry was the only gene that would cause XX mice to develop testes [55]. Conversely, when *Sry* is defective, ovarian development will occur [56]. In summary, mammalian sexual fate is driven by dominant sex determination established by the expression of a Y-linked gene.

1.2.2 *Drosophila melanogaster* Sex Determination

An alternative sex determination mechanism is the ratio of autosomes to sex chromosomes (X: A) [57]. This mechanism is often seen in invertebrates such as *Drosophila*; the ratio of 2X to 2A results in females, and males are 1X to 2A. In *Drosophila*, the genetic elements required for regular sex determination were discovered via loss-of-function mutations in XX flies, resulting in male development. The initiating step in fruit fly sex determination is the X-to-autosomal ratio signal from X-linked and autosome-linked genes. After this initial step, the ratio is no longer the determinant; the transcription of a feminizing (if 2X:2A) gene is continuously expressed to proceed with subsequent development [58]. To describe fly sex determination, the gene *Sxl* (sex-lethal) present on the X is the "switch gene" that feminizes *Drosophila* embryos [59]. *Sxl* is a self-activating gene that binds to its promoter and stimulates transcription [60]. The resulting protein, *Sxl*, is an RNA-binding protein that splices RNA, resulting in females [61]. In the case of *Drosophila*, sex determination is genetic, but the mechanism is X:A dose-dependent [62].

1.2.3 *Caenorhabditis elegans* Sex Determination

Like *Drosophila*, *C. elegans* also utilizes X chromosome counting as a mechanism for sex determination. The wild-type animals have two sexes: XX

hermaphrodites (2X:2A) and XO males (1X:2A) [57]. Due to the prevalence of self-fertilizing XX hermaphrodites, the ratio of males to hermaphrodites is unequal. Male *C. elegans* are relatively uncommon [63]. They occur from either the loss of an X chromosome by nondisjunction during hermaphrodite self-fertilization or as a progeny from a cross between a male and a hermaphrodite [64]. Despite the more favorable odds of hermaphrodite-rich populations, the "master sex-determination switch" is *xol-1*, a gene that drives male development [65]. *xol-1* promotes male development by repressing *sdc* genes **(Fig 1.2A)**. The *sdc* genes specifically lend to hermaphrodite gene regulation by repressing *her-1*, another male developmental fate gene [66,67]. In XX nematodes, *xol-1* transcription is regulated by *sex-1* **(Fig 1.2B)**.

On the X chromosomes are genes known as the X signal element (XSE), and there are autosomal signaling elements (ASE) on the autosomes [68]. The role of XSE in *C. elegans* is to convey the number of X chromosomes within the male or hermaphrodite [69]. SEX-1 binds to the promoter for *xol-1*, the masculinizing XSE, and represses its transcription in XX nematodes [70]. Another XSE, *fox-1*, regulates *xol-1* by dictating the mRNA splicing pathways. FOX-1 renders the *xol-*
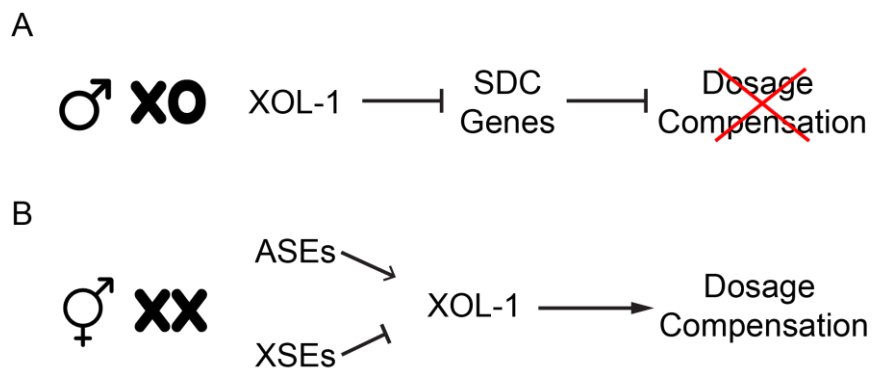
Figure 1.2 XSE and ASE compete to activate or repress *xol-1* to control dosage compensation. (A) In males, the SDC genes are repressed by XOL-1, thus preventing dosage compensation activity. **(B)** The ratio of ASE and XSE expression in the early embryo of XX *C. elegans* results in the inactivation of *xol-1*. Thus, dosage compensation is initiated.

1 transcript inactive by either deleting an exon or preventing the removal of an intron,

thus not permitting transcription maturation [71]. The ratio of the XSE to ASE will signal

sex determination and the need for dosage compensation in early embryos [72]. The

ASE found in *C. elegans* include SEA-1 and SEA-2 [68]. The protein SEX-1 is a

regulator of *xol-1. C. elegans* presents an additional system of chromosome dose-

dependent sex determination. For all sex determination pathways described, the genetic

output must be balanced due to the disproportion in chromosome count. Concurrently

with the evolution of chromosomal sex determination is the propagation of a dosage

compensation system in many organisms [57].

1.3 Dosage Compensation

In organisms with heterogametic sex determination, chromosomal gene expression has an inherent imbalance. This potential imbalance results in sex-specific lethality, necessitating intervention to adjust gene expression [57]. Common model organisms like the

Figure 1.3 Various methods of dosage compensation in commonly studied models. Dosage compensation balances the gene dosage between females, or hermaphrodites, and males by protein complexes and post-translational marks in various organisms. In mammals, dosage compensation is achieved by inactivating one of the X chromosomes; in females, it is achieved by X inactivation. In Drosophila melanogaster, the male-specific lethal (MSL) complex upregulates the male X chromosome by hyperacetylation to match the gene dosage in females. Finally, in *Caenorhabditis elegans*, dosage compensation is achieved in hermaphrodites by down-regulating both X chromosomes by half using a condensin-containing dosage compensation complex.

ones discussed previously, mice, flies, and the nematode *C. elegans*, have developed

molecular mechanisms to ensure equal gene transcription from the sex chromosomes

in both sexes **(Fig. 1.3)**. In 1947, Hermann Muller was the first to name the process of

sex chromosome gene balancing dosage compensation [46]. Although Muller's work

was based on a drosophila model, it is now understood that many approaches exist to

achieve dosage compensation amongst the vast diversity of organisms.

1.3.1 *Mammalian Dosage Compensation*

In mammals and *C. elegans*, the X chromosomes are downregulated in the

homogametic (XX) sex. Dosage compensation in mammals results in the inactivation of

one of the X chromosomes in females starting around the two- to eight-cell stage of

development [73] **(Fig 1.3)**. Thus, X gene transcription equals the singular X output

seen in males [74]. The process of X inactivation was discovered by Mary F. Lyon in

1961. She observed that when coat color genes were translocated onto the X

chromosomes, their coat colors would become "mottled," and spots of various colors

would form only in females. The patches of color found only in female mice suggest the

deactivation of specific X chromosomes, resulting in diverse color patterns [52,75].

Mammals achieve dosage compensation by random X inactivation in XX females,

though in some organisms, X inactivation is imprinted onto the paternal X [76].

The transcriptionally silenced X chromosome becomes tightly compacted into a

Barr body [77]. The factor widely understood as the determining factor of Barr body

formation is X inactivation-specific transcript (Xist). This long non-coding RNA is the

determinant of X inactivation in females. The complete absence of *Xist* on both

chromosomes will result in female-specific lethality [74]. The female lethality that occurs

because of the loss of *XIST* occurs before the mouse reaches adulthood. A small percentage of mice lacking Xist RNA can survive to term [78]. *Xist* functions in *cis*, binding and coating the X that expresses the RNA. The expression of the *Xist* RNA begins in a region of the X chromosome known as the X inactivation center (XIC). The XIC is a region of the X chromosome that contains *Xist,* as well as other non-coding RNA elements that regulate the expression of *Xist* [79]. The XIC includes *Tsix,* the long non-coding RNA that is anti-sense of *Xist* and represses its expression [80].

The inactive X chromosomes have distinct histone modifications regulating gene expression. The RNA binding protein (RBP), HnrnpK, is recruited to the X by *Xist*. On the X chromosome, this RBP facilitates the enrichment of H3K27me3 and H2AK119ub. PRC1 and PRC2 (polycomb repressive complex) place these marks. PRC1 mediates H3K27 methylation on the inactive X, thus limiting the binding of transcription factors [81]. The study identifying PRC2's role in X gene regulation noted that when HnrnpK is depleted, the PRC2 subunit Eed is no longer colocalized to *Xist* [82]. Additionally, *Xist* forms a complex with two proteins, SHARP and SMRT, to recruit HDAC3 (histone deacetylase 3) [83]. HDAC3 silences genes by removing acetyl marks from histones [83,84]. HDAC3 contributes to the efficiency of X inactivation [85]. Further silencing mediated by *Xist* includes associating with the nuclear lamina, a region associated with repression. *Xist* directly interacts with the Lamin B receptor. The binding of the Lamin B receptor to Xist facilitates the reconfiguration of the chromosome architecture, resulting in the spread of *Xist* [86]. However, it has recently been shown that a mutation to the Lamin B receptor does not cause a phenotype in female mice [87]. Furthermore, histone modifications regulate the inactivated X. These marks include H3K9me and H3K4

hypoacetylation [88,89]. The contributions of histone modifications, histone variants, and protein complexes maintain X inactivation throughout an organism's life, even throughout many rounds of cell division [32].

1.3.2 *Drosophila melanogaster Dosage Compensation*

Dosage compensation in *Drosophila melanogaster* occurs in a manner opposite to that seen in *C. elegans* and mammals, but the method achieves the same result. Rather than altering female sex chromosome gene expression, the fruit fly bolsters the expression of the X in males **(Fig 1.3)**. A combination of five proteins composes the male-specific lethal (MSL) and RNA on the X (roX) are considered the core components of dosage compensation in *Drosophila* [90]. The MSL complex is inactive in female Drosophila due to Sxl repression of *msl2* [91]. Conversely, this means that the absence of *Sxl* permits the initiation of dosage compensation in males.

The proteins in MSL include: males absent on first (MOF), maleless (MLE), and male specific lethal 1-3 (MSL1, MSL2, MSL3) [91]. Loading of the complex onto the X begins with the localization by MSL-1 and MSL-2 at chromatin entry sites (CES) [92]. The MSL spreads across the X to nearby genes from the CES due to MSL-3's affinity for binding histone 3 lysine 36 trimethylation (H3K36me3), a marker for active gene expression [93]. MOF is an essential histone acetyltransferase that enriches histone 4 lysine 16 acetylation (H4K16ac) on the male X. This histone mark prevents condensation of the X and causes the hyperactivation of the male X [94]. MLE is an RNA helicase and ATPase, integrating roX into X [95]. The RNAs roX1 and roX2 are predicted to have approximately 35 binding sites on the male X chromosome. Once they bind to the X, roX1 spreads across it similarly to Xist, which coats the inactivated X

14

chromosome in mammals [96]. The functions of roX1 and roX2 appear redundant. However, they contribute to the dosage compensation of a differing set of genes [33].

In summary, Drosophila's dosage compensation complex, MSL, orchestrates a multi-layered regulatory mechanism that equalizes X gene expression between males and females by altering the chromosomal 3D structure. These processes involve the relaxation of nucleosome compaction through H4K16ac and the reduction of supercoiling at the chromosomal level facilitated by helicase activity [95,97]. Thus, emphasizing the synergy of these molecular processes within the multi-subunit protein structure to achieve dosage compensation in male Drosophila.

1.3.3 *Caenorhabditis elegans Dosage Compensation*

In *C. elegans*, the X chromosome to autosome ratio leads to dose-dependent sex determination and necessitates dosage compensation [68,98]. Males only have one X chromosome, meaning they have the potential for half the X gene expression compared to XX hermaphrodites. The primary dosage compensation mechanism in *C. elegans* is the downregulation of *both* X chromosomes in hermaphrodites by half **(Fig 1.3)** [99]. As a result, the transcriptional output is equivalent to a singular X chromosome. The downregulation of the X is achieved by the dosage compensation complex (DCC). This complex comprises a condensin complex and five accessory proteins that combine to alter the 3D structure of the X chromosome, recruit regulatory proteins, and alter nuclear localization [25,27,100]. This alteration of the chromosome's structure and localization by the DCC plays an essential role in the growth and survival of hermaphrodite nematodes, as evidenced by hermaphrodite specific lethality that occurs

in hermaphrodites overexpressing the X's [99]. Further description of the DCC function and its protein subunits are detailed in this chapter.

1.4 Conserved Condensin Protein Complexes in Chromosome Compaction and Gene Regulation

All organisms, from singular cells to multicellular life, utilize at least one condensin protein complex [101]. These protein complexes perform essential roles in condensation, segregation, and the gene regulation of chromosomes [102]. The canonical complex in eukaryotes comprises five protein subunits, two structural maintenance of chromosome proteins (SMCs), and three non-SMC chromatin-associated polypeptide (CAP) proteins. In prokaryotes, the condensin complexes contain only three subunits [103]. Most multicellular eukaryotic cells contain at least two condensin complexes, and yeast contains one that utilizes ATP to extrude and compact DNA [104].
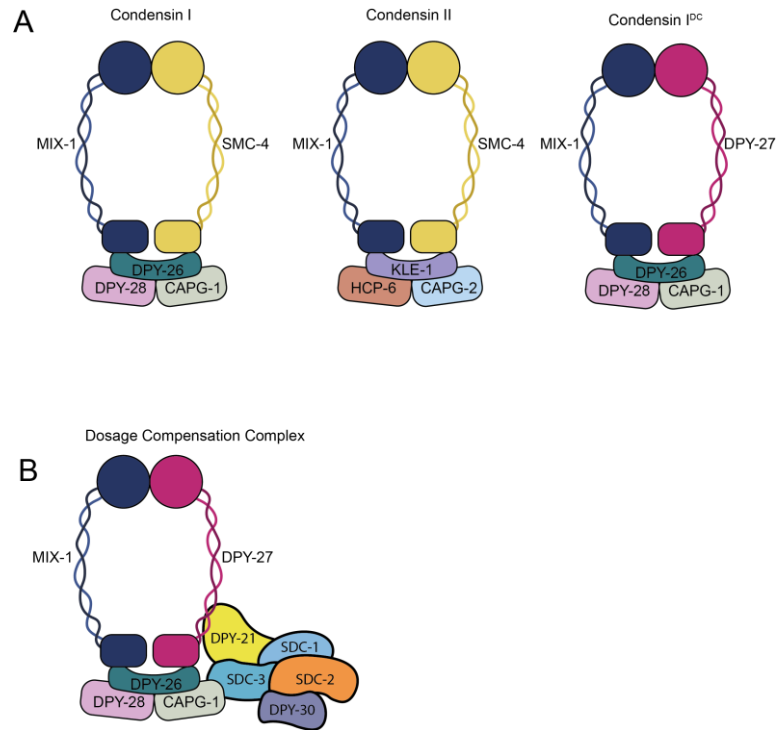
Figure 1.4 Three condensin complexes in *C. elegans* compact chromosomes. A) There are three condensin proteins in *C. elegans*: condensin I, condensin I^{DC}, and condensin II. Condensin I and II are conserved complexes involved in meiosis and mitosis found throughout eukaryotes. Condensin I^{DC} is unique to *C. elegans* and only differs from conserved condensin I by one protein, DPY-27. **B)** The dosage compensation complex (DCC) is condensin I^{DC} and the proteins DPY-21, DPY-30, SDC-1, SDC-2, and SDC-3. The complete DCC is required for successful dosage compensation in *C. elegans* hermaphrodites.

1.4.1 *Condensin I and II are Highly Conserved Complexes Necessary for Meiosis and Mitosis*

Most multicellular eukaryotes use two condensin complexes to segregate their chromosomes [105]. *C. elegans* has three condensin complexes, Condensin I, Condensin II, and a third specialized condensin protein, condensin I^{DC} (dosage compensation) **(Fig 1.4A)** [106]. The two common subunits between Condensin I and II are the structural maintenance proteins (SMCs), SMC2 and SMC4. The SMC proteins function as the core protein subunits that change the structure of chromosomes. SMC proteins are chromosomal ATPases, but it is unclear how their function contributes to the condensation of chromatin in the condensin protein complexes. The non-SMC subunits in Condensin I and Condensin II are CAP proteins. The chromatin-associated polypeptide (CAPs) proteins in Condensin I are CAP-D2, CAP-G, and CAP-H, whereas Condensin II has CAP-D3, CAP-G2, and CAP-H2. CAP proteins are thought to regulate the ATPase function of the SMC subunits [107]. Although the condensin proteins share common protein subunits, they have overlapping and distinct roles in meiosis and mitosis. ATPase function contributes to the role of condensin in altering chromosome structure. The condensin compacts chromosomes by loop extrusion by expending ATP to push DNA through the SMC ring [108] [109]. Condensin I is localized to the cytoplasm during interphase. The condensin I complex accesses the nucleus after nuclear envelope breakdown during the second phase of mitosis, where it then binds to the chromosomes [110]. Condensin II is nuclear localized throughout a cell's life and binds to chromosomes to begin condensation in the prophase of mitosis [111]. The distinction in condensin I and II functions is still not well characterized.

1.4.2 Condensin I^{DC} is a Dosage Compensated X Chromosome-Specific Complex

C. elegans features three condensin complexes. Condensin I and Condensin II function in meiotic and mitotic processes. The third condensin in *C. elegans*, condensin I^{DC}, is specialized for X chromosome compaction **(Fig 1.4B)** [106]. Distinguished by a single subunit difference from condensin I, condensin I^{DC} consists of MIX-1, DPY-26, CAPG-1, DPY-28, and the unique complex member, DPY-27 [106,112–115]. Condensin I features MIX-1, SMC-4, CAPG-1, DPY-28, and DPY-26 among its subunits, while Condensin II comprises MIX-1, SMC-4, CAPG-2, HCP-6, and KLE-2 [106]. Shared subunits between condensin I and condensin I^{DC} and the homology between DPY-27 and SMC-4 suggest functional similarities between the complexes. However, condensin I^{DC} has not demonstrated any mitotic function like the other two condensins [106]. As the name suggests, condensin I^{DC} earns its name from its similarity to Condensin I and its specific role in dosage compensation. The protein complex condensin I^{DC} binds to chromosome X, repressing X-linked genes [114]. The specificity of condensin I^{DC} in gene regulation provides a paradigm to study condensin functions in gene regulation apart from their meiotic and mitotic roles. Of particular interest in our study is the DPY-27 subunit, the sole unique subunit of condensin I^{DC}, which plays a significant role in chromosome regulation alongside other subunits.

1.4.3 DPY-27 is a Unique Protein Component of Condensin I^{DC} and is Necessary for Dosage Compensation During Embryogenesis

The DPY-27 subunit of condensin I^{DC} is essential for the survival of hermaphrodite *C. elegans*. It was evident that DPY-27 is necessary for hermaphrodite development in a developmental assay utilizing a cold-sensitive allele of *dpy-27.* This

mutation, which rendered DPY-27 non-functional at low temperatures, imposed a developmental barrier, preventing hermaphrodites from surviving beyond the comma stage [116]. Further investigations into this protein revealed that DPY-27 is a homolog to condensin I subunit SMC-4 [106]. DPY-27 and SMC-4 dimerize to MIX-1 in their respective complexes [106]. Mutations to either MIX-1 or DPY-27 impede dosage compensation [100,113,114]. The similarity between the complexes and the subsequent observation of chromosome conformational changes supports the hypothesis that condensin I^{DC} binds to the X chromosome to extrude and compact the X chromosomes, similar to condensin I and II by loop extruding DNA [25,27,100]. Data in Chapter 2 explores DPY-27's function after the onset of dosage compensation and provides evidence for its necessity in embryonic development.

1.5 *C. elegans* Dosage Compensation Complex (DCC) is Composed of a Condensin and Five Non-Condensin Subunits

In *C. elegans*, the dosage compensation complex, or DCC, refers to the combination of condensin I^{DC} plus five accessory proteins **(Figure 1.4B)**. These accessory proteins include SDC-1, 2, 3, DPY-30, and DPY-21 [117,118]. Although several members of the DCC have been identified, not all have well-characterized roles in dosage compensation. Among those which have well-characterized roles are SDC-2 and DPY-21 [31,118].

1.5.1 *The DCC is Recruited to the X by SDC-2*

The loading of the DCC onto the X is a process that occurs in two steps. The DCC proteins load onto the X chromosome recruitment element on the X sites (rex sites) and

spread to coat the X [119]. This complex binds to the dosage compensated X starting

around the 30-40 cell stage of embryonic development at the onset of SDC-2

expression [67]. Initially, the SDC-2 protein binds to the X chromosome, which triggers

the assembly of the remaining components of the DCC complex. Additionally, the SDC-

2 subunit in *C. elegans* hermaphrodites has a dual function. It helps to target the DCC

complex to the X chromosomes and also plays a role in sex determination [67]. SDC-2

determines hermaphrodite developmental fate by repressing the transcription of *her-1*, a

gene that promotes male development [66,120]. It is noteworthy that mutations in her-1

lead to the development of hermaphrodite characteristics in worms that have XO

chromosomes [121]. The binding of SDC-2 to the *her-1* gene thus ensures proper

hermaphrodite development. If SDC-2 fails to bind to her-1, it leads to male

development, and if it fails to bind to the X chromosomes, it leads to hermaphrodite-

specific lethality [122]. All members of the dosage compensation complex are

necessary for dosage compensation [116,123]. SDC-2 does not alter the health or

development of X0 nematodes when mutated [122].

1.5.2 *H4K20me1 is Enriched Specifically on Dosage-Compensated X Chromosomes in C. elegans by DPY-21*

Non-condensin complex members of the DCC play a significant role in regulating

and maintaining the expression of genes on the X chromosome. An exceptionally

versatile protein subunit is DPY-21. Of the DCC accessory proteins, DPY-21 is the

member shown to interact with condensin I^{DC} [118]. Studies show that the protein

functions as a demethylase and a scaffold for the DCC. However, the latter function is

not yet well characterized. Evidence for this dual role is revealed by mutations to the

dpy-21 gene [124]. Null mutations for *dpy-21* do not cause hermaphrodite lethality, but there is a significant increase in X gene expression and a decline in hermaphrodite health, including dumpy phenotypic development [125]. The XX hermaphrodite population is about 85% viable relative to the wild type without functional *dpy-21* [65]. In a 2017 study, the domains of DPY-21 were compared to motifs found in other complexes. DPY-21 was found to contain a Jumonji domain.
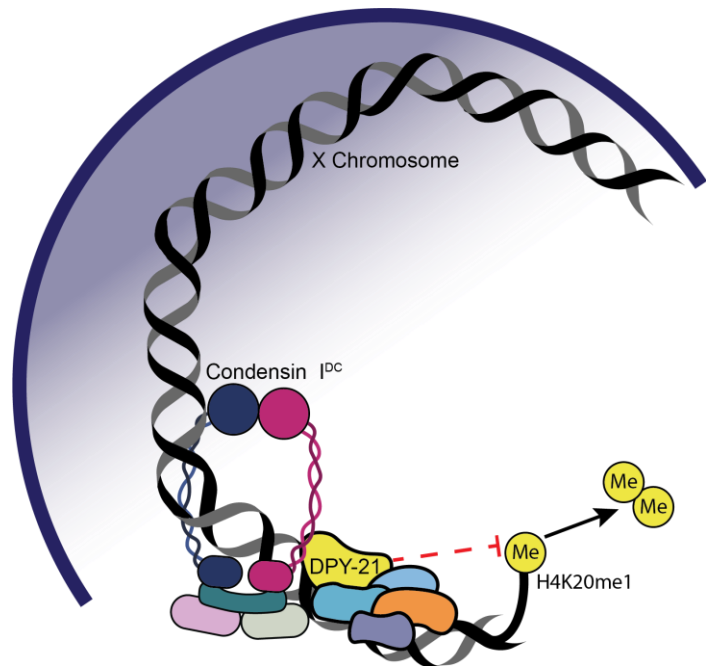
Figure 1.5 The repressive chromatin mark H4K20me1 becomes enriched due to the demethylase activity of the DCC subunit DPY-21. The DCC subunit DPY-21 contains a conserved Jumonji domain in histone demethylases [120]. After the onset of dosage compensation, DPY-21 depletes the di- and trimethylated state of H4K20 to monomethylation, rendering the X chromosome enriched for the repressive H4K20me1 mark [123].

Jumonji domains within proteins are common amongst demethylases. In DPY-21, this domain can demethylate di- and trimethylated H4K20 down to H4K20me1, thus enriching the X chromosomes for the monomethylated mark **(Fig 1.5)**. Notably, mutations in the Jumonji domain of DPY-21 cause a loss in the demethylase function, but the mutants are phenotypically less severe than the *dpy-21* null mutants [126]. The difference in development and survival between catalytic domain mutants and null mutants supports the multipurpose role of DPY-21 as a demethylase and another uncharacterized function.

During late embryonic development, DPY-21 is present on the X chromosomes but appears on the X after condensin I^{DC} [124,127]. However, only after multiple cell divisions is the H4K20me1 mark specifically enriched on the X chromosome [128]. The methyltransferase SET-1 initiates H4K20 modification by placing the monomethylation mark [129]. The monomethylation mark is then modified by SET-4 to di- and trimethylation. This mark is then subsequently reduced to H4K20me1 by DPY-21 during mid-stage embryogenesis [127,129]. In *C. elegans,* the monomethylated H4K20 mark is associated with gene repression [130]. This histone mark is shared between *C. elegans* and mammalian dosage-compensated X chromosomes [131].

1.6 Nuclear Lamina Tethering of the Chromosomes Contributes to Gene Regulation in *C. elegans*

As a cell differentiates, the nuclear lamina interaction with the chromosomes increases [132]. Over time, actively expressed genes migrate toward the nuclear interior, while repressed regions establish a repressive bond with the nuclear lamina through histone modifications [32,133]. As in many other organisms, the nuclear periphery is considered a repressive compartment where histone-modifying proteins linger to place repressive marks on nearby chromosomes and tether them to lamina-associated proteins in *C. elegans* [134]. Notably, both arms of autosomes are bound to the nuclear lamina by the protein LEM-2 in post-meiotic cells. The histone mark that LEM-2, H3K27me3, binds to is abundant in the chromosome arms [135]. The unbound central regions of the chromosomes reach into the central regions of the nucleus and are more actively transcribed [30,136]. Apart from LEM-2 and H3K27me3, other histone modifications and proteins anchor chromosomal domains to the nuclear lamina.

1.6.1 *CEC-4 Relocates the X to the Nuclear Periphery by binding to H3K9me3*

In mammals, the di- and tri-methylated histone 3 lysine 9 is enriched on chromosomal regions bound to the nuclear lamina [137]. In *C. elegans*, the binding of CEC-4 to H3K9me3 regions of the chromosomes results in the anchoring of chromosomal arms to the lamina and promotes the compaction of chromosomes [138]. This mark is a hallmark of gene repression in *C. elegan*s: the histone methyltransferases (HMTs), MET-2, and SET-25 methylate H3K9me

Figure 1.6 The histone modification H3K9me3 is enriched across all chromosomes in *C. elegans*. CEC-4 facilitates DCC spread by relocating the X chromosome to the nuclear periphery and bringing all the components closer together in space [132].

gradually. Beginning with MET-2 binding to H3K9, the histone will be mono- and di-methylated. The methylated histone will then be added to an additional methyl group by the HMT SET-25, resulting in H3K9me3. Interestingly, SET-25 localizes to the nuclear periphery and maintains the tri-methylated state of H3K9 [139]. Both H3K27 and H3K9 maintain repressive environments near the nuclear lamina in many organisms [29,30,137].

In *C. elegans*, both arms of the autosomes and the left arm of the X chromosome will be bound to the inner nuclear membrane [30,136]. In a screen for genes that influence dosage compensation, CEC-4, a lamina-associated protein, was particularly

interesting compared to other lamina tethering proteins and histone modifiers[136].

CEC-4 is a chromodomain-containing protein that recognizes and binds to H3K9me3 in

C. elegans [140]. Loss-of-function mutants for *cec-4* appear superficially wild type.

Changes to the adult mutants are evident upon observation of chromosome

condensation and gene regulatory changes in imaging of the nucleus and by RNA-seq.

The X gene expression was slightly upregulated relative to the wild type without a

functional CEC-4 protein [136]. The chromodomain protein, CEC-4, binds the

methylated domains. CEC-4 is a perinuclear localized protein that contributes to the

regulation of autosomes and the X chromosomes. In hermaphrodites, the X

chromosomes differ from the autosomes as they are bound to the nuclear periphery

only in the left arm, whereas both arms bind the autosomes. However, when there is a

knockout mutation for *cec-4*, only the central portion of the chromosome is released and

moved closer to the central region of the nucleus, which is more active in transcription.

It has been proposed that CEC-4 locks down the dosage compensated X chromosomes

to the nuclear periphery and facilitates the DCC spreading across the chromosome.

Without the contribution of CEC-4, the X is not condensed correctly and becomes more

accessible to transcriptional machinery [136].

The primary focus of the study in Chapter 2 is understanding gene expression in

interphase by utilizing *C. elegans* dosage compensation as a model. *C. elegans* dosage

compensation represents an excellent system for dissecting how the various levels of

chromatin structure affect gene expression by regulating the entire X chromosome. To

further understand how dosage compensation is maintained after initiation, we

conditionally depleted DPY-27. In addition, we interrogated the contributions of DCC-

dependent mechanisms through genetic mutations in *cec-4* and *dpy-21*.

Chapter 2

Condensin I^{DC}, H4K20me1, and Perinuclear Tethering Maintain X Chromosome Repression in *C. elegans*

This chapter is in preparation for submission to the journal PLOS Genetics. Contributing authors include Audry I. Rakozy, Eshna Jash, and Györgyi Csankovszki.

2.1 Abstract

Dosage compensation in Caenorhabditis elegans equalizes X-linked gene expression between XX hermaphrodites and XO males. The process depends on a condensin-containing dosage compensation complex (DCC), which binds the X chromosomes in hermaphrodites to repress gene expression. Condensin I^{DC} and five DCC components must be present on the X during early embryogenesis in hermaphrodites to establish dosage compensation. However, whether the DCC's continued presence is required to maintain the repressed state once established is unknown. Beyond the role of condensin I^{DC} in X chromosome compaction, additional mechanisms contribute to X-linked gene repression. DPY-21, a non-condensin I^{DC} DCC component, is an H4K20me2/3 demethylase whose activity enriches the repressive histone mark, H4 lysine 20 monomethylation, on the X chromosomes. In addition, CEC-4 tethers H3K9me3-rich chromosomal regions to the nuclear lamina, which also

contributes to X-linked gene repression. To investigate the necessity of condensin I^{DC} during the larval

and adult stages of hermaphrodites, we used the auxin-inducible degradation system to deplete the condensin I^{DC} subunit DPY-27. While DPY-27 depletion in the embryonic stages resulted in lethality, DPY-27 depleted larvae and adults survive. In these DPY-27 depleted strains, condensin I^{DC} was no longer associated with the X chromosome, the X became decondensed, and the H4K20me1 mark was gradually lost, leading to X-linked gene derepression. These results suggest that the stable maintenance of dosage compensation requires the continued presence of condensin I^{DC}. A loss-of-function mutation in cec-4, in addition to the depletion of DPY-27 or the genetic mutation of dpy-21, led to even more significant increases in X-linked gene expression, suggesting that tethering heterochromatic regions to the nuclear lamina helps stabilize repression mediated by condensin I^{DC} and H4K20me1.

2.2 Introduction

Conformation, subnuclear localization, and the post-translational modifications of histones on chromosomes are linked closely to gene expression. The relationship between these processes plays a crucial role in an organism's development, growth, and survival. Understanding the mechanisms behind the regulation of gene expression is of fundamental importance. Dosage compensation in the nematode *Caenorhabditis elegans* offers an excellent paradigm for exploring chromosome-wide gene regulation. There is an inherent imbalance in chromosomal gene expression in species with heterogametic sexes [141]. As in numerous other species with chromosome-based sex determination, *C. elegans* has evolved several molecular mechanisms to ensure equal

gene expression from the sex chromosomes between the sexes [99]. This process is known as dosage compensation. In *C. elegans,* hermaphrodites have two X chromosomes (2X:2A), whereas males have only one X and no other sex chromosome (1X:2A) [69]. This difference in chromosome count is essential for sex determination [69,122]. However, without correction, in hermaphrodites, transcription from the X doubles relative to males, leaving the hermaphrodite population inviable [125]. The dosage compensation mechanism in *C. elegans* corrects for the differing numbers of sex chromosomes by reducing the gene expression of the hermaphrodite X chromosomes [98]. Dosage compensation requires orchestrating several gene-regulatory events across X chromosomes in hermaphrodites to decrease gene expression by half.

A core component of the dosage compensation machinery in *C. elegans* involves a specialized condensin complex. Condensins are highly conserved protein complexes used in most cellular life, from prokaryotes to metazoans [107]. Condensin complexes are characterized by their ring-shaped structure, and they hydrolyze ATP to extrude DNA strands through the ring, thus leading to DNA coiling and loop formation [109]. This loop extrusion activity is thought to be essential for chromosome compaction in mitosis and meiosis [142]. Multicellular eukaryotes have two condensin complexes, condensin I and II, functioning in mitosis and meiosis [143]. Similarly, *C. elegans* utilizes condensin I and II complexes for chromosome compaction and segregation [106]. However, *C. elegans* has a third condensin complex that specifically functions in dosage compensation of the X chromosomes of hermaphrodites. The hermaphrodite-specific condensin is known as condensin I^{DC} (Dosage Compensation) [106,144].

Condensins are composed of two structural maintenance of chromosomes (SMC) proteins and three chromosome-associated polypeptides (CAP) [145,146]. Condensin I^{DC} earns its name due to the four shared protein subunits with condensin I. These subunits include the structural maintenance of chromosomes (SMC) protein MIX-1 and the chromosome-associated polypeptides (CAPs) CAPG-1, DPY-26, and DPY-28. The difference between condensin I^{DC} and condensin I is the second SMC subunit, DPY-27, in condensin I^{DC} and its paralog SMC-4 in condensin I [106,114,147]. Condensin I^{DC} compacts the dosage compensated X chromosomes; thus, the X occupies less nuclear volume in hermaphrodites than in males [133]. At a higher resolution, condensin I^{DC} remodels the architecture of the X chromosomes to form topologically associating domains (TADs) characterized by a higher frequency of *cis*-interactions within domains [25,27].

Beyond condensin I^{DC}, the complete dosage compensation complex (DCC) in *C. elegans* includes the proteins SDC-1, SDC-2, SDC-3, DPY-30, and DPY-21 [106,118,120,148]. Together, these ten proteins bind and spread across the X chromosomes in hermaphrodites, inhibiting RNA Pol II binding, thus lowering transcriptional output by half [149]. One of the non-condensin DCC subunits is DPY-21 [118]. It contains a Jumonji C domain found in histone demethylases. DPY-21 has been shown to demethylate dimethylated histone 4 lysine 20 (H4K20me2) [124], previously deposited on histones by the activities of SET-1 and SET-4 [127,130], to the monomethylated form (H4K20me1). Thus, by the X-specific demethylase activity of DPY-21, H4K20me1 is enriched on the X chromosomes in hermaphrodites and contributes to further repression [124,127,130]. In addition to its demethylase function,

DPY-21 has an additional uncharacterized role in dosage compensation [124,126]. Like

other DCC members, DPY-21 activity is required to regulate the X chromosome

effectively, as evidenced by the elevated X gene expression in hermaphrodites with

dpy-21 mutations [31,124]. However, DPY-21 is not necessary to recruit the other DCC

members, and the loss of its function leads to mild defects in hermaphrodite *C. elegans*

but no significant lethality [118].

Nuclear lamina interactions with heterochromatin provide an additional layer of

gene regulation in *C. elegans,* impacting dosage compensation. In *C. elegans,*

heterochromatic regions of chromosomes are located near the nuclear periphery

[30,118,139,148]. Histone methyl transferases (HMTs) MET-2 and SET-25 target H3

lysine 9 (H3K9) on chromatin to deposit mono-, di-, and trimethylation [139]. The

lamina-associated protein CEC-4 binds to heterochromatic H3K9me regions on both the

autosomes and the X [140]. The tethering of heterochromatic regions of the

chromosomes to the nuclear lamina contributes to stabilizing cell fates during *C.*

elegans development [140]. In addition, the loss of nuclear lamina tethering leads to the

decompaction and relocation of the X into a more interior position in the nucleus and a

mild increase of X-linked gene expression without impacting autosomal gene

expression, indicating dosage compensation defects [136]. Despite defects in the

chromosomal organization, mutants with non-functional CEC-4 survive with no apparent

phenotypes [140].

Dosage compensation is set up stepwise throughout development in *C. elegans*.

The process is initiated at about the 40-cell stage, when the DCC subunit SDC-2 is

expressed and localizes to hermaphrodite X chromosomes [67], which leads to the

recruitment of the other DCC subunits [150]. This initiation step coincides with the loss

of pluripotency of embryonic blastomeres [128,151]. DPY-21 localizes to the X after the

initial loading of condensin I^{DC}, and H4K20me1 becomes enriched on the X between the

bean and comma stages of embryogenesis [124,128]. By the end of embryogenesis,

most cells exit mitosis [152], after which the dosage-compensated state is maintained in

postmitotic cells. We refer to this stage as the maintenance phase. Earlier studies using

cold-sensitive *dpy-27* alleles suggested that DPY-27 activity is essential during a critical

developmental time window in mid-embryogenesis, after which loss of its function has a

lesser impact on viability [116]. These results suggest that while condensin I^{DC} is

required to initiate dosage compensation, other mechanisms can maintain dosage

compensation, including ones mediated by DPY-21 and CEC-4.

The requirement for CEC-4 also changes with the differentiation state of

embryonic cells. CEC-4 is required to tether heterochromatic transgenic arrays to the

nuclear lamina in embryos but not in L1 larvae [140]. At the larval stages and beyond,

additional mechanisms, including ones mediated by MRG-1 and CBP-1, contribute to

sequestering heterochromatin to the nuclear lamina [153]. However, X chromosome

compaction and nuclear lamina tethering affect *cec-4* adults, even in fully differentiated

postmitotic cells [136]. We hypothesize that by sequestering the chromosome to the

nuclear lamina, CEC-4 stabilizes the repression of the X chromosomes during the

maintenance phase of dosage compensation.

In this study, we used the auxin-inducible degradation (AID) system to deplete

the condensin I^{DC} subunit DPY-27 at various stages of development. We assessed the

importance of condensin I^{DC} to X chromosome repression and organismal viability

during the establishment and maintenance phases of dosage compensation. Our findings reveal that the continued presence of DPY-27 is required to maintain X chromosome repression after initial establishment, although continued repression is less essential for viability during the maintenance phase. Additionally, we evaluated the hypothesis that the nuclear lamina protein CEC-4 helps stabilize the repressed state by combining *cec-4* mutations with depletion of DPY-27 or mutations in the histone demethylase *dpy-21.* We show that the loss of lamina associations resulting from mutations in *cec-4* exacerbates the defects caused by the lack of DPY-27 or DPY-21 function. Our results reveal the differential contributions of the various repressive pathways to X chromosome dosage compensation.

2.3 Results

2.3.1 *The impact of DPY-27 depletion on hermaphrodite embryos and larvae*

Using a strain containing an auxin-inducible degron (AID)-tagged *dpy-27* allele [40] and expressing the plant F-box protein TIR1 under a ubiquitous promoter (*eft-3*) [38] (referred to as *TIR1; dpy-27::AID*, to see complete genotype and allele information for all strains see the Materials and Methods), we were able to time the depletion of DPY-27 by moving worms to auxin-containing plates during or after embryogenesis. To evaluate whether the lack of CEC-4 exacerbates the defects, we also generated a strain containing the *cec-4 (ok3124)* mutation in addition to *TIR1 and dpy-27::AID* (referred to as *TIR1; dpy-27::AID; cec-4*). For controls, we used wild-type worms (N2), cec-4 mutants, and a strain with AID-tagged dpy-27 but no TIR1 expressing transgene (referred to as *dpy-27::AID*).

Our first experiment investigated the ability of embryos exposed to auxin to survive in the absence of DPY-27 throughout the entirety of embryonic development. To ensure that the maternally loaded DPY-27 is also depleted, we initiated our assay at the L4 larval stage of the parent before oocyte production begins **(Fig 2.1A)** [114]. L4 larvae were placed on auxin-containing plates for a 24-hour egg-laying period, after which the parents were removed. This procedure ensures that both *in-utero* and *ex-utero* development occurs in the presence of auxin. Strains not exposed to auxin were viable primarily, although the *dpy-27::AID*-containing strains had a very low, but statistically significant, level of lethality (**Fig 2.1B**, Fisher's exact test, p values listed in **Table 2.1**). While auxin treatment did not significantly impact the survival of control embryos (N2, *cec-4, dpy-27::AID),* 100% of *TIR1; dpy-27::AID and TIR1; dpy-27::AID; cec-4* worms died as embryos or L1 larvae **(Fig 2.1B)**. These results indicate that DPY-27 function during embryonic development is essential for the survival of hermaphrodite worms, which is consistent with previous studies [116].

At the onset of dosage compensation during early embryogenesis, condensin I^{DC} loads onto the X chromosomes in hermaphrodites [106]. However, it is unclear whether the sustained presence of the complex is essential once dosage compensation is established. To assess the requirement for DPY-27 to remain on the X during larval development, we exposed our strains to auxin, starting at the L1 larval stage for a period of three days. We compared survival on auxin-containing plates to survival on plates without auxin **(Fig 2.1C)**. Strains developing without auxin exposure grew to adulthood and produced viable offspring in the timeframe of the experiment. In contrast to embryonic exposure, exposing larvae to auxin had a much lesser effect on survival.

Most *TIR1; dpy-27::AID* larvae survived similarly to N2, *cec-4*, or *dpy-27::AID* controls **(Fig 2.1E,** Chi-square test, p values listed in **Table 2.2)**. However, DPY-27 depleted strains developed slowly and exhibited developmental defects, including stunted growth **(Fig 2.1D)**. The rare embryo produced by these hermaphrodites did not hatch. Adding *cec-4* to the background lowered the survival rate, suggesting that lack of both DPY-27 and CEC-4 results in more severe defects than lack of DPY-27 alone **(Fig 2.1E)**

2.3.2 *Exposure to auxin depletes DPY-27, disrupts DCC binding and H4K20me1 enrichment on the X*

We next investigated the degree of DPY-27 depletion in auxin-treated strains relative to untreated. DPY-27 was visualized in each strain by immunofluorescence (IF) after worms were exposed to auxin for three days starting at the L1 larval stage. Due to the underdeveloped nature of the DPY-27 depleted strains, we based the timing of IF staining on the growth of the wild type. After 3 days, wild-type N2 worms have developed into young adults. IF images were captured in intestinal nuclei. Intestinal cells are 32-ploid, and their large size facilitates analyses of the nucleus. Before auxin treatment, all our strains had a wild-type pattern of DPY-27 localization within the nucleus of intestinal cells **(Fig 2.2A)**, consistent with the lack of any visible defects or lethality in these strains. Auxin treatment in N2, *cec-4*, and *dpy-27::AID* strains led to no observable changes. However, in the *TIR1*-containing strains, *TIR1; dpy-27::AID* and *TIR1; dpy-27::AID; cec-4,* auxin treatment resulted in depletion of DPY-27 to background levels **(Fig 2.2B)**, suggesting that auxin-induced degradation was successful.

The observation that *TIR1; dpy-27::AID* and *TIR1; dpy-27::AID; cec-4* larvae can survive despite complete or near complete depletion of DPY-27 prompted us to investigate the degree to which dosage compensation is maintained in these larvae. To assess the binding of other Condensin I^{DC} subunits to the X chromosome following DPY-27 depletion, we performed IF staining for CAPG-1. In N2, *cec-4*, and *dpy-27::AID* strains, CAPG-1 maintains a signal pattern indicative of X chromosome binding. However, in *TIR1; dpy-27::AID* and *TIR1; dpy-27::AID; cec-4,* the CAPG-1 signal becomes non-specific, and it diffuses throughout the entire nucleus **(Fig 2.2C)**. Our results indicate that condensin I^{DC} no longer maintains localization to the X chromosomes following DPY-27 depletion.

We next assessed the enrichment of the histone modification H4K20me1 as a readout for functional DCC binding. In wild-type N2 hermaphrodites, this histone modification is specifically enriched on dosage-compensated X chromosomes [127,130], and this pattern was maintained in *cec-4* and *dpy-27::AID* strains. After exposure to auxin in *TIR1; dpy-27::AID* and *TIR1; dpy-27::AID; cec-4* strains, H4K20me1 was no longer specifically localized within the nucleus, resembling the pattern observed for CAPG-1 localization with the IF signal spread throughout the entirety of the nucleus **(Fig 2.2C)**. H4K20me1 first becomes enriched on dosage-compensated X chromosomes in mid-embryogenesis [128,130] well before the L1 stage, when auxin treatment was initiated. We conclude that the continued presence of DPY-27 and the DCC is required to maintain this chromatin mark on the X chromosomes. The *TIR1; dpy-27::AID* and *TIR1; dpy-27::AID; cec-4* strains appeared

similar in this assay, suggesting that the presence or absence of CEC-4 does not contribute to the maintenance of the H4K20me1 mark.

2.3.3 *The continued presence of DPY-27 is required to maintain X chromosome condensation and subnuclear localization*

The X chromosomes of wild-type hermaphrodites occupy a surprisingly low proportion of space in the nucleus compared to what is predicted based on DNA content [100]. We previously showed that in DCC mutants and in *cec-4* mutant hermaphrodites, the X chromosomes decondense and relocate toward the more actively transcribed central region of the nucleus [136]. The DCC starts to compact the X chromosomes in early embryogenesis [100]. We tested if the continued presence of DPY-27 is necessary for maintaining the compact conformation of the X. We performed whole chromosome X paint fluorescence *in situ* hybridization (FISH) to mark the X chromosome territories in intestinal nuclei. Without auxin treatment, the X chromosome signal appeared as expected: compact and near the nuclear periphery in all strains without a *cec-4* mutation and more diffuse in strains with a *cec-4* mutation **(Fig 2.3A).** After auxin treatment, the X chromosomes appeared enlarged in *TIR1; dpy-27::AID* as well **(Fig 2.3B)**. We quantified these changes by measuring the proportion of nuclear volume occupied by the X chromosome (see Methods). The X chromosome occupied about 12-13% of the nuclear volume in wild type and close to 20% in *cec-4* mutants **(Fig 2.3C, Table 2.3** for complete statistical analysis)**, which is consistent with previous results [136]. In the *TIR1; dpy-27::AID* strain, depletion of DPY-27 led to decondensation of the X chromosome to a degree similar to *cec-4* mutants or to what was previously observed in worms treated with *dpy-*27 RNAi [100]. These findings demonstrate the critical role of

36

DPY-27 in maintaining the compact conformation of the X chromosome in wild-type hermaphrodites. In the *TIR1; dpy-27::AID; cec-4* strain, the X was already decondensed without auxin treatment due to the presence of the *cec-4* mutation, and depletion of DPY-27 led to a measurable level of additional decondensation **(Fig 3C)**. These results can be interpreted in several ways. These results indicate that the presence of DPY-27 maintains X compaction, and the additional loss of *cec-4* exacerbates decondensation.

The dosage compensation mechanisms make the X chromosomes not only compact but also position the chromosomes near the nuclear periphery [136]. To assess any changes in subnuclear localization, we analyzed our X chromosome FISH signals in the various strains using a three-zone assay (see Methods) **(Fig 3A**The localization of the X within the nucleus was assessed in these three concentric zones, and the portion of the X signal in the central zone was quantified from a singular focal plane taken from the middle of the nucleus. ImageJ defined the boundaries of the nucleus (DAPI) and the X chromosome paint signal (left and center image, respectively). The nucleus was then divided into three concentric circles: peripheral (blue), intermediate (pink), and center (yellow). **(Fig 3D)**. In wild-type hermaphrodites, we observed the expected X localization. Only a small portion of the signal reaches into the center ring. At the same time, the bulk of the X is located in the intermediate and peripheral zones of the nucleus **(Fig 3E, S1 Fig, S4 File** for complete statistical analysis**),** as observed before [136]. In *cec-4* mutants (*cec-4* and *TIR1; dpy-27::AID; cec-4)*, significantly more of the X signal is in the center, as expected. The relocation is even more significant in DPY-27 depleted strains **(Fig 3E)**. In both *TIR1; dpy-27::AID* and *TIR1; dpy-27::AID; cec-4* strains, over 40% of the signal is localized in the central

region, suggesting that the depletion of DPY-27 has a more significant impact on X nuclear localization than the *cec-4* mutation. Adding *cec-4* mutation did not significantly increase the degree of movement to the middle region compared to DPY-27 depletion alone. Overall, this data indicates that the continued presence of DPY-27 is required to maintain X compaction and peripheral localization and that adding a *cec-4* mutation led to further X decompaction.

2.3.4 *The continued presence of DPY-27 is required in fully differentiated postmitotic cells*

Thus far, we analyzed worms for which the auxin treatment began at the L1 larval stage and ended three days later (the duration of time in which N2 reaches adulthood). In this timeframe, intestinal nuclei undergo four rounds of endoreduplication and reach the stage of 32-ploidy [154]. To analyze the continued need for DPY-27 after these altered cell cycles have taken place and the cells have fully differentiated, we performed experiments where the auxin treatment began in adulthood (3 days past L1). The auxin-degron system is very effective in *C. elegans,* with protein degradation observable within 30 minutes [155]. We subjected adult hermaphrodites to auxin for one hour to assess whether one hour was sufficient for DPY-27 degradation. In *TIR1; dpy-27::AID* and *TIR1; dpy-27::AID; cec-4* strains, we observed significant protein depletion, comparable to longer treatments as visualized by IF staining **(Fig 2.4A)**.

Given the rapid depletion of DPY-27, we investigated potential alterations in mechanisms linked to dosage compensation. To assess whether H4K20me1 enrichment is sustained after DPY-27 loss, intestinal nuclei of young adult hermaphrodites exposed to auxin for one hour were stained with an antibody targeting

H4K20me1 and the DCC subunit CAPG-1. Auxin exposure for one hour resulted in the

CAPG-1 signal appearing diffuse throughout the nucleus in *TIR1; dpy-27::AID* with and

without *cec-4*, but with partial enrichment over a portion of the nucleus, presumably the

X chromosome **(Fig 2.4B, left)**. These results indicate that after DPY-27 depletion, the

rest of the DCC also rapidly dissociates from the X, but with a slight delay compared to

the DPY-27. Notably, H4K20me1 staining also appeared somewhat limited to this

region but more diffuse than in controls. Strains in which DPY-27 was not depleted (*cec-*

4 and *TIR1; dpy-27::*AID) exhibited a clear overlap in the enrichment of H4K20me1 and

the DCC protein CAPG-1, comparable to no auxin controls. However, the changes in

staining of H4K20me1 and CAPG-1 after one hour of auxin treatment are not as drastic

as in hermaphrodites exposed to auxin during larval development for three days. To test

whether prolonged exposure would lead to a complete loss of enrichment, we exposed

young adult hermaphrodites to auxin for 24 hours. After 24 hours on plates containing

auxin, *TIR1; dpy-27::AID* and *TIR1; dpy-27::AID; cec-4* exhibited a complete loss of the

X-enrichment of the CAPG-1 and H4K20me1 signals **(Fig 2.4B, right)**, indistinguishable

from results obtained with worms treated with auxin for three days of larval development

(Fig 2.2C). We performed whole X paint FISH on strains exposed to auxin for 24 hours

(Fig 2.4C). We observed X chromosome decondensation to levels similar to worms

exposed to auxin for three days **(Fig 2.4D)**. Hence, we conclude that the continued

presence of DPY-27 is required to maintain the dosage-compensated state even in fully

differentiated postmitotic cells and that depletion of DPY-27 leads to the rapid loss of

features associated with dosage compensation.

2.3.5 *X-linked genes are derepressed after DPY-27 depletion*

We next tested whether these changes in X chromosome compaction, nuclear organization and the depletion of repressive histone marks led to increases in X chromosome gene expression in the *TIR1; dpy-27::AID* and *TIR1; dpy-27::AID; cec-4* strains when treated with auxin. Although nuclear organization and H4K20me1 enrichment were not significantly different with and without a mutation in *cec-4*, the reduced viability of auxin-treated *TIR1; dpy-27::AID; cec-4* larvae compared to *TIR1; dpy-27::AID* larvae also suggested that the X may be more derepressed in the strain lacking *cec-4.* To test these hypotheses, we extracted total mRNA from synchronized L3 populations, which were grown in the presence of auxin starting at L1 or grown in the absence of auxin for controls. We performed these experiments at the L3 stage rather than at a later stage because, at this stage the delay in growth and development of the DPY-27 depleted strains is not yet apparent, and also to avoid complications arising from the contributions from the germline where the X chromosomes are subject to regulation unrelated to dosage compensation [156]. At the L3 stage, the germline consists of only about ~60 cells; thus, the RNA extracted from whole worms represents predominantly somatic tissues [157]. The mRNA-seq readout is plotted as a log2-fold change in gene expression on autosomes and the X in auxin-treated samples compared to controls **(Fig 2.5)**.

Without exposure to auxin, the *dpy-27::AID* strain has gene expression levels similar to N2, suggesting again that tagging DPY-27 with the degron tag did not disrupt its function **(Fig 2.9)**. *cec-4* strains treated with auxin displayed a very slight X depression compared to both N2 and *cec-4* mutants without auxin exposure, indicating a minimal influence of auxin treatment on gene expression regulation **(Fig 2.10)**. The

TIR1; dpy-27::AID and the *TIR1; dpy-27::AID; cec-4* strains also had a small degree of X derepression compared to wild type even in the absence of auxin, possibly due to somewhat leaky *TIR1* activity, which is a phenomenon noted by other research groups as well **(Fig 2.9)** [158–160]. Therefore, to assess the increase in X-linked gene expression due to the loss of DPY-27 during the maintenance phase of dosage compensation, we compared gene expression levels in the same strain with and without auxin and in auxin-treated strains with and without TIR1 expression **(Fig 2.5)**. In comparison to *dpy-27::AID*, the strain *TIR1; dpy-27::AID* had significant upregulation of the X chromosome when treated with auxin, while autosomal gene expression remained unchanged (median X gene expression – median autosomal gene expression, M(X) - M(A) = 0.503) **(Fig 2.5A)**. Similarly, auxin-treated *TIR1; dpy-27::AID* exhibited X derepression compared to non-auxin-treated samples (median X-media A=0.435) **(Fig 2.5B)**. These results demonstrate that depletion of DPY-27 during the maintenance phase of dosage compensation leads to significant X derepression.

We then investigated whether the absence of CEC-4 further enhanced X derepression. Comparing the mRNA-seq gene expression profiles of *TIR1; dpy-27::AID; cec-4* treated with auxin to untreated populations of the same genotype, we observed a significant increase in X-linked gene expression (M(X) – M(A)= 0.78) **(Fig 2.5C)**. The degree of X derepression was greater than that caused by auxin treatment in *TIR1; dpy-27::AID* without the *cec-4* mutation. These results suggest that the loss of *cec-4* may exacerbate X dosage compensation defects. To confirm, we compared *TIR1; dpy-27::AID; cec-4* to *TIR1; dpy-27::AID* after auxin treatment. The difference between these two populations was substantial (M(X) – M(A)= 0.13), suggesting that depletion of DPY-

41

27 leads to a greater level of X derepression in a strain that lacks CEC-4 **(Fig 2.5D)**.

These results are consistent with CEC-4's support in maintaining stable X chromosome

repression in differentiated cells.

2.3.6 *Loss of cec-4 Activity Exacerbates Dosage Compensation Defects Caused by a Mutation in dpy-21*

Our experiments showed that the loss of CEC-4 further sensitizes hermaphrodite

C. elegans to dosage compensation defects caused by DPY-27 depletion **(Fig 2.5D)**. To

test whether loss of CEC-4 also exacerbates defects caused by other dosage

compensation mutations, we sought to understand the interplay between CEC-4, known

for its role in tethering the X chromosomes to the nuclear lamina [136], and DPY-21,

whose activity leads to X-specific enrichment H4K20me1 [124]. Individually, the

mutations in these pathways lead to phenotypes related to dosage compensation

defects and changes in X-linked gene expression, but despite these changes, the

mutants are viable [118,124,127,136,140]. Since *dpy-21* null mutants (*dpy-21(e428))*

are viable [118], we performed these experiments with the null mutant rather than using

the AID system. Therefore, our experiment tested the impact of these mutations

throughout the lifespan of the animals, including both the establishment and the

maintenance phases of dosage compensation. We constructed a double mutant *cec-4*

(ok3124) IV*; dpy-21(e428)* V strain (referred to as *cec-4; dpy-21).* The strain is viable

and produces progeny with visible defects, such as a Dpy phenotype.

We first evaluated the ability of embryos lacking functional *cec-4* and *dpy-21* to

develop into adulthood. Most wild-type (N2) and *cec-4* mutant embryos developed into

adulthood. While the viability of *dpy-21* mutants was somewhat reduced, it was not

significantly different from the viability of *cec-4; dpy-21* double mutants **(Fig 2.6B).**

However, the total brood count of *cec-4; dpy-21* hermaphrodites was significantly

smaller than all other strains observed, including the *dpy-21* and *cec-4* single mutants

(Fig 2.6A). In all strains, most embryos emerged as L1 within 24 hours **(Fig 2.6B)**. As

the progeny developed to adulthood, there was a significant drop off in survival in

strains containing *cec-4* and/or *dpy-21* in the background **(Fig 6C)**. Overall, these

results suggest the addition of the *cec-4* mutation does decrease the overall fitness of

dpy-21 mutants.

We employed DPY-27 staining to mark the X chromosomes to assess the level

of X chromosome compaction. All mutants exhibited a prominently decondensed X

chromosome **(Fig 2.6C)**. Further quantitative analysis, comparing the domain of the

DPY-27 signal to the overall nuclear volume, revealed that the X chromosomes were

decondensed in *cec-4* and *dpy-21* single mutants, but in the *cec-4; dpy-21* strain, the X

occupied an even more significant proportion of the nucleus, **(Fig 2.6D)**. Remarkably,

the double mutant strain, *cec-4; dpy-21*, displayed particularly enlarged X chromosomes

visible via IF **(Fig 2.6E)**. The localization of DPY-27 to the X chromosome was not

influenced by the loss of *cec-4* and/or *dpy-21* **(Fig 2.6F)**. This observation shows that

adding the *cec-4* mutation to *dpy-21* mutants augments some defects associated with

dosage compensation.

To determine the impact of these mutations on X chromosome gene repression,

mRNA-seq was performed in L3 hermaphrodites. We previously reported subtle

upregulation of the X chromosomes in *cec-4* mutant L1 larvae compared to the wild type

[136]. In L3 larvae, this upregulation was even more modest and not statistically

significant (median X - median A = 0.027) **(Fig 2.7A)**, suggesting that lack of CEC-4

alone does not have a significant impact on X-linked gene regulation despite the

observed changes in X chromosome compaction and nuclear localization. In contrast,

the *dpy-21* mutant displayed a more pronounced derepression of the X chromosome

(median X - median A = 0.612) **(Fig 2.7B)**, consistent with previous results [31,124].

When we compared the *cec-4; dpy-21* double mutant to the wild type, we observed an

even more drastic change in gene expression (median X - median A = 0.721) **(Fig**

2.7C). Furthermore, when juxtaposing the double mutant *cec-4; dpy-21* against its

single mutant counterparts, the results underscored that *cec-4; dpy-21* expressed X-

linked genes at a higher level than either single mutant (*cec-4; dpy-21* vs *cec-4*: median

X - median A = 0.669, and *cec-4; dpy-21* vs *dpy-21*: median X - median A = 0.09).

Given the relatively minor derepression of the X chromosome in *cec-4* mutants, a

significant increase in the X-linked gene expression levels of *cec-4; dpy-21* compared to

cec-4 alone was expected **(Fig 2.7D)**. The *dpy-21* single mutant already exhibited an

upregulation in X chromosome gene expression; however, the *cec-4; dpy-21* double

mutant significantly surpassed it in X derepression **(Fig 2.7E)**. While *cec-4*, as a single

mutation, does not substantially impact X-linked gene expression, our results show that

the loss of *cec-4* sensitizes hermaphrodites to additional dosage compensation defects.

2.4 Discussion

In this study, we investigated the relative contributions of the DCC to two phases

of dosage compensation: establishment and maintenance. We depleted DPY-27, a core

protein subunit of the dosage compensation machinery, condensin I^{DC}, using the auxin-

inducible degron system during embryonic and larval development. Our data indicated

that DPY-27 function is essential during embryonic development, but the protein is dispensable for hermaphrodite survival during larval and adult stages. In an additional dosage compensation mechanism, the non-condensin DCC member DPY-21 significantly contributes to X-linked gene repression by enriching H4K20me1 on the X chromosome [124]. We show that the enrichment of H4K20me1 is lost rapidly after DPY-27 depletion, indicating that the mark must be continuously maintained, presumably by DPY-21 recruited to the X by DPY-27. In addition, DPY-27 depletion leads to X chromosome decondensation and relocation to a more central position in the nucleus, as well as significant increases in X-linked gene expression. In addition to the contributions of the DCC, nuclear lamina association of the X chromosome via H3K9me3 binding to CEC-4 also contributes to X morphology and repression [136]. We found that a loss-of-function mutation in *cec-4* amplifies the sensitivity of hermaphrodites to the depletion/mutation of other dosage compensation processes. These results suggest that nuclear lamina anchoring by CEC-4 serves to stabilize repression initiated by condensin I^{DC} or H4K20me1. By genetic loss-of-function mutations in *cec-4* and *dpy-21* and depletion of DPY-27, we unexpectedly revealed that larval and adult hermaphrodites are resilient to depletion of known dosage compensation mechanisms and substantial increase in X-linked gene expression.

2.4.1 *Condensin I^{DC} Function is Required for Embryonic Viability but not for Larval and Adult Viability*

A previous study using a cold-sensitive mutant for *dpy-27* demonstrated that inactivating DPY-27 during the comma stage of embryonic development leads to more extensive lethality than inactivation of the protein at later stages. However, the

differences in viability counts at the different temperatures were only about 20% [116]. We re-examined this question using the auxin-mediated degradation system, where adding auxin leads to rapid and near complete depletion of DPY-27. Prior to auxin treatment, the strains had essentially 100% viability, while auxin treatment during embryogenesis led to essentially 100% lethality. These results demonstrate that condensin I^{DC} activity is essential during embryonic development when cell fates are being specified and cells begin to differentiate into different cell types. At the end of embryonic development, the embryo consists of about 500 cells, the majority of which have exited the cell cycle and begun terminal differentiation [152]. Depletion of condensin I after embryogenesis is not incompatible with viability despite developmental abnormalities in depleted larvae. This result raised two possibilities. First, it is possible that dosage compensation, once established, can be maintained in the absence of condensin I^{DC}. Second, it is possible that X chromosome repression is not maintained, but larvae can tolerate defects in X-linked gene regulation. Our results, discussed below, are consistent with the second scenario.

2.4.2 Condensin I^{DC} Must Remain on the X to Maintain the Condensed Conformation

We show that compaction of the dosage compensated X cannot be maintained without DPY-27. By varying durations of auxin exposure and observing the condensin IDC subunit CAPG-1, we saw the gradual loss of condensin I^{DC} enrichment on the X **(Figs 2.2 and 2.4)**. We propose that the absence of DPY-27 leads to the destabilization of the condensin I^{DC} ring, resulting in the eventual release of the complex from the X. The X chromosome also decondenses after condensin I^{DC} loss, indicating that

46

chromosome compaction must be actively maintained. Previous research investigating the maintenance of mitotic or meiotic chromosome architecture demonstrated that depletion or inactivation of mitotic condensin subunits after chromosome condensation has taken place led to disorganized chromosome structure with reduced rigidity or a more extensive surface area measurements [161–164]. Similar to what we observed about the continued need for condensin I[DC] to maintain the compact structure of dosage compensated X chromosomes, maintenance of mitotic chromosome architecture also requires the continued presence of condensin. However, in the studies of mitotic chromosomes, compaction was maintained after condensin loss; only the organization or rigidity of chromosomes was altered. In our study, the interphase X chromosome was decondensed after condensin loss. It's been suggested that during mitosis, additional mechanisms, such as posttranslational histone modifications, contribute to chromosome condensation [165]. We hypothesize that condensin function is necessary for compaction in the absence of these mitosis-specific histone modifications in interphase. We note that two posttranslational histone modifications associated with mitosis, namely enrichment of H4K20me1 and depletion of H4K16ac, are also features of interphase dosage compensated X chromosomes of *C. elegans* [127,130,165–167]. However, additional mitotic histone modifications that are not present on dosage compensated X chromosomes (for example, H3S10Ph or depletion of additional acetylation marks) may also contribute to condensin condensin-independent chromosome compaction in mitosis [168]. Our findings indicate that the complete condensin complex must remain associated with the X for the maintenance of compaction during developmental stages in which most cells are post-mitotic. It will be interesting to investigate the maintenance

47

of chromosome architecture changes on dosage compensated Xs at higher resolution, such as the formation of TADs using Hi-C.

2.4.3 *The Presence of DPY-27 is Required to Actively Maintain the Enrichment of H4K20me1 on the X*

Concurrently with the loss of CAPG-1 signal, the H4K20me1 mark exhibits a loss of specific localization on the X with increasing auxin exposure time **(Figs 2.2 and 2.4)**. We propose that the continued presence of DPY-21 (presumable recruited by DPY-27) on the X is necessary to maintain H4K20me1 enrichment on the X. Notably, the presence of DPY-21 is not essential for the localization of condensin I^{DC} on the X; however, for DPY-21 to bind the X, the presence of condensin I^{DC} is required [118]. Our results are similar to what was seen for the H3K9me2 by MET-2. Maintenance of this chromatin mark in *C. elegans* also requires the continued presence of the enzyme that places it [169]. Our results suggest that functional Condensin I^{DC} plays a role in maintaining the localization of DPY-21 on the X, and its continued presence is required even in post-mitotic developmental stages. We hypothesize that in the absence of DPY-21, either there is frequent enough histone turnover to lose the H4K20me1 enrichment or that the X is rendered accessible to histone modifiers that remove the H4K20me1 or modify the mark to di- or trimethylation.

2.4.4 *Condensin I^{DC} is Required to Maintain X-linked Gene Repression in Hermaphrodites*

Severe depletion or mutation of dosage compensation in *C. elegans* is hermaphrodite lethal. Unexpectedly, we observed that hermaphrodites survive as larvae in the absence

of DPY-27, albeit with major phenotypic defects **(Fig 2.1C).** Furthermore**,** they survive

without other vital contributors to X gene regulation in addition to DPY-27 depletion,

namely, nuclear lamina tethering by CEC-4 and H4K20me1 **(Fig 2.6B)**. In short, auxin-

treated *TIR1; dpy-27::aid; cec-4* larvae survive without measurable activity of any known

dosage compensation mechanism. Our study revealed increases in X-linked gene

expression beyond levels reported in *dpy-27* null mutants in the past [31]. The embryos

and larvae used in this study lacked both maternal and zygotic contributions of DPY-27

and did not survive. In these *dpy-27* null mutant embryos and L1 populations, the

reported log2 fold change in X-linked gene expression level was less than 0.3 [31].,

significantly less than what we observed when depletion took place in the maintenance

phase. Our most significant increase in X-linked gene expression was measured in

TIR1; *dpy-27::AID; cec-4* L3 larvae with a log2 fold change in X-linked gene expression

at a value of 0.78 **(Fig 2.5)**. These larvae survive despite more significant gene

expression defects than previously reported for embryos dying of dosage compensation

defects. We suggest that the absence of these dosage compensation processes is

acceptable in these animals because the continued repression of the X is no longer

essential after early development once cell fates have been specified and the cells have

begun differentiating.

In mice, the critical contributor to dosage compensation, the long non-coding

RNA *Xist*, can be deleted with minimal change to X repression as long as it is deleted

during the maintenance phase after X chromosome inactivation is fully established

[170,171]. However, unlike the continued repression of the mouse X despite the loss of

Xist, we observed a significant derepression of X-linked genes in *C. elegans*

hermaphrodites after the depletion of DPY-27. The difference might be due to the nature of the repressive mechanisms. In mice, X chromosome inactivation involves the establishment of facultative heterochromatin on the X chromosomes, including DNA methylation and heterochromatic histone modifications [172]. Studies in other organisms have shown that these chromatin marks can be maintained by propagating them during the S phase [173–176], even without the initial trigger. The repressive mechanisms involved in *C. elegans* dosage compensation are different. H4K20me1 patterns are not propagated during the DNA replication; in fact, H4K20me1 levels decrease in the S phase due to the activity of an H4K20me1 demethylase PHF8 [177]. Instead, H4K20me1 is thought to be established during mitosis [166] and then converted to H4K20me2/3 methylation after mitotic exit [166]. Our results suggest that maintenance of this mark on dosage compensated X chromosomes requires the continued presence of DPY-27, presumably recruiting the H4K20me2 demethylase DPY-21 [124].

2.4.5 *The Loss of Function of cec-4 Sensitizes Hermaphrodites to the loss of DPY-27 or DPY-21*

The *cec-4* mutation, combined with DPY-27 depletion, showed no significant changes in nuclear compartmentalization and chromosome compaction compared to DPY-27-depleted strains with functional CEC-4. Quantitative microscopy revealed that, in post-mitotic intestinal nuclei of all dosage compensation mutants, the X chromosome occupied 18-24% of the nucleus **(Figs 3E, 4D)**. Although we did not observe a measurable difference in X compaction or nuclear localization, there was a notable decrease in hermaphrodite viability of DPY-27 depleted larvae with a *cec-4* mutation

compared to DPY-27 depleted larvae without a *cec-4* mutation, suggesting disruption to X gene regulation approaching unacceptable limits for survival. When a *cec-4* mutation was combined with a *dpy-21* mutation, there was an observable increase in X decompaction and a decrease in brood size in the double mutant compared to single mutants, again suggesting a more significant disruption to dosage compensation. mRNA-seq analysis indicated that the loss-of-function mutation of *cec-4* alone minimally increased X-linked gene expression **(Fig 2.7)**. However, in scenarios where *cec-4* was non-functional, coupled with DPY-27 depletion or *dpy-21* mutation, we observed a substantial increase in X-linked gene expression, significantly more than in strains without the *cec-4* mutation **(Figs 5** and **7)**. Previous studies have highlighted the involvement CEC-4 in cellular differentiation and stabilizing cell fates [140]. Cells actively undergoing differentiation demand precise gene expression levels. However, we hypothesize that the loss of some repressive mechanisms after differentiation is acceptable, partly because CEC-4 may help lock down established gene expression patterns, including the repressed state of dosage-compensated X chromosomes. It should be noted, however, that the loss of *cec-4* challenges the health of *C. elegans* larvae and depletes other dosage compensation proteins, but most of the larvae survive. We hypothesize that losing these mechanisms, including the CEC-4 function, at the larval developmental stage does not result in outright lethality because cellular differentiation is more complete.

While DCC-mediated mechanisms are crucial for viability during the establishment of dosage compensation, our results demonstrate that they are not essential for survival during the maintenance stage. During larval and adult developmental stages,

hermaphrodites survive without any known dosage compensation activity. This resilience raises questions about the necessity of continued X repression after embryonic development.

2.5 Acknowledgments

2.6 Materials and Methods

2.6.1 *Caenorhabditis elegans Strains*

The strains used are shown in the table below. Strains were maintained at 20°C on nematode growth media (NGM) plates seeded with the *Escherichia coli* strain OP50 as a food source, as described in [179]. For some experiments requiring larger number of worms, strains were grown on high-growth media (HGM) plates were seeded with *E. coli* strain NA22, as described in [180].

Genotype	Strain	Source
Wild Type	Bristol N2	CGC
dpy-21(e428) V	EKM71	This study
cec-4 (ok3124) IV	EKM121	This study
cec-4 (ok3124) IV; *dpy-21(e428)* V	EKM222	This study
ieSi57[Peft-3::*TIR1*::mRuby::unc-54 3'UTR, cb-unc-119(+)] II; *dpy-27::AID::MYC* (xoe41) III	EKM237	This study
dpy-27::AID::MYC (xoe41) III	EKM227	[178]
dpy-27::AID::MYC (xoe41) III; *cec-4* (ok3124) IV	EKM233	This study
ieSi57[Peft-3::*TIR1*::mRuby*::unc-54* 3'UTR, *cb-unc-119*(+)] II; *dpy-27::AID::MYC*(xoe41) III; *cec-4*(ok3124) IV	EKM238	This study
wrdSi3 [*sun-1*p::*TIR1*::F2A::mTagBFP2::AID*::NLS::tbb-2 3'UTR] II; *dpy-27*(*xoe41*[*dpy-27::AID::myc*]) III; *him-8* (*me4*) IV	JEL1197	[178]
unc-119 (*ed3*); ieSi57 [*Peft-3*::*TIR1*::mRuby::*unc-54* 3'UTR, *cb-unc-119*(+)] II	CA1200	[155]

The alleles for *dpy-21 (e428)* and *cec-4 (ok3124)* were initially acquired from the *Caenorhabditis* Genetics Center (CGC) as the strains CB428 and RB2301, respectively. Each strain was backcrossed to Bristol N2 six times to generate the strains EKM71 *dpy-21 (e428)* and EKM121 *cec-4 (ok3124)*. EKM222 was obtained by crossing EKM71 to EKM121.

The strain JEL1197 was received from and generated by [178]. To isolate the *dpy-27::AID::MYC* (xoe41) allele, JEL1197 was crossed to wild type to produce EKM227. EKM227 was then crossed to CA1200 [155] to create EKM237. To add *cec-4 (ok3124)* to the background, EKM227 was crossed with EKM121. The subsequent strain, EKM233, was crossed with CA1200 to generate EKM238.

2.6.2 *Antibodies*

Antibodies used in this study include rabbit anti-H4K20me1 (Abcam ab9051), rabbit anti-DPY-27 [106], and goat anti-CAPG-1 [136]. Secondary antibodies for anti-goat and anti-rabbit were purchased from Jackson Immunoresearch.

2.6.3 *Synchronized worm growth and collection*

To obtain synchronized worm populations, gravid adults were bleached to collect embryos [181]. During bleaching, the hermaphrodites degrade and leave only embryos, which are then collected. After washing with sterile 1X M9 salt solution [182], the embryos are isolated and shaken slowly overnight in a flask containing M9 buffer to allow them to hatch. Synchronized L1s were plated onto either NGM with OP-50 or HGM with NA22 plates as needed. Synchronized L1s were used in RNA-seq, IF, and

54

larval development assays. After synchronization, L1s were grown to L3 or adult as needed per assay.

2.6.4 *Auxin Treatment*

Strains were subjected to auxin (Thermo Fisher Alfa Aesar Indol-3-Acetic Acid #A10556) by incorporation into NGM or HGM plates. A final concentration of 4mM diluted in ethanol was added to 1L of media, as described in [155,183]. Auxin-containing plates were maintained in the dark at 4°C for up to a month.

2.6.5 *Assay of viability upon auxin exposure initiated during embryogenesis*

L4 hermaphrodites were placed on an auxin-containing plate to ensure all embryonic development occurs while exposed to auxin. Plates were maintained in the dark at 20°C. Worms were placed on plates with or without auxin for an egg-laying period of 24 hours. After this period, the adult was removed from the plate, and the embryos laid were counted. 24 hours later, the number of dead larvae and dead embryos were quantified. Live adults were counted 3 days after the initial egg-laying period. Three independent replicates were performed. Differences were evaluated using Fisher's exact test comparing the numbers of dead and live progeny for each genotype.

2.6.6 *Assay of viability upon auxin exposure initiated during larval development*

Experiments testing larval development began with synchronized L1 larvae. The synchronized population was resuspended in M9 and split evenly between an auxin plate and a plate without auxin for 3 days. Worms surviving after three days were counted. Assuming an equal number of larvae initially plated, the final counts are reported as a ratio of survival on auxin to survival off auxin. Three independent

replicates were performed. Differences were evaluated using a Chi-square test comparing the number of surviving worms on auxin to the number surviving off auxin of each genotype.

2.6.7 *Brood Count Assay*

Young adult hermaphrodites were allowed to lay eggs on NGM and moved to new plates each day until fertilized embryos were no longer produced. For each plate, after the removal of the parent, the number of embryos laid was counted, and after 24 hours, the number of dead embryos was counted. After 3 days of development, the number of surviving adults was counted. We quantified the adult viability by comparing the number of surviving adults after 3 days of development to the initial number of embryos. Brood counts

2.6.8 *Immunofluorescence (IF)*

Hermaphrodite worms were dissected in 1x sperm salts (50 mM Pipes pH 7, 25 mM KCl, 1 mM MgSO$_4$, 45 mM NaCl, and 2 mM CaCl$_2$) and fixed in 4% paraformaldehyde (PFA) diluted in 1X sperm salts on a glass slide for 5 minutes in a humid chamber containing PBS-T (PBS with 0.1% and Triton X-100). Slides were frozen on dry ice for at least 20 minutes with a 20x20 mm coverslip over the diluted PFA and dissected *C. elegans*. Using a razor blade, the coverslip was removed by flicking the coverslip off the slide. The slides were then washed in PBS-T 3 times for 10 minutes each. 30µL of diluted primary antibody was applied to each slide, and a piece of parafilm was placed over the spot with the antibody to slow evaporation. The slides were incubated in a humid chamber at room temperature overnight. Slides were

washed in PBS-T 3 times for 10 minutes and stained with corresponding secondary antibodies diluted 1:100 in PBS-T at 37°C for 1 hour. Three more washes in PBS-T were completed after the secondary antibody incubation. In the third wash, the nucleus was stained using DAPI diluted in PBS-T for 10 minutes at room temperature. Slides are mounted in Vectashield (Vector Labs).

2.6.9 *Fluorescence in situ Hybridization (FISH)*

Degenerate Primer PCR was used to amplify purified yeast artificial chromosomes (YACs) containing sequences corresponding to regions of the X chromosome and then labeled with dCTP-Cy3 alongside standard nucleotides using random priming as in [136,184]. The X paint FISH probe generated this way covers about 90% of the X. Adult hermaphrodites were dissected on glass slides in 1x sperm salts and fixed in 4% PFA. After 5 minutes of fixation, the specimen was covered with a 20x20 coverslip and placed on dry ice for at least 20 minutes. The coverslip was then flicked off the slide with a razor blade. Slides were washed in PBS-T three times and subjected to an ethanol series of increasing concentrations (70%, 80%, 90%, 100% EtOH) for 2 minutes each, after which the slides were air dried. To each slide, 10uL of X paint probe was added and incubated at 37°C overnight. The next day, the slides were washed in a 39°C water bath in 2x SSC/50% formamide three times, in 2X SSC solution three times for 5 minutes each, then in 1x SSC once for 10 minutes, followed by a room temperature wash in 4x SSC. DAPI was included in the final 4x SSC wash, and slides were mounted using Vectashield. DAPI was excluded in the final 4X SSC wash for FISH followed by IF, after which IF was performed as described above.

2.6.10 *Microscopy*

Microscopy was performed using an Olympus BX61 microscope and a 60X APO oil immersion objective. Images were taken with a Hamamatsu ORCA-ER High-Resolution Monochrome Cooled CCD (IEEE 1394) camera. 3D images of nuclei were captured using 0.2-micrometer Z-spacing. The nuclei presented in this study are from intestinal cells. To observe signal depletion, exposure times were standardized to wild type.

2.6.11 *Analysis of X Volume*

Z-stacked images of intestinal nuclei of hermaphrodites were trimmed to 10-15 slices at 0.2 µM apart to include only planes with nuclear signals. Background signal was subtracted in ImageJ Fiji with a rolling ball radius of 50 pixels. After splitting the channels, the 3dManager from the 3dSuite plugin was used to create a three-dimensional ROI of the DAPI signal and a three-dimensional ROI of the FISH signal in the Cy3 channel [185]. The area of the Cy3 channel ROI inside the DAPI ROI was then compared in the 3dSuite 3DManager to find the X chromosome volume in the nucleus. The mask for the X chromosomes was limited to the area that overlaps with the DAPI mask signal, ensuring that the quantifications do not include non-specific staining of X paint FISH. The volume of the nucleus occupied is a ratio of the X signal relative to the DAPI signal measured in voxels (volumetric pixels). The proportion of the X signal overlapping with the nuclear volume also normalizes the amount of signal to nuclear size.

2.6.12 *Three-Zone Assay*

A mask containing all the X chromosome (X paint FISH) signals within the nucleus (DNA, DAPI) across a single plain near the center of intestinal nuclei in adult hermaphrodites. The background was subtracted in ImageJ FIJI with a rolling ball radius of 50 pixels. Using the native ROI manager in ImageJ FIJI, the threshold of the DAPI mask was used to draw three concentric ellipses that formed three zones of equal area in the nucleus. The Cy3 signal overlap with each zone was calculated using the ROI Manager to return the X chromosome FISH signal percentage in each zone.
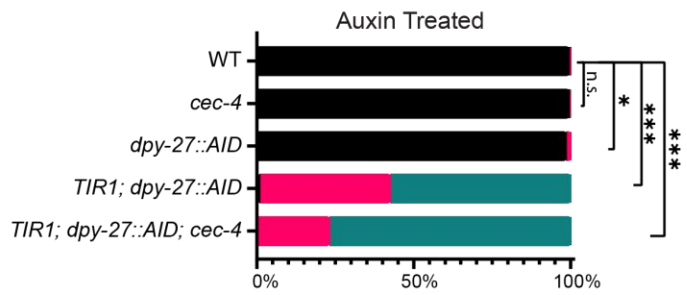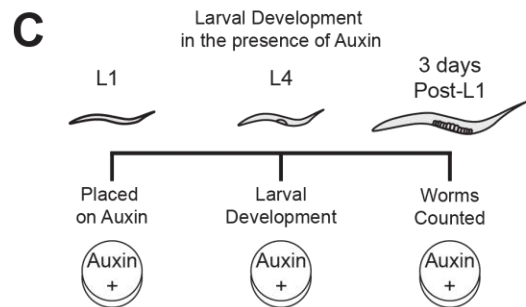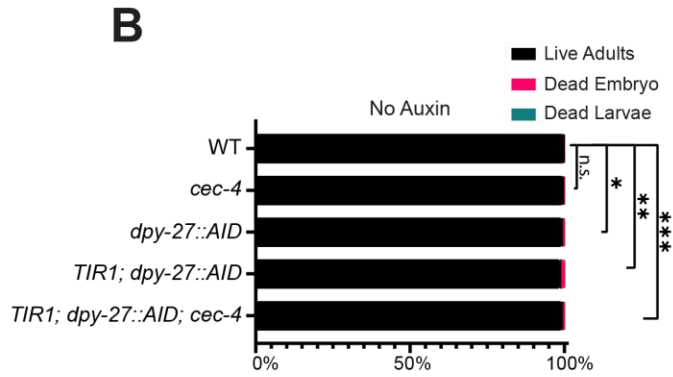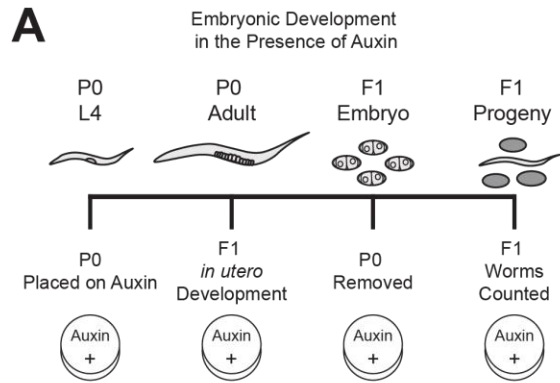
2.6.13 *mRNA-seq*

Synchronized L1s were placed on HGM plates with or without auxin and NA22 [186]. 24-hours later, L3 larvae were collected in M9. After pelleting, excess M9 was removed, and the remaining pellet was snap-frozen in liquid nitrogen with 1mL of Trizol. RNA was extracted and cleaned from the collected *C. elegans* using Qiagen RNeasy Kit. Reads were trimmed for quality use. Poly-A enrichment, library prep, and next-generation sequencing were conducted in the Advanced Genomics Core at the University of Michigan. RNA was assessed for quality using the TapeStation or Bioanalyzer (Agilent). Samples with RINs (RNA Integrity Numbers) of 8 or greater were subjected to Poly-A enrichment using the NEBNext Poly(A) mRNA Magnetic Isolation Module (NEB catalog number E7490). NEBNext Ultra II Directional RNA Library Prep Kit for Illumina (catalog number E7760L) and NEBNext Multiplex Oligos for Illumina Unique dual (catalog number E6448S) were then used for library prep. The mRNA was fragmented and copied into first-strand cDNA using reverse transcriptase and random primers. The 3' ends of the cDNA were then adenylated, and adapters were ligated. The PCR products were purified and enriched to create the final cDNA library. Qubit hsDNA
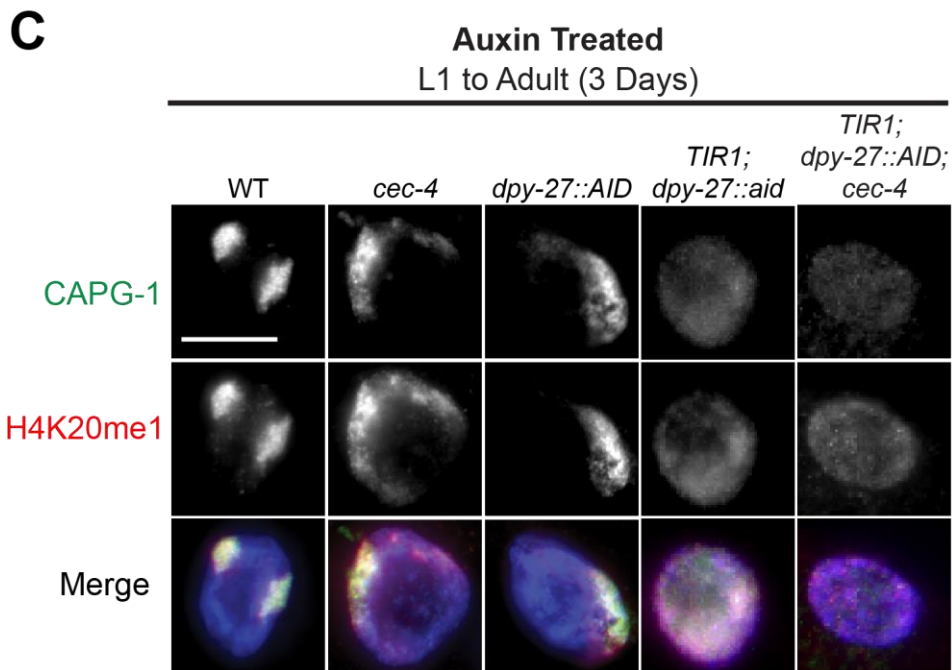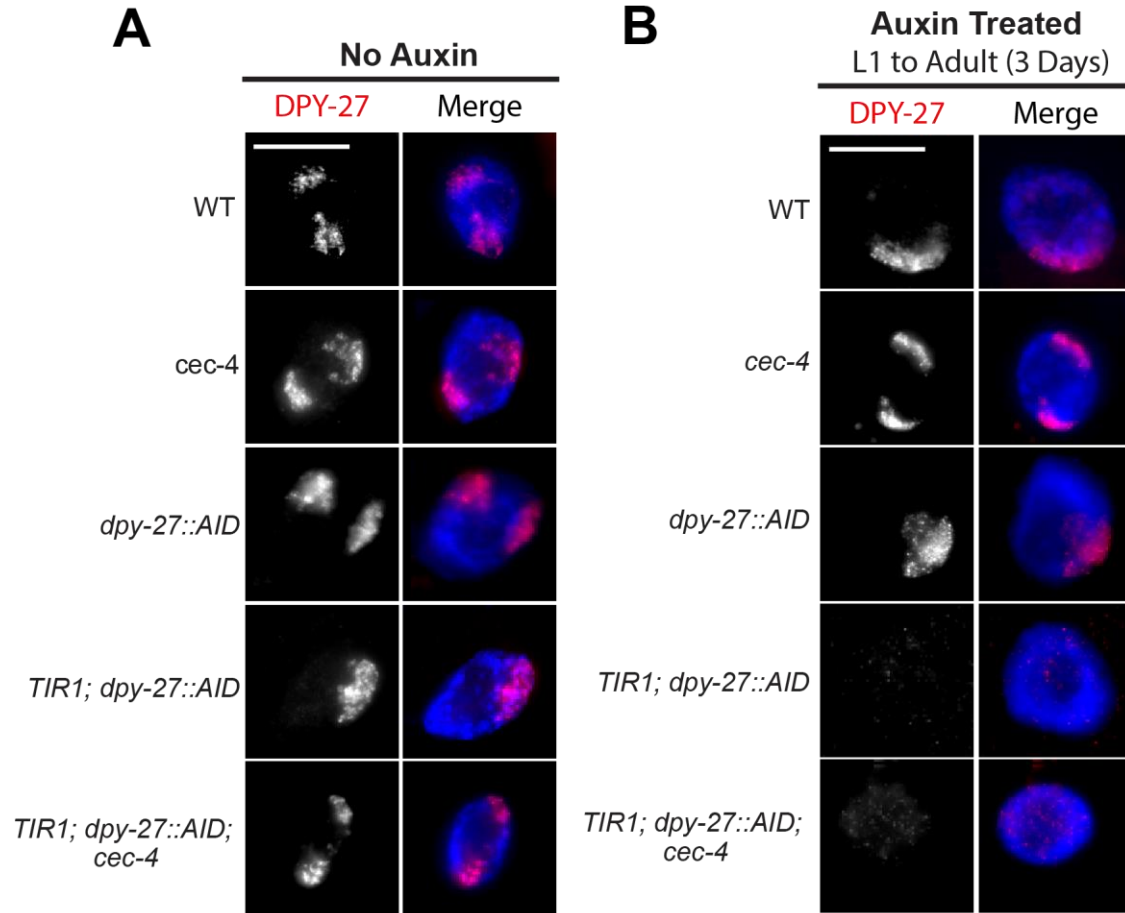
(Thermofisher) and LabChip (Perkin Elmer) checked the final libraries for quality and quantity. The samples were pooled and sequenced on the Illumina NovaSeqX 10B paired-end 150bp, according to the manufacturer's recommended protocols. BCL Convert Conversion Software v4.0 (Illumina) generated de-multiplexed Fastq files. The reads were trimmed using CutAdapt v2.3. FastQC v0.11.8 was used to ensure the quality of data [187,188]. Reads were mapped to the reference genome WBcel235, and read counts were generated using Salmon v1.9.0 [189]. Differential gene expression analysis was performed using DESeq2 v1.42.0 [190]. Downstream analyses were performed using R scripts and packages.
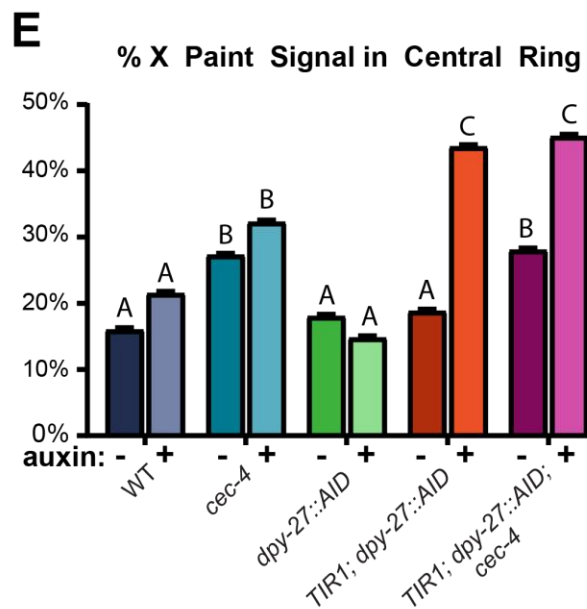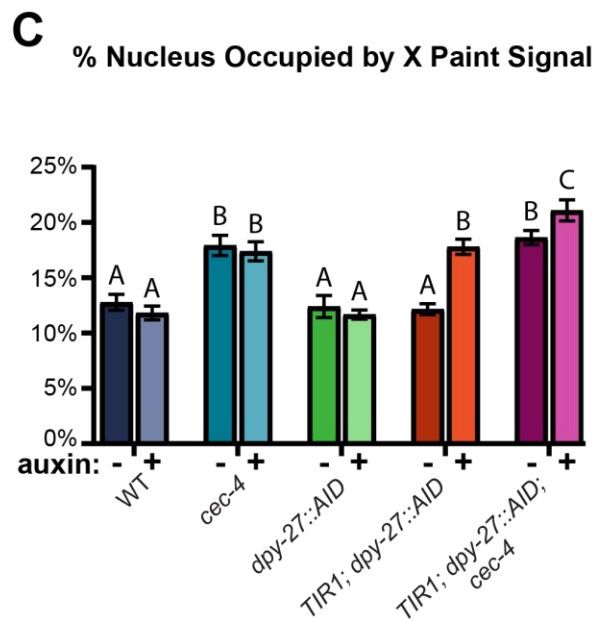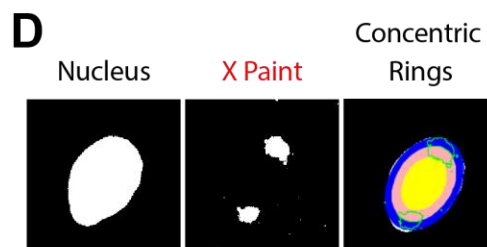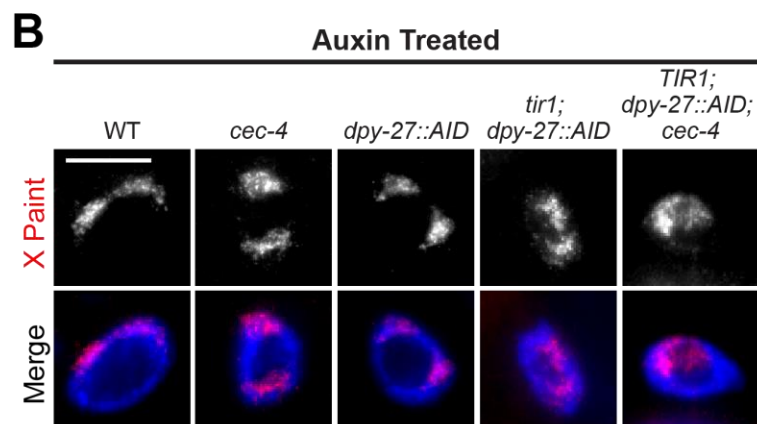
2.7 Figures

A Embryonic Development in the Presence of Auxin

B

No Auxin

Auxin Treated

C Larval Development in the presence of Auxin

E Survival after 3 Days on Auxin (Auxin/No Auxin)

D
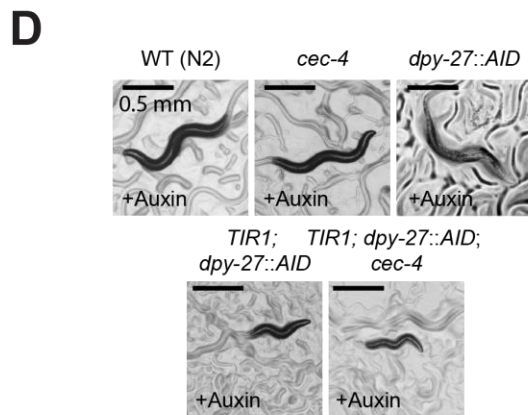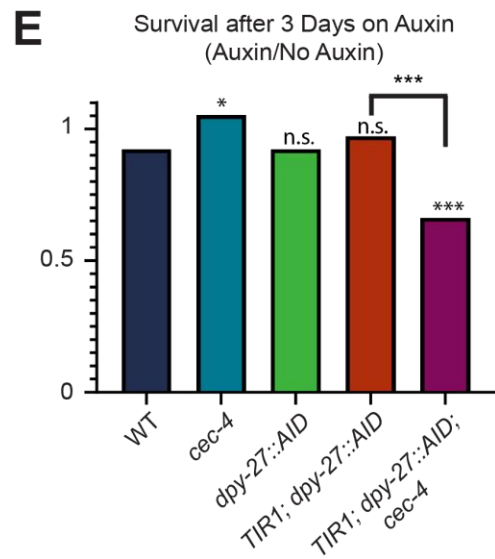
Figure 2.1. Depleting DPY-27 using the auxin-inducible degradation (AID) system leads to lethality and developmental defects in hermaphrodites. (A) Overview of the timeline of auxin exposure initiated from parental age L4 to F1 embryogenesis. **(B)** Survival outcomes upon auxin exposure throughout embryogenesis result in compromised viability in *TIR1; dpy-27::AID* and *TIR1; dpy-27::AID* strains, as indicated by significant differences in the dead embryo and dead larvae counts. Significance was determined by Student's t-test relative to wild-type values. Dead embryos and dead larvae were summed as one value for statistical analy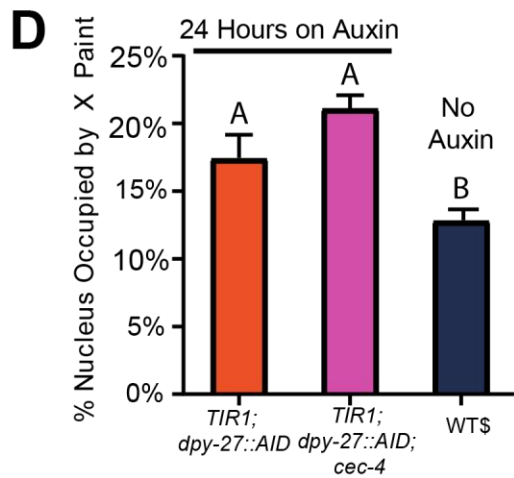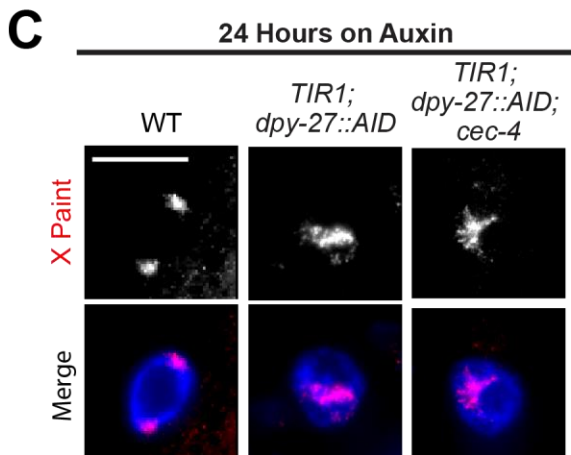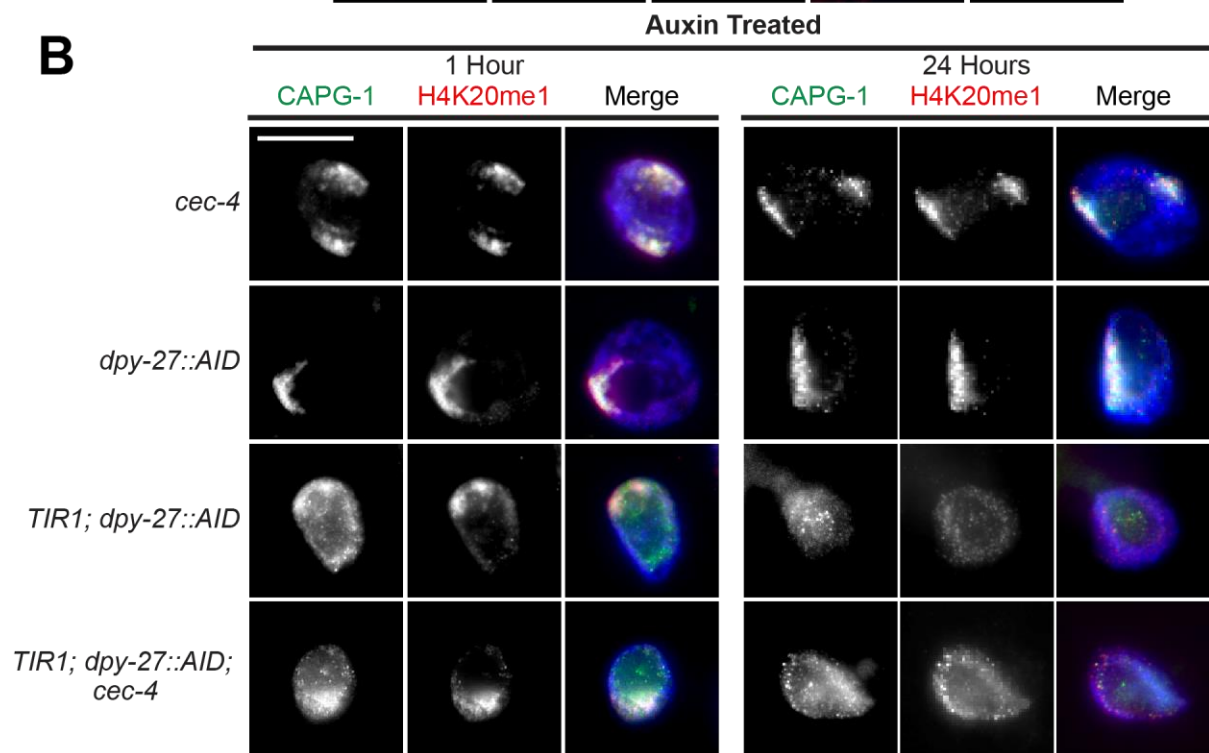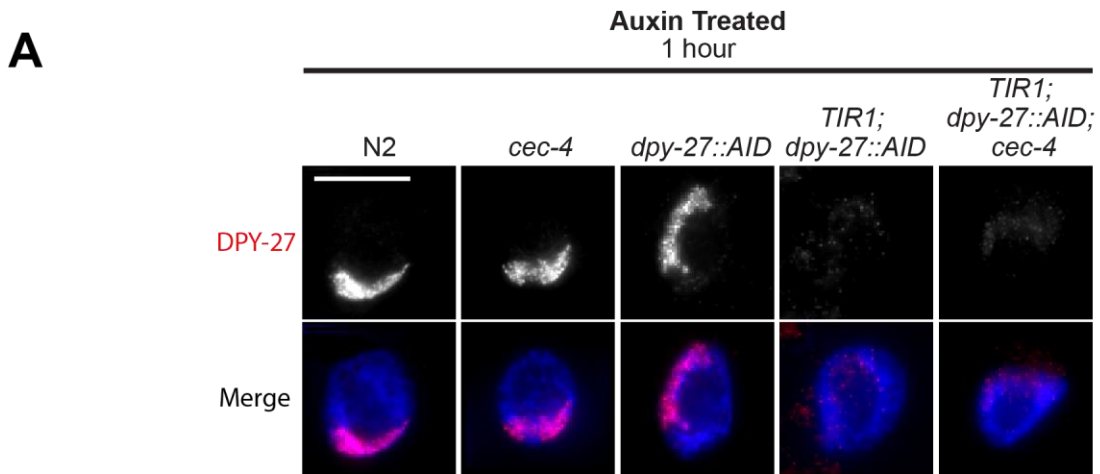ses. The n of progeny counted was at least 463. A complete statistical analysis can be found in **Table 2.1**. **(C)** Overview of the timeline of auxin exposure from the L1 stage for three days. N2 worms in this time frame grow to young adults (24 hours post-L4 adults. Subsequent assays of auxin treatments began and are. **(D)** Phenotypic images of hermaphrodites exposed to auxin from the L1 stage for three days. Scale bar, 0.5 mm. **(E)** Larval survival on auxin relative to survival off auxin. Synchronized L1 larvae were split into equal aliquots, and results are reported as a ratio of surviving adults on auxin compared to those without auxin exposure. Statistical significance represented in the figure is the value compared to WT (N2) (n.s., p>0.05). Complete statistical analyses can be found in **Table 2.2**. Significance was determined by a chi-squared test for variance (p<0.05).

A No Auxin

	DPY-27	Merge
WT		
cec-4		
dpy-27::AID		
TIR1; dpy-27::AID		
TIR1; dpy-27::AID; cec-4		

B Auxin Treated
L1 to Adult (3 Days)

	DPY-27	Merge
WT		
cec-4		
dpy-27::AID		
TIR1; dpy-27::AID		
TIR1; dpy-27::AID; cec-4		

C Auxin Treated
L1 to Adult (3 Days)

	WT	cec-4	dpy-27::AID	TIR1; dpy-27::aid	TIR1; dpy-27::AID; cec-4
CAPG-1					
H4K20me1					
Merge					

Figure 2.2 Auxin treatment leads to depletion of DPY-27, loss of DCC binding to the X, and disruption of the X-enrichment of H4K20me1 (A) Immunofluorescent staining of DPY-27 within the intestinal nuclei of young adult hermaphrodites (24-hours post-L4 adults) is depicted in the left columns. DAPI staining of DNA (blue) is overlayed with DPY-27 signal (red) in the columns to the right. Representative images show that DPY-27 is present within the nuclei in strains not exposed to auxin. **(B)** Over three days, exposure to auxin from L1 to adulthood significantly depletes the DPY-27 signal (red) by immunofluorescence in strains that express *TIR1*. **(C)** DPY-27 depletion from synchronized L1 for three days leads to loss of CAPG-1 localization and H4K20me1 enrichment on the X. CAPG-1 (top row, green), H4K20me1 (middle row, red), and a merged image of all three channels, including DAPI DNA staining (bottom row, blue), are shown. **(A-C)** Scale bars, 10 μm.

A No Auxin

WT | cec-4 | dpy-27::AID | TIR1; dpy-27::AID | TIR1; dpy-27::AID; cec-4

X Paint

Merge

B Auxin Treated

WT | cec-4 | dpy-27::AID | tir1; dpy-27::AID | TIR1; dpy-27::AID; cec-4

X Paint

Merge

D Nucleus | X Paint | Concentric Rings

C % Nucleus Occupied by X Paint Signal

E % X Paint Signal in Central Ring

A No Auxin

WT | cec-4 | dpy-27::AID | TIR1; dpy-27::AID | TIR1; dpy-27::AID; cec-4

X Paint

Merge

B Auxin Treated

WT | cec-4 | dpy-27::AID | tir1; dpy-27::AID | TIR1; dpy-27::AID; cec-4

X Paint

Merge

D Nucleus | X Paint | Concentric Rings

C % Nucleus Occupied by X Paint Signal

E % X Paint Signal in Central Ring

Figure 2.3 The continued presence of DPY-27 is required for X compaction and peripheral localization within the nucleus. (A) Adult hermaphrodite intestinal nuclei were stained with whole X chromosome paint FISH probe (top row, red), and DNA was labeled with DAPI (blue). Representative images are from young adult 24-hour post-L4 hermaphrodites not exposed to auxin. **(B)** X chromosome paint 3D FISH was performed in intestinal cells of synchronized hermaphrodites exposed to auxin from L1 for three days. **(C)** Quantifications of the X chromosome paint FISH signal volume normalized to nuclear size (n = 20 nuclei). Hermaphrodites grown without auxin are indicated by a - (bars on the left), and auxin-treated worms are designated by a + (bars on the right). For a complete statistical analysis, see **Table 2.3** (D). A singular slice from the middle of an intestinal nucleus demonstrates three-zone assay segmenting. ImageJ defined the boundaries of the nucleus (DAPI) and the X chromosome paint signal (left and center image, respectively). The nucleus was then divided into three concentric circles: peripheral (blue), intermediate (pink), and center (yellow). The amount of X signal (outlined in green) in each ring was quantified. **(E)** The proportion of the whole chromosome X paint signal seen in the center of the nucleus was quantified (n = 20 nuclei). Values for only the central ring are reported as a representation of the degree of relocating the X chromosome away from the periphery of the nucleus. Relocation to the center of the nucleus is increased in auxin-treated *TIR1* mutants. Hermaphrodites grown without auxin are indicated by a = (bars on the left), and auxin-treated worms are designated by a + (bars on the right). For complete statistical analysis, see **Table 2.4. (A-B)** Scale bars, 10 µm. **(C, E)** Values sharing the same letter are considered statistically similar (n.s. = p>0.05). Distinct letters indicate significant differences between the corresponding values (significant difference = p<0.05) as determined by Student's t-test. Error bars indicate the standard error of the mean. Complete signal analyses in all concentric rings can be found in **Table 2.3**.
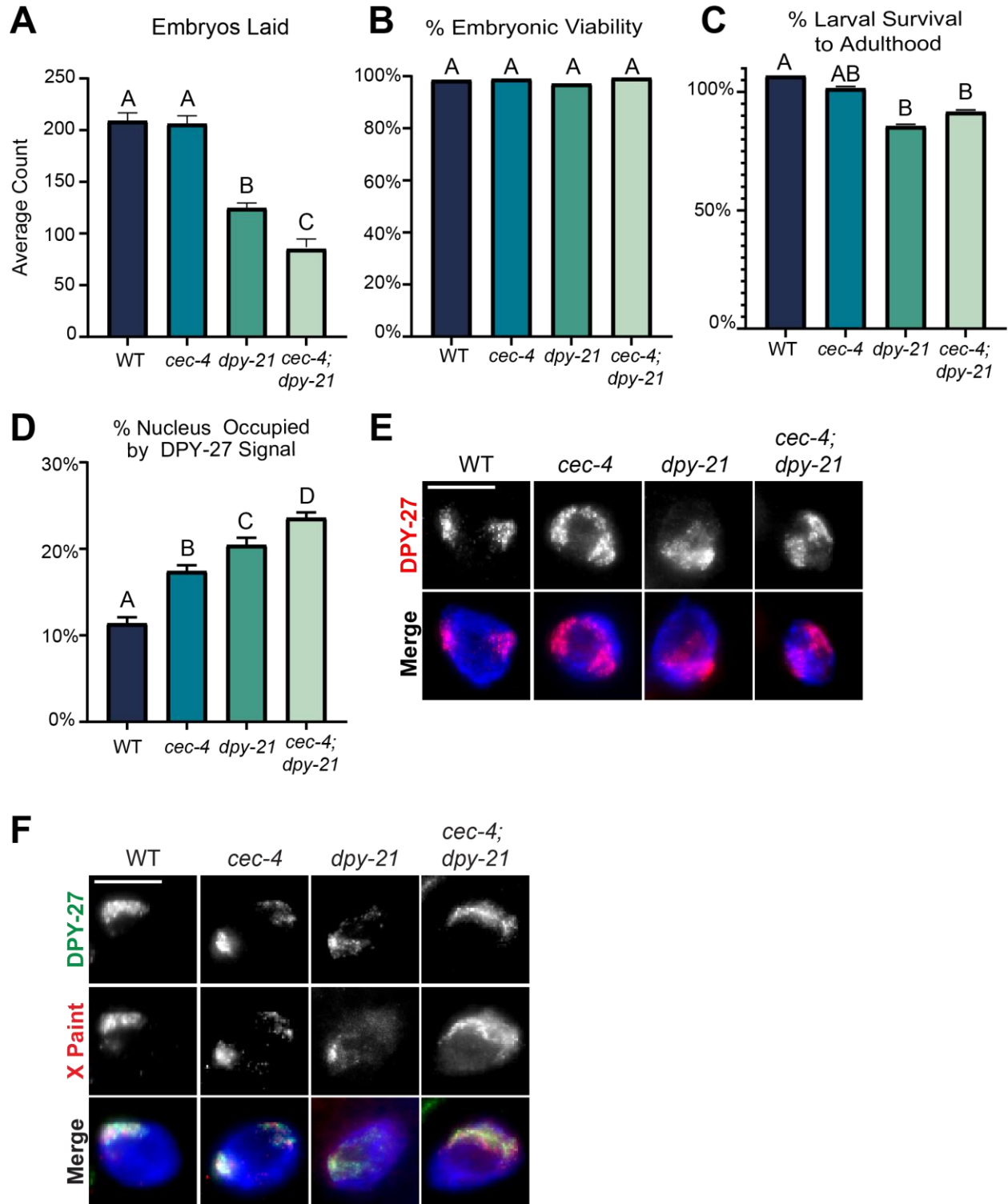
A

Auxin Treated
1 hour

| | N2 | *cec-4* | *dpy-27::AID* | *TIR1;*
dpy-27::AID | *TIR1;*
dpy-27::AID;
cec-4 |

DPY-27

Merge

B

Auxin Treated

| | 1 Hour | | | 24 Hours | | |
| | CAPG-1 | H4K20me1 | Merge | CAPG-1 | H4K20me1 | Merge |

cec-4

dpy-27::AID

TIR1; dpy-27::AID

TIR1; dpy-27::AID;
cec-4

C

24 Hours on Auxin

| WT | *TIR1;*
dpy-27::AID | *TIR1;*
dpy-27::AID;
cec-4 |

X Paint

Merge

D

24 Hours on Auxin

% Nucleus Occupied by X Paint

TIR1;
dpy-27::AID

TIR1;
dpy-27::AID;
cec-4

WT$

Figure 2.4 Rapid depletion of DPY-27 leads to a subsequent gradual loss of CAPG-1 and H4K20me1 enrichment on the X. (A) Young adult hermaphrodites were exposed to auxin for one hour before dissection, fixation, and IF staining for DPY-27 (red) and DNA (DAPI, blue). DPY-27 signal was significantly depleted in *TIR1; dpy-27::AID* and *TIR1; dpy-27::AID; cec-4* strains **(B)** Immunofluorescent analysis of young adult hermaphrodites using antibodies for CAPG-1 (green) and H4K20me1 (red) after auxin exposure for one hour (columns on the left) and 24 hours (columns on the right). **(C)** X paint FISH (red) staining of adult *TIR1; dpy-27::AID* and *TIR-1; dpy-27::AID; cec-4* after 24-hours of auxin exposure. **(D)** Quantification of the 3D volume of the nucleus occupied by the X paint FISH signal. Student's t-test determined significance. Values sharing the same letter are not significantly different. WT data is repeated from Fig 3C ($). Error bars indicate the standard error of the mean. **(A-D)** Scale bars, 10 μm. See **Table 2.3** for complete statistical analysis.
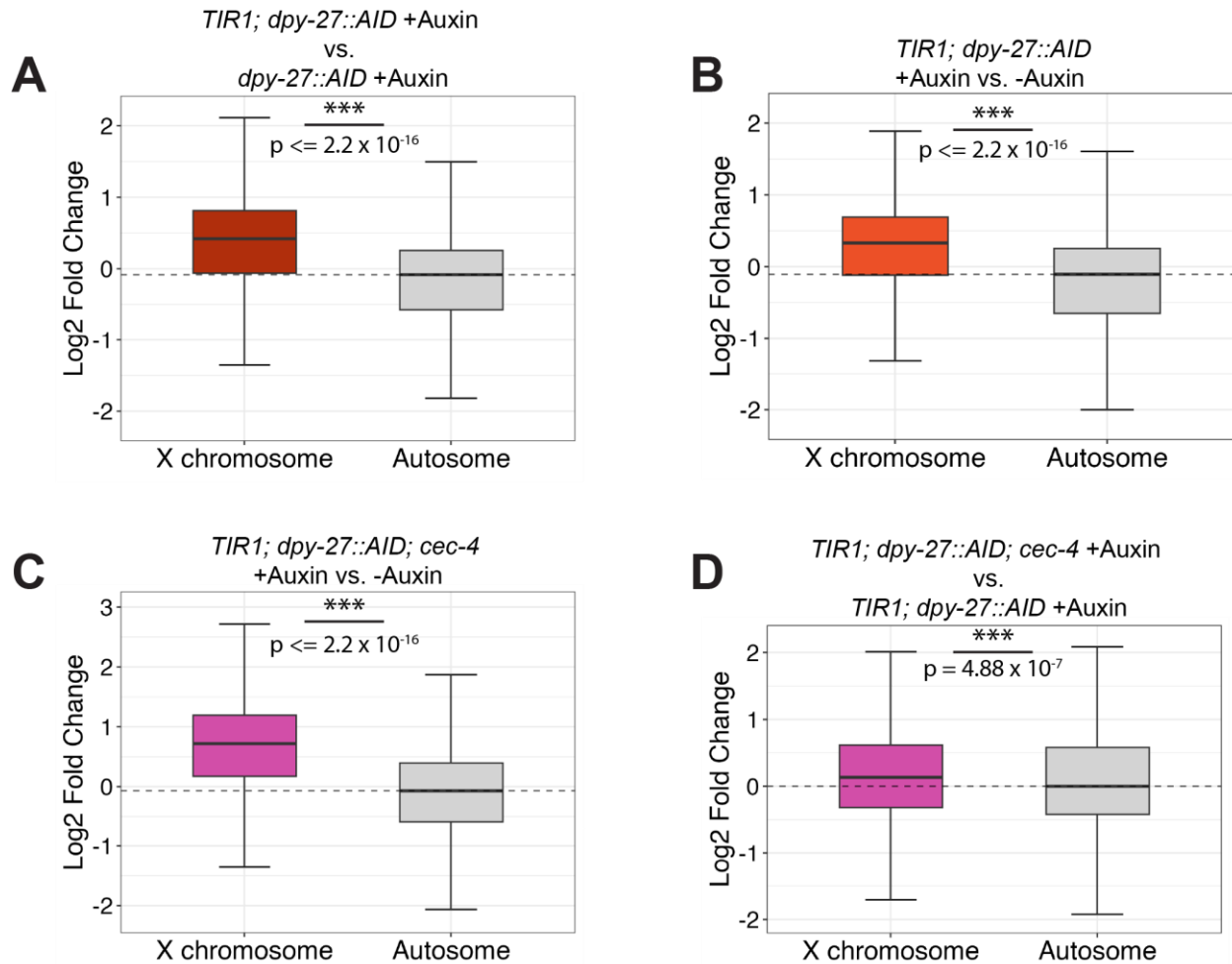
Figure 2.5 The X-linked gene expression is derepressed in strains depleted of DPY-27 during larval development. (A-D) Boxplots depicting the distribution of the expression of the X-linked genes and expression of the autosomal genes. Gene expression is plotted as the log2 ratio of the strains being compared. A Wilcoxon rank-sum test was used to determine the statistical significance of the differential gene expression between the X and autosomes. (n.s. = not significant, * = $p < 0.05$, ** = $p < 0.01$, *** = $p < 0.001$) **(A)** The log2 fold change in gene expression of the autosomes and the X chromosomes of *TIR1; dpy-27::AID* relative to the *dpy-27::AID* after both strains were exposed to auxin (X derepression of 0.502). **(B)** *TIR1; dpy-27::AID* treated with auxin compared to the same genotype grown without auxin (X derepression of 0.435). **(C)** *TIR1; dpy-27::AID; cec-4* treated with auxin was compared to no auxin treatment. **(D)** *TIR1; dpy-27::AID; cec-4* compared to *TIR1; dpy-27::AID,* both treated with auxin (X derepression of 0.13). See **Table 2.5** for complete statistical analysis.

A Embryos Laid

B % Embryonic Viability

C % Larval Survival to Adulthood

D % Nucleus Occupied by DPY-27 Signal

E

F

Figure 2.6 Loss of CEC-4 exacerbates dosage phenotypes caused by mutations in dpy-21.(A) Total average lifetime brood counts are reported (n = 6-8 hermaphrodites). **(B)** The percentage of the average embryo that hatched after 24 hours (unhatched embryo after 24 hours/total embryo). A mutation in *dpy-21* decreases the number of average brood size. The double mutant, *cec-4; dpy-21*, yields the smallest brood. Error is reported as the standard error of the mean (n = 6-8 hermaphrodites). See **Table 2.6** for complete statistics. **(C)** The percentage of the average embryo that survived to adulthood. The few embryos laid by the *cec-4; dpy-21* strain can survive to adulthood but at a frequency lower than that of the wild type. The error is reported as the standard error of the mean (n = 6-8 hermaphrodite broods). **(D)** The extent of X chromosome decompaction was assessed by quantifying the percentage of overlap between DPY-27 and DNA (DAPI stain). Error was calculated by standard deviation (n = 20). See **Table 2.7** for a complete statistical analysis. **(E)** Representative images of adult hermaphrodite intestinal nuclei IF stained for DPY-27 (left column, red) and DNA (DAPI, blue). **(F)** DPY-27 (green) co-localizes to the X signal (red) in all assayed strains. **(E, F)** Scale bar, 10 μm. **(A-D)** Values sharing the same letter are considered not statistically significantly different (n.s. = p>0.05). Distinct letters indicate significant differences between the corresponding values (p<0.05, Student's t-test).
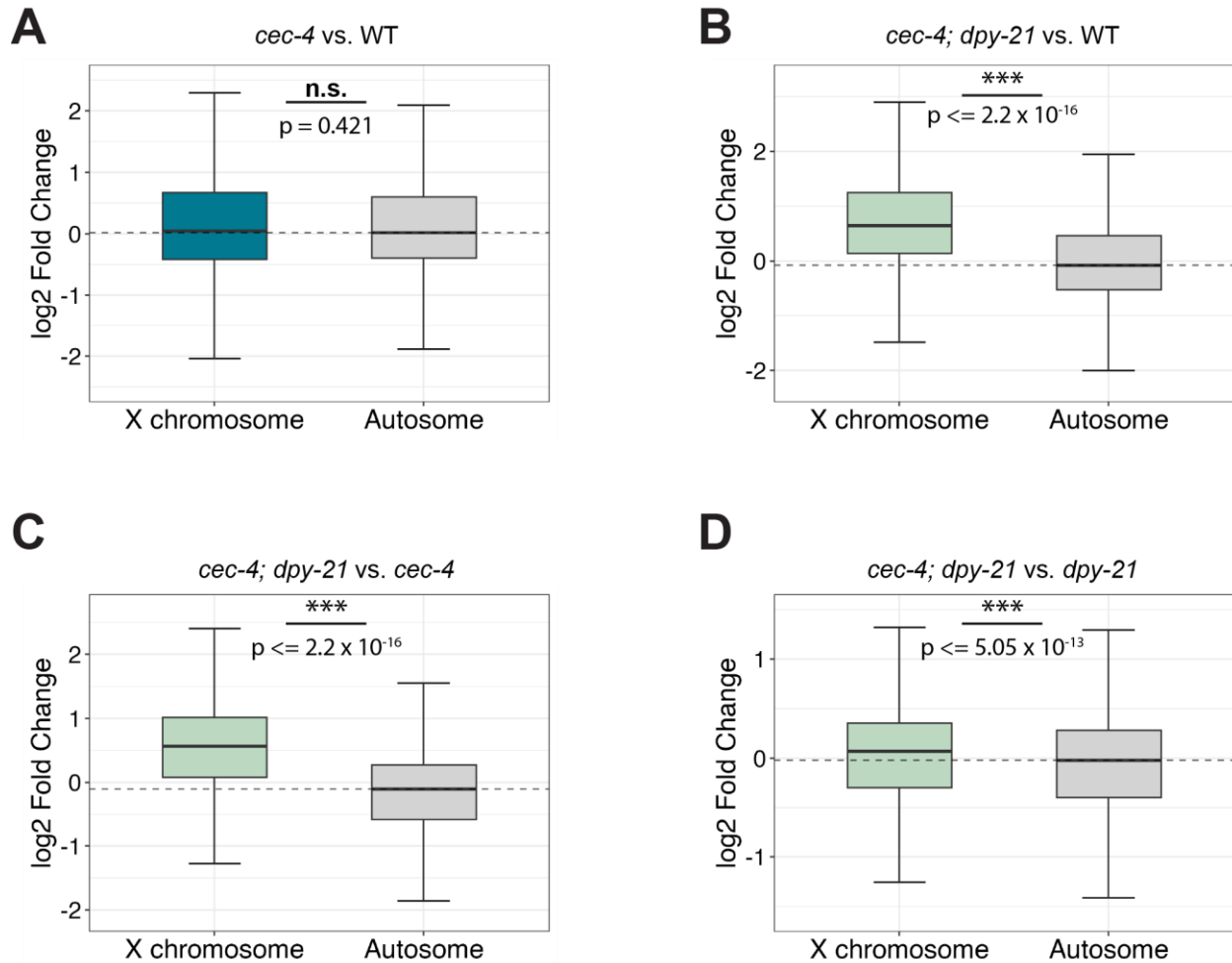
Figure 2.7 Loss of CEC-4 exacerbates gene expression defects caused by mutations in *dpy-21*. (A-D) Boxplots depicting the distribution of the expression of X-linked genes and expression of genes on autosomes. Gene expression is plotted as the log2 ratio of the strains being compared. Statistical significance is determined by the differences in gene expression between the X and autosomes by a Wilcoxon rank-sum test. (n.s. = not significant, * = $p < 0.05$, ** = $p<0.01$, *** = $p < 0.001$) **(A)** The log2 fold change in gene expression of the autosomes and the X chromosomes in the *cec-4* mutant relative to the wild type (N2). The difference is not significantly different ($p = 0.421$). **(B)** The log2 fold change in gene expression of the autosomes and the X chromosomes relative to *cec-4; dpy-21*. The double mutant, *cec-4; dpy-21*, has a significantly upregulated X chromosome relative to the wild type (X derepression of 0.721). **(C)** The log2fold change in gene expression of the X and autosomes of *cec-4; dpy-21* compared to cec-4. The X to autosomal difference in gene expression is significantly different (X derepression of 0.669). **(D)** Log2 fold change in gene expression of *cec-4; dpy-21* compared to *dpy-21* alone. The derepression of the X chromosome genes is significantly different from autosomes (X derepression of 0.09). See **Table 2.5** for complete statistical analysis.
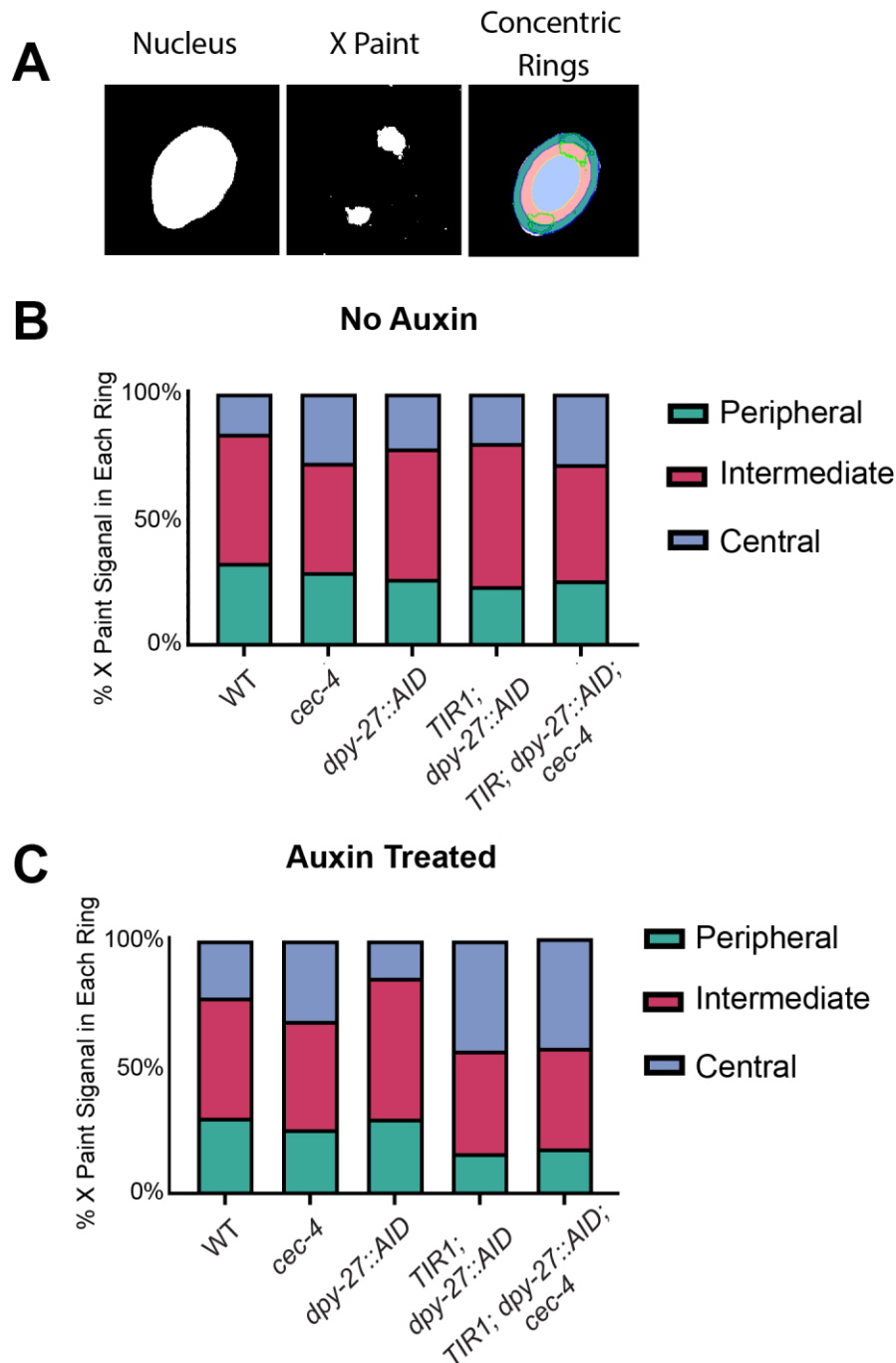
Figure 2.8 Comparison of all rings from the concentric circle analysis of X localization within the nucleus with and without auxin treatment. (A) Three-zone assay segmenting demonstrated by a singular slice from the middle of an intestinal nucleus. ImageJ defined the boundaries of the nucleus (DAPI) and the X chromosome paint signal (left and center image, respectively). The nucleus was then divided into three concentric circles: peripheral (green), intermediate (pink), and center (light blue). The amount of X signal (outlined in green) in each ring was quantified. **(B)** Three-zone assay for the X paint FISH signal (n = 20 nuclei) in strains grown without auxin. **(C)** Three-zone assay for the X paint FISH signal (n = 20 nuclei) in strains grown with auxin. **(B-C)** See **Table 2.4** for complete statistical analysis.
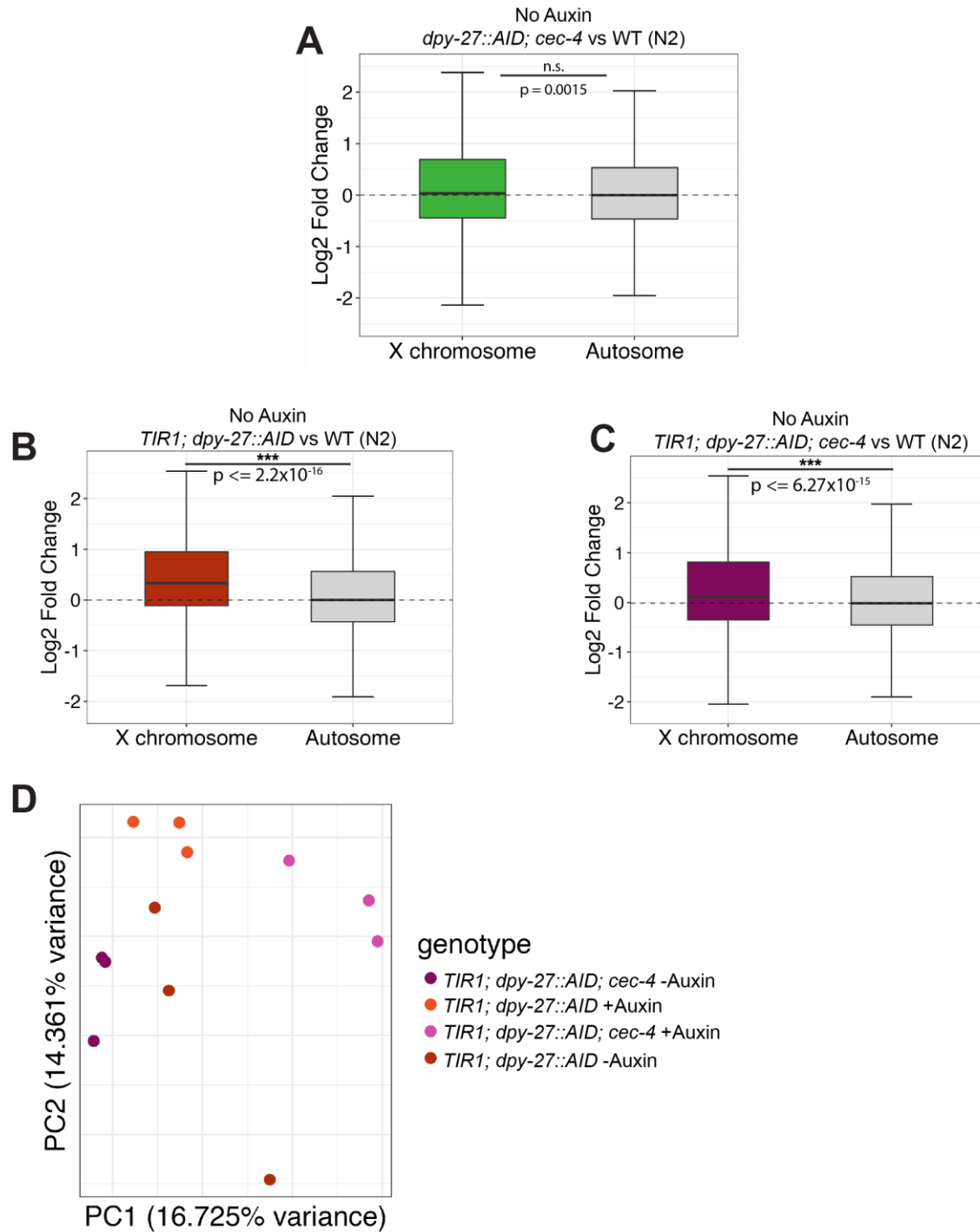
Figure 2.9 Principal component analysis (PCA) of mRNA-seq data. (A-C) Boxplots depicting the distribution of the expression of X-linked genes and expression of genes autosomes. Gene expression is plotted as the log2 ratio of the strains being compared. Statistical significance is determined by the differences in gene expression between the X and autosomes by a Wilcoxon rank-sum test. (n.s. = not significant, * = p < 0.05, ** = p<0.01, *** = p < 0.001) **(D)** Principal component analysis (PCA) plot depicting the relationships among wild-type, *TIR1; dpy-27::AID*, *TIR1; dpy-27::AID; cec-4*. Auxin treatment is indicated alongside the corresponding genotype in the figure.

74
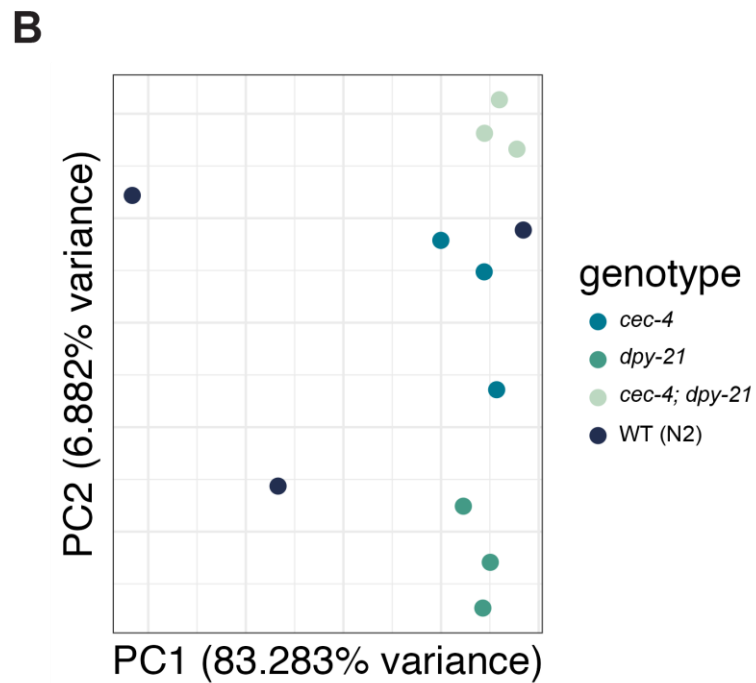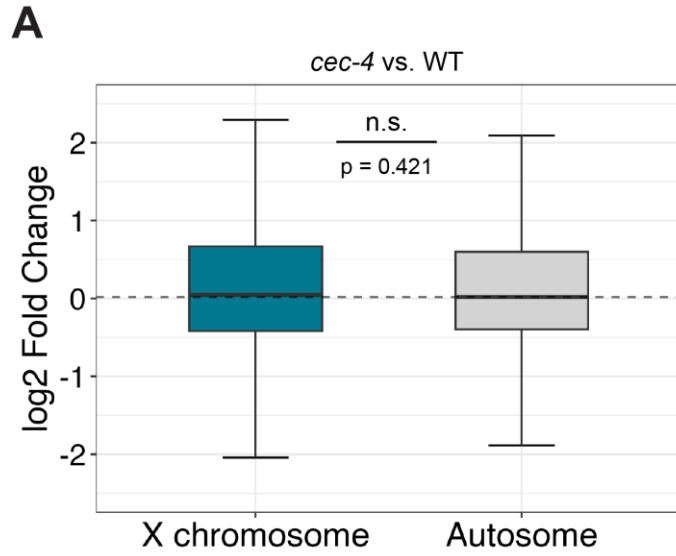
Figure 2.10 RNA seq analysis of *cec-4* and *dpy-21* mutants. Principal component analysis (PCA) plot depicting the relationships among wild-type, single mutants (*cec-4 and dpy-21*), and double mutants (*cec-4; dpy-21*) based on gene expression profiles.

2.8 Tables

Raw numbers

no auxin

Genotype	Dead Larvae	Dead Embryo	Live Adults	total progeny	dead progeny
N2	0	3	897	900	3
cec-4	0	9	873	882	9
dpy-27::AID	0	14	876	890	14
TIR1; dpy-27::AID	0	13	622	635	13
TIR1; dpy-27::AID; cec-4	0	18	611	629	18
auxin					
Genotype	Dead Larvae	Dead Embryo	Live Adults	total progeny	dead progeny
N2	0	6	1132	1138	6
cec-4	0	5	1216	1221	5
dpy-27::AID	0	13	886	899	13
TIR1; dpy-27::AID	266	193	4	463	459
TIR1; dpy-27::AID; cec-4	534	161	0	695	695

Statistics Fisher's exact test (dead progeny vs live adults)

no auxin   p values

	vs N2	*vs cec-4*	*vs dpy-27::AID*	*vs TIR1; dpy-27::AID*
N2				
cec-4	0.0877			
dpy-27::AID	0.007	0.4019		
TIR1; dpy-27::AID	0.0015	0.1268	0.5562	
TIR1; dpy-27::AID; cec-4	<0.0001	0.0098	0.1487	0.3691
auxin				
	vs N2	*vs cec-4*	*vs dpy-27::aid*	*vs TIR1; dpy-27::AID*
N2				
cec-4	0.7674			
dpy-27::AID	0.0374	0.0146		
TIR1; dpy-27::AID	<0.0001	<0.0001	<0.0001	
TIR1; dpy-27::AID; cec-4	<0.0001	<0.0001	<0.0001	0.0254

Statistics Fisher's exact test (dead larvae vs dead eggs)

auxin	*vs N2*	*vs cec-4*	*vs dpy-27::AID*	*vs TIR1; dpy-27::AID*
N2				
cec-4	NA			
dpy-27::AID	NA	NA		
TIR1; dpy-27::AID; cec-4	NA	NA	NA	
TIR1; dpy-27::AID; cec-4	NA	NA	NA	0.0001

Table 2.1 Comparison of embryonic and larval survival in strains on and off auxin. Fisher's exact test determined statistical significance.

Raw numbers

Genotype	Totals surviving worms from 3 replicates		auxin/no auxin ratio
	no auxin	auxin	
N2	1018	939	0.92
cec-4	1230	1296	1.05
dpy-27::AID	1244	1149	0.92
TIR1; dpy-27::AID	688	669	0.97
TIR1; dpy-27::AID; cec-4	1158	768	0.66

Statisctics (Chi square tests)

p values

Genotype	vs N2	vs cec-4	vs dpy-27::AID	dpy-27::AID
N2				
cec-4	0.027236			
dpy-27::AID	0.984043	0.021022		
TIR1; dpy-27::AID	0.455269	0.233107	0.449346	
TIR1; dpy-27::AID; cec-4	< .00001	< .00001	< .00001	< .00001

Table 2.2 Larval survival to adulthood on and off auxin. A Chi-squared test of homogeneity determined statistical significance.

Raw numbers

Genotype	Auxin +/-	avg. X volume (%)	STDEV	SEM	n
N2	No auxin	12.79	3.18	0.71	20
cec-4	No Auxin	17.92	4.59	0.92	25
dpy-27::AID	No Auxin	12.41	4.46	1.00	20
TIR1; dpy-27::AID	No Auxin	12.15	2.22	0.50	20
TIR1; dpy-27::AID; cec-4	No Auxin	18.64	2.89	0.65	20
N2	3 days	11.68	2.77	0.62	20
cec-4	3 days	17.39	4.12	0.86	23
dpy-27::AID	3 days	11.68	1.87	0.42	20
TIR1; dpy-27::AID	3 days	17.79	3.07	0.69	20
TIR1; dpy-27::AID; cec-4	3 days	21.10	4.32	1.02	20
TIR1; dpy-27::AID	24 hours	17.47	6.15	1.71	13
TIR1; dpy-27::AID; cec-4	24 hours	21.07	4.91	1.00	24

Statistics (Student's t-test)

p values		No auxin					auxin (3days)				
		N2	cec-4	dpy-27::AID	TIR1; dpy-27::AID	TIR1; dpy-27::AID; cec-4	N2	cec-4	dpy-27::AID	TIR1; dpy-27::AID	TIR1; dpy-27::AID; cec-4
no auxin	vs N2		6.74E-05	0.75562	0.4660192	4.51E-07	0.310317	0.00018	0.188603	1.11E-05	4.8E-08
	vs cec-4			0.000207	2.896E-06	0.529426	2.25E-06	0.67402	5.4E-07	0.909422	0.021845
	vs dpy-27::AID				0.8205883	9.44E-06	0.621375	0.00052	0.509213	9.04E-05	2.53E-07
	vs tir1;dpy-27::AID					2.05E-09	0.679808	7.2E-06	0.474735	1.15E-07	5.16E-09
	vs tir1;dpy-27::AID; cec-4						3.78E-09	0.25435	2.18E-10	0.377156	0.041693
auxin 3 days	vs N2							5.7E-06	0.854547	1.45E-07	2.86E-09
	vs cec-4								1.24E-06	0.717501	0.006632
	vs dpy-27::AID									1.36E-08	2.12E-09
	vs tir1;dpy-27::AID										0.008593
	vs TIR1; dpy-27::AID; cec-4										

p values		no auxin	auxin (24 hr)	
		N2	TIR1; dpy-27::AID	TIR1; dpy-27::AID; cec-4
no auxin	vs N2		0.022088	4.49E-08
auxin	vs tir1;dpy-27::AID			0.08295
24 hr	vs tir1;dpy-27::AID; cec-4			

Table 2.3 Comparison of X decondensation in strains exposed to auxin for 1 hour, 24 hours, and 3 days. Statistical significance was compared using Student's t-test. The standard deviation and standard error of the mean calculated error.

78

Proportion of X in each concentric circle

- Auxin	N2	cec-4	dpy-27::AID	TIR1; dpy-27::AID	TIR1; dpy-27::AID; cec-4
Peripheral	32.78%	27.89%	29.82%	23.46%	25.65%
Intermediate	51.28%	43.54%	52.19%	57.79%	46.38%
Central	15.94%	28.57%	17.99%	18.75%	27.98%
N	21	19	20	19	20
+ Auxin	N2	cec-4	dpy-27::AID	TIR1; dpy-27::AID	TIR1; dpy-27::AID; cec-4
Peripheral	30.86%	25.31%	29.52%	15.85%	15.69%
Intermediate	47.68%	42.84%	55.74%	40.54%	39.15%
Central	21.46%	31.85%	14.74%	43.60%	45.16%
N	19	20	20	20	19

Statistics for localization in the central zone

- Auxin	N2	cec-4	dpy-27::AID	TIR1; dpy-27::AID	TIR1; dpy-27::AID; cec-4
ST DEV	0.16025019	0.139307423	0.114844992	0.098487136	0.164125996
SEM	0.03583303	0.031959315	0.025680121	0.022594499	0.036699688
+ Auxin	N2	cec-4	dpy-27::AID	TIR1; dpy-27::AID	TIR1; dpy-27::AID; cec-4
ST DEV	0.13314739	0.154569352	0.064341376	0.149390846	0.033404809
SEM	0.03054611	0.034562758	0.014387169	0.185737642	0.042611137

p values (Student's t-test)

No auxin

vs	N2	cec-4	dpy-27::AID	TIR1; dpy-27::AID	TIR1; dpy-27::AID; cec-4
N2		0.011225541	0.639763193	0.504326575	0.02260643
cec-4			0.014220262	0.017318706	0.904147543
dpy-27::AID				0.824890003	0.032428736
TIR1; dpy-27::AID					0.040131653
TIR1; dpy-27::AID; cec-4					

Auxin

vs	N2	cec-4	dpy-27::AID	TIR1; dpy-27::AID	TIR1; dpy-27::AID; cec-4
N2		0.030363956	0.057293639	1.98173E-05	7.68772E-05
cec-4			0.000109775	0.01920441	0.02057291
dpy-27::AID				2.16027E-08	8.37394E-07
TIR1; dpy-27::AID					0.776183586
TIR1; dpy-27::AID; cec-4					

Auxin vs no Auxin

	N2	cec-4	dpy-27::AID	TIR1; dpy-27::AID	TIR1; dpy-27::AID; cec-4
	0.24192932	0.500559915	0.278621206	5.92653E-07	0.004228738

Table 2.4 Concentric ring analysis, "3-zone assay", for X localization within the nucleus. Statistical significance was compared using Student's t-test. The standard deviation and standard error of the mean calculated error.

	Median log2 fold change on A	Median log2 fold change on X	difference (X-A)	p-value
cec-4 vs N2	0.0177784	0.04480026	0.02702185	0.421
dpy-21 vs N2	-0.04555933	0.5674185	0.6129778	< 2.2e-16
cec-4; dpy-21 vs N2	-0.07518271	0.6464376	0.7216203	< 2.2e-16
cec-4; dpy-21 vs cec-4	-0.1039192	0.5652231	0.6691423	< 2.2e-16
cec-4; dpy-21 vs dpy-21	-0.02000659	0.07085425	0.09086083	5.05E-13
TIR1; dpy-27::AID +auxin vs tir-1; dpy-27::AID -auxin	-0.1069557	0.3289617	0.4359175	< 2.2e-16
TIR1; dpy-27::AID +auxin vs dpy-27::AID +auxin	-0.08351502	0.4192456	0.5027606	< 2.2e-16
TIR1; dpy-27::AID; cec-4 +auxin vs tir-1; dpy-27::AID; cec-4 -auxin	-0.06942255	0.7181707	0.7875932	< 2.2e-16
TIR1; dpy-27::AID; cec-4 +auxin vs TIR1-1; dpy-27::AID +auxin	0	0.1309671	0.1309671	4.88E-07
cec-4 +auxin vs cec-4 -aux	-0.01026743	0.02368716	0.03395459	1.61E-11
dpy-27::AID -auxin vs N2	0	0.03444444	0.03444444	0.001599
TIR1; dpy-27::AID -auxin vs N2	-0.004027541	0.3347476	0.3347476	< 2.2e-16
TIR1; dpy-27::AID; cec-4 -auxin vs N2	0.0127948	0.1214531	0.1342479	6.27E-15

Table 2.5 Comparisons of differential gene expression as determined by mRNA-seq. The Wilcoxon rank-sum test determined the p-value.

Average counts

	N2	cec-4	dpy-21	cec-4; dpy-21
N	8	6	7	7
embryos laid	208.88	206.50	124.57	69.86
ST DEV	61.00	62.54	24.89	45.95
SEM	21.57	25.53	9.41	17.37
embyonic viability	0.986	0.990	0.971	0.994
ST DEV	0.013	0.014	0.049	0.010
SEM	0.005	0.006	0.018	0.004
Larval viability	1.068	1.015	0.826	0.916
ST DEV	0.092	0.117	0.151	0.104
SEM	0.033	0.048	0.057	0.039

Student's T-test (embyos laid), p values

Genotype	N2	cec-4	dpy-21	cec-4; dpy-21
N2				
cec-4	0.944650674			
dpy-21	0.005400028	0.022066832		
cec-4; dpy-21	0.000248063	0.001623698	0.021238593	

Student's T-test (embryonic viability)

Genotype	WT (N2)	cec-4	dpy-21	cec-4; dpy-21
N2				
cec-4	0.607865361			
dpy-21	0.463083774	0.364824379		
cec-4; dpy-21	0.215523365	0.55930081	0.268519163	

Student's T-test (larval viability)

Genotype	N2	cec-4	dpy-21	cec-4; dpy-21
N2				
cec-4	0.384456218			
dpy-21	0.00439616	0.026952961		
cec-4; dpy-21	0.011363235	0.137966294	0.220189019	

Table 2.6 shows Total lifetime brood counts and survival to adulthood. Statistical significance was compared using Student's t-test. Error was calculated by the standard deviation and standard error of the mean.

Genotype	n	Avg of X/nucleus volume	ST DEV	SEM
N2	20	11.38	3.36	0.75
cec-4	20	17.41	3.28	0.73
dpy-21	20	20.43	4.00	0.90
cec-4, dpy-21	20	23.56	3.07	0.69

Student's T-Test	P Val.
N2 vs cec-4	<0.0001
N2 vs dpy-21	<0.0001
cec-4 vs dpy-21	0.0131
cec-4 vs cec-4 dpy-21	<0.0001
dpy-21 vs cec-4 dpy-21	0.0084

Table 2.7 X occupancy in the nucleus measured by whole X-paint FISH relative to nuclear volume.

Chapter 3

Conclusions and Future Directions

In many organisms, sex is determined by the genetic content of allosomes. While this chromosome-based sex determination is common, variations in chromosome count are generally not well tolerated and can lead to disease, if not outright lethality [191]. To address this, dosage compensation has evolved in many organisms to mitigate the detrimental effects of chromosomal discrepancies while still allowing for sex determination based on these differences. Although the goal of dosage compensation in organisms utilizing the chromosome-based sex system is similar, the mechanism of achieving this varies [56–58].

This study explored dosage compensation in the nematode *C. elegans*. In this organism, the XX hermaphrodites downregulate both of their X chromosomes to equalize X-linked gene expression to levels expressed in XO males. We utilized this system to further the understanding of dosage compensation and study chromosome-wide gene regulation via histone modifications, nuclear lamina interactions, and a specialized condensin complex.

The significance of the condensin I^{DC} and accessory proteins within the dosage compensation complex is apparent in regulating X-linked genes on the hermaphrodite X, balancing expression to levels to what is measured in males [133]. While this highlights the crucial role of the condensin I^{DC}, the mechanisms orchestrating global

83

Downregulation across the entire hermaphrodite X chromosome by half is not fully understood. Furthermore, prior studies did not address the necessity of a dosage compensation mechanism during the maintenance phase of regulating X-linked gene expression. My thesis work aimed to explore how condensin I^{DC} and DCC-dependent dosage compensation processes contribute to X-linked gene regulation during the maintenance phase of dosage compensation. The data in this dissertation contributed to understanding dosage compensation in *C. elegans* during a period of development where most cells are post-mitotic. To address our questions, we utilized the auxin-inducible degron (AID) system to conditionally deplete DPY-27 as well as genetic mutants for *cec-4* and *dpy-21*. This concluding chapter will discuss findings in relation to other studies and propose additional experiments to expand upon our results.

3.1.1 *DPY-27 is Required During Embryonic Development for Hermaphrodite Survival*

Current knowledge places the loading of the complete DCC to the X around the 26-40 cell stage of embryogenesis [67,192]. Additionally, prior studies identified the requirement for the condensin I^{DC} subunit DPY-27 in the viability of hermaphrodites, specifically during the 30-cell to comma stage of embryonic development, as demonstrated using a cold-sensitive allele of *dpy-27* [116]. In these experiments, cold-sensitive mutants exposed to a lower temperature rendered DPY-27 non-functional. When placed at lower temperatures around the 30-cell stage, hermaphrodite specific lethality resulted. It is worth noting, however, that the viability of this strain before exposure to low-temperature was reported at 20%, making it not ideal for quantifying lethality as a baseline for the necessity of DPY-27 [116]. While previous investigations

have explored the essential role of DPY-27 during the initiation of dosage compensation, we aimed to use contemporary methodologies to define precisely when DPY-27 is essential during varying stages of development.

Our study reaffirmed the role of condensin I^{DC} in embryonic development by employing targeted depletion of DPY-27 during embryogenesis by the auxin-inducible degron system. The loss in hermaphrodite viability of DPY-27 depleted strains was observed in our data, which agrees with observations in past research. At the onset of dosage compensation, *C. elegans* hermaphrodites must decrease X gene production to continue to develop. However, our assay depleted DPY-27 throughout the entirety of embryonic development and did not specifically look at individual developmental stages. The timing for dosage compensation onset is confirmable by carefully administered auxin exposure in *TIR1; dpy-27::AID*.

3.1.2 *Additional Auxin-Inducible degron Assays to Interrogate the Developmental Timeline for the Requirement of DPY-27*

The modern auxin-inducible degron system is a powerful tool that directly depletes proteins of interest temporally and spatially efficiently in *C. elegans.* Using the auxin-inducible degron system can facilitate the understanding of when DPY-27 is necessary for embryonic survival. Evidence shows that the auxin molecule can penetrate the eggshell and the cuticle of *C. elegans*, providing a distinct advantage over RNAi. Additionally, the auxin-degron system targets proteins, whereas RNAi will only deplete mRNA while the protein remains [155]. Standard RNAi methods require worms to feed on bacteria containing double-stranded RNA (dsRNA) specific to the gene of interest or microinjection of dsRNA [193]. Furthermore, RNAi may not be sufficient for

the depletion of lowly expressed genes, as many DCC members are during interphase [194]. Auxin treatment is easily administered to *C. elegans* in all life stages, including embryogenesis. Spatially, the *TIR1* transgene-containing strains with varying tissue-specific promoters allow for tissue-specific depletion of the protein of interest [155]. The AID system provides the means to interrogate the developmental requirement of condensin I^{DC}.

To investigate the viability of DPY-27 depleted strains in older embryos, auxin exposure coupled with live imaging can provide insights into the necessity of DPY-27 during later embryonic stages. By carefully staging embryos, development can be observed while embryos are depleted of DPY-27 by auxin exposure. Live imaging of *C. elegans* is possible on a thin pad of agarose placed on a glass slide. Adding auxin to the agarose pad will ensure the continuous delivery of auxin to the embryo. Cell divisions, or the lack of divisions, can be tracked throughout development. Additionally, the embryo can be rescued from the agarose pad, and the number of larvae that survive the larval stages can be evaluated. This experiment would not only lend to the understanding of dosage compensation during embryonic development but would also provide additional insight into the *in vivo* functions of condensin complexes.

3.1.3 *The Loss of DPY-27 Results in the Destabilization of the Condensin I^{DC} Ring from the X Chromosomes*

In this study, it is evident that the rapid degradation of DPY-27, as facilitated by the AID system, has significant consequences for the stability of the condensin I^{DC} complex on the X chromosome. Our observations, illustrated in **Fig 2.4A**, revealed visible changes in DPY-27 presence within an hour of auxin exposure. The subsequent

gradual depletion of CAPG-1, another condensin I^{DC} subunit, further supports the notion

of complex destabilization. This result indicates destabilization of the condensin I^{DC}

complex on the X chromosome. The signal for CAPG-1 appears diffuse throughout the

nucleus of DPY-27 depleted strains exhibiting a non-specific pattern of staining by 24

hours **(Fig 2.4B)**. This phenomenon aligns with findings in mitotic avian cells where the

depletion of the condensin protein SMC2 resulted in the loss of chromosomal

organization [161]. We speculate that the depletion of DPY-27 renders the condensin

I^{DC} ring incomplete, thus destabilizing the complex from the X chromosome.

3.1.4 *X Chromosome Condensation and Nuclear Lamina Tethering Potentiates Gene Repression by Bringing Repressive Mechanisms Closer Together Spatially within the Nucleus*

In our study, as well as in past research in our lab, we have shown that the

mutation in *cec-4* leads to significant decompaction of the X chromosome **(Fig 2.6D)**.

Despite this significant change in X composition, there is no change in autosomal gene

regulation [136]. Furthermore, the X chromosomes are slightly upregulated, but in our

study, this change was not significant **(Fig 2.7A)**. In our study, we observed that the

addition of a cec-4 mutation in the background of other dosage compensation-depleted

strains there was an additive influence on gene derepression on the X **(Fig 5.C** and **7B)**.

The lack of gene expression changes when there is a loss of *cec-4* despite the

chromosomal conformation change, suggesting that the role of the protein in dosage

compensation is indirect. Additionally, when generally considering the process of

dosage compensation in *C. elegans*, the primary mechanism is often regarded as

condensin I^{DC}. Our lab and others have demonstrated that condensin I^{DC} must load onto

the X to initiate and maintain X condensation [100]. However, I propose that despite the importance of nuclear lamina tethering of the X and X compaction, these are not repressive events. Rather, the compaction of the X chromosome is necessary for the spreading of repressive events across the X chromosomes in *C. elegans* hermaphrodites.

To test the hypothesis that condensation and nuclear lamina tethering serve as potentiators, several experiments could be conducted. First, employing Global Run-On Sequencing (GRO-seq) analysis would allow for the assessment of transcriptional activity on the X chromosome and autosomes in wild-type, *cec-4*, and *TIR1; dpy-27::AID* auxin-treated mutant backgrounds, providing insight into nascent RNA synthesis and transcriptional changes.

3.1.5 *Looking beyond the necessity of DPY-27 in maintaining condensin I^{DC} on the X chromosome*

It is currently unknown whether certain complex members bear more functional weight in stabilization. Further experiments are needed to confirm the necessity of each condensin I^{DC} subunit in stabilizing the complex on the X chromosome. To conduct this assay, adding the auxin-degron tag will provide the means to deplete the subunits individually. The non-DPY-27 condensin I^{DC} protein subunits are shared between the condensin I and condensin I^{DC} complexes. Therefore, the loss of these by means other than auxin degradation may prove difficult due to the entanglement with the cross-functioning with condensin I. Incorporating auxin exposure during larval stages in these experiments will provide a comprehensive understanding of the dynamic interactions

88

within the condensin I^{DC} complex and its subunits on the X chromosome. In addition to confirming the necessity of each condensin I^{DC} subunit, further exploration can delve into the temporal dynamics of subunit interactions during different developmental stages. Understanding whether certain subunits play more prominent roles at specific points in development could shed light on the nuanced regulation of the condensin I^{DC} complex. Additionally, investigating the consequences of individual subunit depletion on X chromosome morphology and gene expression patterns could provide valuable insights into the functional hierarchy within the complex. These experiments would provide further information about how condensin complexes maintain their associations with chromosomes and at what developmental time point they are necessary.

3.1.6 *Nuclear volume occupied by the X in males versus hermaphrodites*

In mammals, as well as *C. elegans*, changes in chromosome topology result in gene misregulation [136,195]. Due to this association, we measured the nuclear volume occupied by the X chromosomes. The singular male X chromosome encompasses 10% of the total genome, whereas the hermaphrodite X chromosomes make up 18% of the total DNA content in the nucleus [100]. In a previous publication, we showed that the proportion of the nucleus occupied by the singular male X chromosome alone was much more significant than expected, about 16%. These results imply that two X chromosomes have the potential of reaching a maximal occupancy of 32%. To observe the nuclear organization of the X chromosomes in hermaphrodites depleted of DPY-27, *cec-4*, and *dpy-21*, we utilized whole chromosome X paint fluorescent *in situ* hybridization (FISH) as well as immunofluorescent staining (IF). By IF for DPY-27, which colocalizes to the X, in *cec-4 and dpy-21* mutants, we observed the most

significant level of X volume within the nucleus at 24%. The caveat of this data is that the volume was quantified based on the protein DPY-27 rather than the X FISH signal as performed in the quantifications of the male X. Even so, we anticipated that both the depletion of DPY-27 and loss of *cec-4* function would cause massive X chromosome decompaction. Yet, the X FISH signal quantifications capped at a maximum of 21% of the nucleus occupied by two X chromosomes. Considering the male X occupancy level, we predict that two X chromosomes, when maximally decondensed, could occupy about 32% of the nucleus. Despite the X chromosomes in our dosage compensation, deficient hermaphrodites did not decompact to quite the extent of what is predicted based on the male X; the X chromosome volumes in this study are larger than we previously reported [136]. There is the potential that the X chromosomes in the hermaphrodites have hit a maximum level of decompaction that is also acceptable for permitting survival. This is supported by comparing our quantifications of X volume in our DPY-27 depleted and *cec-4* loss-of-function strains in Chapter 2 **(Fig 2.3C)**. Regardless of any combination of disruption to dosage compensation, there is no significant difference in the nuclear occupancy of the X. There are undoubtedly additional dosage compensation mechanisms yet unknown that could be maintaining the hermaphrodite X compaction.

3.1.7 *Depletion of DPY-21 in Combination with DPY-27*

In this study, we examined impaired dosage compensation by concurrently introducing loss-of-function mutations in *cec-4* and *dpy-21*. While we also combined *cec-4* mutation with DPY-27 depletion, we did not explore the effect of adding *dyp-21* loss of function in this background. Initially, we hypothesized that the loss of DPY-27 would coincide with the loss of DPY-21 on the X chromosome. Our results in **Fig 2.2C**

indicate there may be an impairment in DPY-21 after the depletion of DPY-27, as indicate by the decrease in H4K20me1 signal colocalization with the condensin I^{DC} subunit CAPG-1. However, this observation only indirectly provides insight into the role of DPY-21. As a result, further questions arise from our study. Future experiments should explore the role of H4K20me1 enrichment via DPY-21. Specifically, these experiments should be designed to answer whether the act of demethylation of H4K20me2/3 is the dosage compensatory event or if the presence of H4K20me1 itself is contributing to dosage compensation.

The contribution of H4K20me1 to dosage compensation mutations in set-4 and dpy-21 can be delineated using the same background. The knockout allele for *set-4* (n4600) is available via the *Caenorhabditis* Genetics Center. The protein SET-4 is a histone methyltransferase that modifies H4K20me to di- and trimethylation across all chromosomes. It was observed that H4K20me1 itself is not a downstream effector of dosage compensation [31]. However, there is more to uncover about the loss of H4K20me2/3 that does influence dosage compensation. By using double mutants for *dpy-21* and *set-4,* both the methylation of H4K20me2/3 and the demethylation process will be disabled. In these experiments, we would observe the viability of hermaphrodite progeny of these double mutants. Severe defects in dosage compensation result in hermaphrodite specific lethality. As in our data in **Fig 2.1A** and **Fig 2.1C**, we would expect a decrease in embryo laid by the *set-4; dpy-21* double mutants.

Both *set-4* and *dpy-21* have been shown to influence dosage compensation. In a prior study, via RNA-seq, a group observed X-specific gene upregulation [31]. However, this study did not investigate the nuclear architecture in *set-4, dpy-21* double mutants.

To further examine alterations in hermaphrodites lacking proper methylation states due to the absence of *set-4* and *dpy-21*, we propose utilizing immunofluorescence and fluorescent in situ hybridization techniques to evaluate the nuclear organization. Specifically, staining for histone modifications associated with H4K20me1/2/3 can elucidate the methylation status within the nucleus of adult hermaphrodites with the double mutation background. It is anticipated that the prevalent methylation state within the nucleus will be the H4K20me1 mark, albeit in a widespread manner. The expected methylation state that will be prevalent within the nucleus is the H4K20me1 mark but in a ubiquitous manner. These mutants should lack X-specific enrichment of H4K20me1. This is due to the ability of SET-1 to enrich H4K20me1 on chromosomes [130].

To add upon previous research on *set-1, set-4,* and *dpy-21* mutants, the addition of these mutant backgrounds, or RNAi-depletion of these genes, in addition to *TIR1; dpy-27::AID* treated with auxin can be used to further assess changes that occur in the absence of H4K20 methylation states. Replicating assessments seen in Chapter 2, such as strain viability post-DPY-27 depletion, analyzing nuclear organizational changes using fluorescent in situ hybridization targeting the X chromosome, and conducting subsequent RNA-seq analyses on these mutants can give information about how these processes interact. These combined experiments serve as initial steps toward unraveling the intricate interplay between H4K20 methylation dynamics and X chromosome gene repression.

3.1.8 *Nuclear Localization of the X and the Limitations of Fluorescent Microscopy*

Results from Chapter 2 revealed a threshold for maximal nuclear occupancy by the X for dosage compensation for defective hermaphrodites in our study. Yet we

observed substantial alterations in nuclear organization, evident in DPY-27 depleted strains. Reduction in DPY-27 levels led to a pronounced migration of X chromosomes toward the nuclear center. Without a proportional increase in X volume, this shift in X localization mirrors findings in avian cell lines depleted of a condensin subunit. In SMC2-depleted avian cells, X volume remained constant, but significant changes in surface area were noted in the absence of SMC2 [161]. Future investigations could benefit from employing confocal microscopy to enhance the resolution of nuclear organization and X-chromosome decompaction. Our 3D quantifications in this study faced limitations due to the challenge of accurate 3D observation. While we selected 10-15 slices per nucleus in our Z-stacked images, approximating the correct size for intestinal nuclei, the out-of-focus planes did not resolve as a closed spherical shape in fluorescent microscopy. Confocal microscopy offers a promising solution to overcome these limitations, allowing for a more accurate depiction of the complete 3D cellular structure [196]. Future experiments should utilize confocal microscopy for improved resolution in 2D (3-zone assay) and 3D quantifications (X volume).

3.1.9 *In strains depleted of DPY-27 during larval development, mRNA-seq revealed an increase in X-linked gene expression in hermaphrodites*

In this study, we conducted mRNA-seq analysis to investigate alterations in the regulation of X-linked genes following the depletion of DPY-27. Our experiments considered both the impact of the protein's reduction compared to strains with and without DPY-27 and the changes in expression levels compared to autosomes. Our strains depleted of DPY-27, *TIR1; dpy-27::AID,* and *TIR1; dpy-27::AID; cec-4* exhibited

an increase in X-linked gene expression. Notably, these increases in X gene expression are not accompanied by a change in autosomal gene expression.

Prior studies into the effects of DPY-27 depletion utilized either RNAi depletion or mutants maintained via a genetic balancer. A past study in our laboratory partially depleted DPY-27 by RNAi feeding of dsRNA at a stage where most cells in hermaphrodites are in interphase, similar to our study [136]. However, DPY-27 is not a highly expressed gene past early development. Thus, the effects of RNAi on DPY-27 are minimal, as intended in the article. In other studies, DPY-27 loss-of-function mutation was maintained as a heterozygote with a balancer chromosome. In this study, the progeny that did not have DPY-27 maternally or zygotically expressed were selected and analyzed by mRNA-seq [31]. To our surprise, our strains depleted of DPY-27 only during larval stages could reach similar levels of derepression of the X chromosome with a shorter developmental timeline in the absence of the protein.

The auxin-inducible degron system offers an abundance of opportunities for investigating protein function in *C. elegans*. However, since its development for worms in 2015 [155], it has become apparent, though unsurprising, that the system exhibits leaky activation of *TIR1*, and the AID tag itself hinders optimal protein function [158,159]. Consequently, protein depletion in the absence of auxin has been observed, consistent with our study results **(Fig 2.9A)**. Our experiment noted a significant change in X gene expression between wild-type and *TIR1; dpy-27::AID* off auxin, although not as severe as observed under auxin treatment. The notable difference in auxin presence underscores our study's ongoing value in understanding DPY-27 and X gene regulation in larvae. The specificity of the expression change, indicating exclusive X derepression,

suggests that DPY-27 must be depleted to some extent in *TIR1; dpy-27::AID* in the absence of auxin. To address this issue, future experiments can benefit from using the auxin-inducible degron 2 (AID2) system [197]. In this system, the basal degradation caused by *TIR1* was solved by replacing the gene with AtTIR1 in *C. elegans*. The authors that developed the AID2 system in *C. elegans* noted that AtTIR1 allowed lower doses of auxin to induce protein degradation, allowing them to study temporal functions of proteins of interest more precisely. To further improve the AID2 system, they also synthesized a form of auxin that includes an acetoxymethyl group (5-Ph-IAA). The addition of this group increased the efficacy of auxin penetrating the eggshell to induce protein depletion in *C. elegans* embryos [197]. The strains containing AtTIR1 and 5-PH-IAA were unavailable at the beginning of the study in this dissertation. However, the strains are now orderable from the *Caenorhabditis* Genetics Center, and 5-Ph-IAA is available from various sellers. Future studies will greatly benefit from applying the AID2 system to interrogating DPY-27 throughout the *C. elegans* life cycle.

3.1.10 *Dosage compensation sensitive genes*

C. elegans exhibits a unique mechanism of dosage compensation, whereby both X chromosomes in hermaphrodites are halved in expression to match that of a single X chromosome in males. Perturbations in various dosage compensation factors lead to different levels of lethality and gene derepression on the X chromosome. In our study, we generated multiple RNA-seq datasets from hermaphrodites with impaired dosage compensation resulting from genetic mutations or depletion of DPY-27 using the auxin-mediated degron system. Leveraging these datasets, we conducted comparative analyses of upregulated genes on the X across different genetic mutants and DPY-27

depletion strains. Subsequently, genes identified in these datasets were prioritized as potential candidates sensitive to dosage compensation. These genes are crucial for hermaphrodite viability and warrant further investigation for their role in dosage compensation regulation. Future experiments studying the functional roles of these genes in dosage compensation may expand upon our understanding of X gene regulation. The loss of cec-4 further sensitizes C. elegans hermaphrodites to the depletion of dosage compensation mechanisms

The chromodomain-containing protein, CEC-4, is known for contributing to cell fate as differentiation progresses [140]. The left arm of the X chromosome in *C. elegans* is enriched for the histone mark, H3K9me3, to which CEC-4 binds [136]. The mRNA-seq profile of *cec-4* mutants, especially in comparison to wild type, caught our attention. Although we noted a subtle increase in X-linked gene expression in *cec-4* mutant L1 larvae in a previous study in our lab [136], our current investigation did not find this change statistically significant when *cec-4* mutant L3 larvae were off auxin. However, when we exposed a population of *cec-4* mutants to auxin as a control, we observed a significant alteration in gene expression compared to the wild type. The variability among populations with the same *cec-4* mutant allele may stem from random variation or different developmental stages. While *cec-4* mutants can achieve a significantly higher level of X-linked gene expression than the wild type, the magnitude of this difference is so small that it might escape detection depending on biological replicates and experimental variations or may not be evident at every developmental stage. The minuscule nature of X derepression is consistent with the phenotype of *cec-4* mutants. The strain is relatively healthy and does not exhibit phenotypes associated with the loss

of dosage compensation. Nevertheless, our consistent observation remains: the loss-of-functional *cec-4* in strains depleted of DPY-27 markedly increases X-linked gene expression.

As mentioned previously, introducing *cec-4* into strains depleted of DPY-27 during larval development led to lethality. Notably, DPY-27 depletion alone during larval development did not induce lethality, and most nematodes survived for three days despite the absence of complete condensin I^{DC}. This outcome prompted an investigation into the mRNA-seq variations between populations with and without functional CEC-4. To examine this hypothesis, we introduced a mutation in the DCC subunit *dpy-21* into the *cec-4* mutant strain, creating a "double mutant." The strain exhibited compromised survival to adulthood, similar to DPY-27 depleted strains lacking *cec-4*. According to Student's T-test, the double mutant did not display a survival rate distinct from that of *dpy-21* single mutants. However, the brood size of the double mutant was significantly smaller than that of single mutants for *cec-4* and *dpy-21*. I hypothesize that the larvae capable of emerging from the embryo are the ones that survive to adulthood, giving the strain the appearance of a standard survival rate. As expected, adding *cec-4* mutation to d*py-21* loss-of-function strains caused a significant increase in X-linked gene expression. Given the additive effect observed in X-linked gene derepression within DPY-27 depleted hermaphrodite populations, our hypothesis posited that CEC-4 might similarly compound the negative influence on other dosage compensation mechanisms.

We believe that sensitization occurs from the combination of DPY-27 reduction and the loss of CEC-4 function. Without either of these processes, the X chromosome

97

decondenses and becomes centrally localized within the nucleus. The central region of the nucleus is considered a region of active transcription within the nucleus [198]. In addition to the X's relocation, the X's decompaction allows activating marks and transcriptional machinery to access the X chromosome. Together, the X chromosome is poised to become transcriptionally derepressed.

3.1.11 *H4K20me1 depletion after the loss of dpy-21 and dpy-27*

Progress in studies using *C. elegans* as a model organism has several dosage compensation mechanisms beyond condensin I^{DC}. One mechanism is interactions with the nuclear lamina via CEC-4, as mentioned previously [136]. Another DCC-mediated mechanism is the enrichment of H4K20me1 on the X [127]. The DCC subunit DPY-21 has recently emerged as a multi-functional complex component. When bound to the X chromosome, DPY-21 enriches the repressive mark H4K20me1 [124]. This localized enrichment of H4K20me1 on the X significantly contributes to the repression of X-linked genes in hermaphrodites [126]. Despite the discovery of these two dosage compensation processes and the increasing knowledge regarding their underlying mechanisms, there is still much to uncover about how these findings synergistically contribute to the overall dosage compensation mechanism.

An intriguing observation was made when considering the levels of H4K20me1 between auxin-treated and untreated samples. While H4K20me1 is typically abundant on the dosage-compensated X chromosomes of hermaphrodites, its decrease after DPY-27 depletion suggests a process that diminishes the presence of H4K20me1 on the X, thereby emphasizing the mark in other nuclear regions. This shift in H4K20me1 staining pattern could arise from either DPY-21 mislocalization onto other chromosomes

or failing to bind, thereby reducing H4K20me2/3 marks or the X becomes susceptible to methyltransferases or demethylases that modify H4K20me in the absence of DPY-21. Following through with the logic of the latter suggestion, we propose the hypothesis that DPY-27 prevents histone methyltransferases, such as SET-4, from binding to H4K20 throughout the worm's lifetime by maintaining the inaccessibility of the X to methyltransferases.

To determine the role of DPY-27 in the localization of DPY-21 and its implications for chromatin structure, an experiment assessing the subnuclear distribution of DPY-21 would be beneficial. Given the observed alterations in H4K20me1 patterns following DPY-27 depletion **(Fig 2C)**, it becomes pertinent to discern whether this is attributed to potential mislocalization of DPY-21 to non-X chromosomes or histone turnover depleting H4K20me1 enrichment on the X. Chromatin Immunoprecipitation followed by sequencing (ChIP-seq) of DPY-21 in *TIR-1; dpy-27::AID* strains treated with auxin could unveil its binding patterns. If DPY-21 is found to be associated with chromosomes other than the X post-DPY-27 depletion, it would suggest a crucial role of DPY-27 in preserving DPY-21 localization on the X and averting its interaction with other chromosomal regions. To test this, adding a mutant allele for *set-4* to the background of *TIR1*-expressing mutants or depleting *set-4* via RNAi after DPY-27 degradation could be explored. Immunofluorescence observations of changes in H4K20me1/2/3 distribution within the nucleus may offer valuable insights into the DCC's ability to repel gene-activating histone marks and proteins by preventing histone modifiers from accessing the X. Quantitative Western blotting for the H4K20me states will provide further insights into the histone mark's presence. These experiments will reveal the

functional roles of the DCC in preventing histone methyltransferases from accessing the X chromosomes in dosage compensated regions.

3.2 Summary

In conclusion, our study delves into the combination of dosage compensation mechanisms in *C. elegans*, focusing on the roles of condensin I^{DC} and its associated components. Through targeted depletion experiments using the AID system, we confirmed the indispensable nature of DPY-27 during embryonic development, aligning with previous findings but providing contemporary evidence while expanding beyond prior knowledge. Using the AID paradigm to deplete DPY-27 in larvae, we discovered that dosage compensation is no longer necessary for survival. The interplay between DPY-27, CEC-4, and DPY-21 showcased the complexity of dosage compensation, with unexpected consequences and heightened sensitivity in mutants containing a loss-of-function allele for *cec-4*. Our exploration of H4K20me1 dynamics and its connection to DPY-27 depletion unveiled novel insights into the regulatory networks governing gene expression on the X chromosome. While shedding light on the nuances of dosage compensation, our study underscores the need for continued research to unveil the full spectrum of regulatory elements orchestrating X-linked gene expression in *C. elegans*.

Bibliography

1. Alberts B, Johnson A, Lewis J, Raff M, Roberts K, Walter P. Chromosomal DNA and Its Packaging in the Chromatin Fiber. Molecular Biology of the Cell 4th edition. Garland Science; 2002. Available: https://www.ncbi.nlm.nih.gov/books/NBK26834/

2. Jung N, Kim T-K. Advances in higher-order chromatin architecture: the move towards 4D genome. BMB Rep. 2021;54: 233–245. doi:10.5483/BMBRep.2021.54.5.035

3. McGinty RK, Tan S. Nucleosome Structure and Function. Chem Rev. 2015;115: 2255–2273. doi:10.1021/cr500373h

4. Jenuwein T, Allis CD. Translating the Histone Code. Science. 2001;293: 1074–1080. doi:10.1126/science.1063127

5. Henikoff S, Smith MM. Histone Variants and Epigenetics. Cold Spring Harb Perspect Biol. 2015;7: a019364. doi:10.1101/cshperspect.a019364

6. Vyas P, Brown DT. N- and C-terminal Domains Determine Differential Nucleosomal Binding Geometry and Affinity of Linker Histone Isotypes H10 and H1c. J Biol Chem. 2012;287: 11778–11787. doi:10.1074/jbc.M111.312819

7. Role of the histone tails in histone octamer transfer - PMC. [cited 8 Mar 2024]. Available: https://www-ncbi-nlm-nih-gov.proxy.lib.umich.edu/pmc/articles/PMC10164550/

8. Horn PJ, Peterson CL. Chromatin higher order folding--wrapping up transcription. Science. 2002;297: 1824–1827.

9. Marmorstein R, Trievel RC. Histone Modifying Enzymes: Structures, Mechanisms, and Specificities. Biochim Biophys Acta. 2009;1789: 58–68. doi:10.1016/j.bbagrm.2008.07.009

10. Van Bortle K, Corces VG. Nuclear organization and genome function. Annu Rev Cell Dev Biol. 2012;28: 163–187. doi:10.1146/annurev-cellbio-101011-155824

11. C R. Uber zellthilung. Morphol Jahrb. 1885;10: 214–330.

12. Cremer T, Cremer M. Chromosome Territories. Cold Spring Harb Perspect Biol. 2010;2: a003889. doi:10.1101/cshperspect.a003889

13.   eine Anzahl P. Die Blastomerenkerne von Ascaris megalocephala und die Theorie der Chromosomenindividualität. Arch Für Zellforsch. 1909;3: 181.

14.   Boveri T. Die Blastomerenkerne von Ascaris megalocephala und dieTheorie der Chromosomenindividualitit. Arch. Zellforschung. 3: 181-268. Boveri1813Arch Zellforsch. 1909.

15.   Neusser M, Schubel V, Koch A, Cremer T, Müller S. Evolutionarily conserved, cell type and species-specific higher order chromatin arrangements in interphase nuclei of primates. Chromosoma. 2007;116: 307–320. doi:10.1007/s00412-007-0099-3

16.   Cremer M, Grasser F, Lanctôt C, Müller S, Neusser M, Zinner R, et al. Multicolor 3D Fluorescence In Situ Hybridization for Imaging Interphase Chromosomes. In: Hancock R, editor. The Nucleus: Volume 1: Nuclei and Subnuclear Components. Totowa, NJ: Humana Press; 2008. pp. 205–239. doi:10.1007/978-1-59745-406-3_15

17.   Chaumeil J, Le Baccon P, Wutz A, Heard E. A novel role for Xist RNA in the formation of a repressive nuclear compartment into which genes are recruited when silenced. Genes Dev. 2006;20: 2223–2237. doi:10.1101/gad.380906

18.   Zirbel RM, Mathieu UR, Kurz A, Cremer T, Lichter P. Evidence for a nuclear compartment of transcription and splicing located at chromosome domain boundaries. Chromosome Res Int J Mol Supramol Evol Asp Chromosome Biol. 1993;1: 93–106. doi:10.1007/BF00710032

19.   Mahy NL, Perry PE, Bickmore WA. Gene density and transcription influence the localization of chromatin outside of chromosome territories detectable by FISH. J Cell Biol. 2002;159: 753–763. doi:10.1083/jcb.200207115

20.   Nora EP, Lajoie BR, Schulz EG, Giorgetti L, Okamoto I, Servant N, et al. Spatial partitioning of the regulatory landscape of the X-inactivation centre. Nature. 2012;485: 381–385. doi:10.1038/nature11049

21.   de Wit E, Vos ESM, Holwerda SJB, Valdes-Quezada C, Verstegen MJAM, Teunissen H, et al. CTCF Binding Polarity Determines Chromatin Looping. Mol Cell. 2015;60: 676–684. doi:10.1016/j.molcel.2015.09.023

22.   Rajderkar S, Barozzi I, Zhu Y, Hu R, Zhang Y, Li B, et al. Topologically associating domain boundaries are required for normal genome function. Commun Biol. 2023;6: 1–10. doi:10.1038/s42003-023-04819-w

23.   Lupiáñez DG, Kraft K, Heinrich V, Krawitz P, Brancati F, Klopocki E, et al. Disruptions of Topological Chromatin Domains Cause Pathogenic Rewiring of Gene-Enhancer Interactions. Cell. 2015;161: 1012–1025. doi:10.1016/j.cell.2015.04.004

24. Rao SSP, Huntley MH, Durand NC, Stamenova EK, Bochkov ID, Robinson JT, et al. A 3D Map of the Human Genome at Kilobase Resolution Reveals Principles of Chromatin Looping. Cell. 2014;159: 1665–1680. doi:10.1016/j.cell.2014.11.021

25. Crane E, Bian Q, McCord RP, Lajoie BR, Wheeler BS, Ralston EJ, et al. Condensin-driven remodelling of X chromosome topology during dosage compensation. Nature. 2015;523: 240–244. doi:10.1038/nature14450

26. Heger P, Marin B, Schierenberg E. Loss of the insulator protein CTCF during nematode evolution. BMC Mol Biol. 2009;10: 84. doi:10.1186/1471-2199-10-84

27. Kim J, Jimenez DS, Ragipani B, Zhang B, Street LA, Kramer M, et al. Condensin DC loads and spreads from recruitment sites to create loop-anchored TADs in C. elegans. Tyler JK, editor. eLife. 2022;11: e68745. doi:10.7554/eLife.68745

28. Manzo SG, Dauban L, van Steensel B. Lamina-associated domains: Tethers and looseners. Curr Opin Cell Biol. 2022;74: 80–87. doi:10.1016/j.ceb.2022.01.004

29. Guelen L, Pagie L, Brasset E, Meuleman W, Faza MB, Talhout W, et al. Domain organization of human chromosomes revealed by mapping of nuclear lamina interactions. Nature. 2008;453: 948–951. doi:10.1038/nature06947

30. Ikegami K, Egelhofer TA, Strome S, Lieb JD. Caenorhabditis elegans chromosome arms are anchored to the nuclear membrane via discontinuous association with LEM-2. Genome Biol. 2010;11: R120. doi:10.1186/gb-2010-11-12-r120

31. Kramer M, Kranz A-L, Su A, Winterkorn LH, Albritton SE, Ercan S. Developmental Dynamics of X-Chromosome Dosage Compensation by the DCC and H4K20me1 in C. elegans. PLoS Genet. 2015;11: e1005698. doi:10.1371/journal.pgen.1005698

32. Meister P, Towbin BD, Pike BL, Ponti A, Gasser SM. The spatial dynamics of tissue-specific promoters during C. elegans development. Genes Dev. 2010;24: 766–782. doi:10.1101/gad.559610

33. Ohnesorg T, Vilain E, Sinclair AH. The Genetics of Disorders of Sex Development in Humans. Sex Dev. 2014;8: 262–272. doi:10.1159/000357956

34. Carthew RW. Gene Regulation and Cellular Metabolism: An Essential Partnership. Trends Genet TIG. 2021;37: 389–400. doi:10.1016/j.tig.2020.09.018

35. Fraser JA, Diezmann S, Subaran RL, Allen A, Lengeler KB, Dietrich FS, et al. Convergent Evolution of Chromosomal Sex-Determining Regions in the Animal and Fungal Kingdoms. PLoS Biol. 2004;2: e384. doi:10.1371/journal.pbio.0020384

36. Charlesworth B, Charlesworth D. A Model for the Evolution of Dioecy and Gynodioecy. Am Nat. 1978;112: 975–997.

37. Otto SP, Lenormand T. Resolving the paradox of sex and recombination. Nat Rev Genet. 2002;3: 252–261. doi:10.1038/nrg761

38. Kanzaki N, Kiontke K, Tanaka R, Hirooka Y, Schwarz A, Müller-Reichert T, et al. Description of two three-gendered nematode species in the new genus Auanema (Rhabditina) that are models for reproductive mode evolution. Sci Rep. 2017;7: 11135. doi:10.1038/s41598-017-09871-1

39. Chasnov JR. The evolution from females to hermaphrodites results in a sexual conflict over mating in androdioecious nematode worms and clam shrimp. J Evol Biol. 2010;23: 539–556. doi:10.1111/j.1420-9101.2009.01919.x

40. Charlesworth D, Willis JH. The genetics of inbreeding depression. Nat Rev Genet. 2009;10: 783–796. doi:10.1038/nrg2664

41. Nagahama Y, Chakraborty T, Paul-Prasanth B, Ohta K, Nakamura M. Sex determination, gonadal sex differentiation, and plasticity in vertebrate species. Physiol Rev. 2021;101: 1237–1308. doi:10.1152/physrev.00044.2019

42. Gilbert SF. Sex determination. Developmental Biology 6th edition. Sinauer Associates; 2000. Available: https://www.ncbi.nlm.nih.gov/books/NBK9985/

43. Stévant I, Papaioannou MD, Nef S. A brief history of sex determination. Mol Cell Endocrinol. 2018;468: 3–10. doi:10.1016/j.mce.2018.04.004

44. Bull JJ. Sex Determination in Reptiles. Q Rev Biol. 1980;55: 3–21.

45. Lang JW, Andrews HV. Temperature-dependent sex determination in crocodilians. J Exp Zool. 1994;270: 28–44. doi:10.1002/jez.1402700105

46. Paliulis L, Fabig G, Müller-Reichert T. The X chromosome still has a lot to reveal - revisiting Hermann Henking's work on firebugs. J Cell Sci. 2023;136: jcs260998. doi:10.1242/jcs.260998

47. H H. Untersuchungen uber die ersten Entwicklungsv-organge in den Eiern der Insekten. H. Uber Spermatogense und deren Beziehung zur Eientwicklung bei Pyrrhocoris apertus L. Zeit Wiss Zool. 1891;51: 685–736.

48. Mcclung CE. THE ACCESSORY CHROMOSOME—SEX DETERMINANT? Biol Bull. 1902;3: 43–84. doi:10.2307/1535527

49. Beukeboom LW, Perrin N. The Evolution of Sex Determination. Oxford University Press; 2014.

50. Carey SB, Aközbek L, Harkess A. The contributions of Nettie Stevens to the field of sex chromosome biology. Philos Trans R Soc B Biol Sci. 377: 20210215. doi:10.1098/rstb.2021.0215

51. Wallis MC, Waters PD, Graves JAM. Sex determination in mammals — Before and after the evolution of SRY. Cell Mol Life Sci. 2008;65: 3182–3195. doi:10.1007/s00018-008-8109-z

52. Balderman S, Lichtman MA. A History of the Discovery of Random X Chromosome Inactivation in the Human Female and its Significance. Rambam Maimonides Med J. 2011;2: e0058. doi:10.5041/RMMJ.10058

53. Stevens L. Sex chromosomes and sex determining mechanisms in birds. Sci Prog. 1997;80 (Pt 3): 197–216.

54. Sinclair AH, Berta P, Palmer MS, Hawkins JR, Griffiths BL, Smith MJ, et al. A gene from the human sex-determining region encodes a protein with homology to a conserved DNA-binding motif. Nature. 1990;346: 240–244. doi:10.1038/346240a0

55. Koopman P, Gubbay J, Vivian N, Goodfellow P, Lovell-Badge R. Male development of chromosomally female mice transgenic for Sry. Nature. 1991;351: 117–121. doi:10.1038/351117a0

56. Larney C, Bailey TL, Koopman P. Switching on sex: transcriptional regulation of the testis-determining gene *Sry*. Development. 2014;141: 2195–2205. doi:10.1242/dev.107052

57. Meyer BJ. Mechanisms of sex determination and X-chromosome dosage compensation. Genetics. 2022;220: iyab197. doi:10.1093/genetics/iyab197

58. Sánchez L, Granadino B, Torres M. Sex determination in Drosophila melanogaster: X-linked genes involved in the initial step of sex-lethal activation. Dev Genet. 1994;15: 251–264. doi:10.1002/dvg.1020150307

59. Penalva LOF, Sánchez L. RNA Binding Protein Sex-Lethal (Sxl) and Control of Drosophila Sex Determination and Dosage Compensation. Microbiol Mol Biol Rev. 2003;67: 343–359. doi:10.1128/MMBR.67.3.343-359.2003

60. Sánchez L, Nöthiger R. Sex determination and dosage compensation in Drosophila melanogaster: production of male clones in XX females. EMBO J. 1983;2: 485–491.

61. Schüpbach T. NORMAL FEMALE GERM CELL DIFFERENTIATION REQUIRES THE FEMALE X CHROMOSOME TO AUTOSOME RATIO AND EXPRESSION OF SEX-LETHAL IN DROSOPHILA MELANOGASTER. Genetics. 1985;109: 529–548. doi:10.1093/genetics/109.3.529

62. Parkhurst SM, Bopp D, Ish-Horowicz D. X:A ratio, the primary sex-determining signal in Drosophila, is transduced by helix-loop-helix proteins. Cell. 1990;63: 1179–1191. doi:10.1016/0092-8674(90)90414-a

63. Hodgkin J. Male Phenotypes and Mating Efficiency in CAENORHABDITIS ELEGANS. Genetics. 1983;103: 43–64.

64. Chasnov JR. The evolutionary role of males in C. elegans. Worm. 2013;2: e21146. doi:10.4161/worm.21146

65. Miller LM, Plenefisch JD, Casson LP, Meyer BJ. xol-1: a gene that controls the male modes of both sex determination and X chromosome dosage compensation in C. elegans. Cell. 1988;55: 167–183.

66. Perry MD, Li W, Trent C, Robertson B, Fire A, Hageman JM, et al. Molecular characterization of the her-1 gene suggests a direct role in cell signaling during Caenorhabditis elegans sex determination. Genes Dev. 1993;7: 216–228. doi:10.1101/gad.7.2.216

67. Dawes HE, Berlin DS, Lapidus DM, Nusbaum C, Davis TL, Meyer BJ. Dosage compensation proteins targeted to X chromosomes by a determinant of hermaphrodite fate. Science. 1999;284: 1800–1804.

68. Farboud B, Nix P, Jow MM, Gladden JM, Meyer BJ. Molecular antagonism between X-chromosome and autosome signals determines nematode sex. Genes Dev. 2013;27: 1159–1178. doi:10.1101/gad.217026.113

69. Madl JE, Herman RK. Polyploids and sex determination in Caenorhabditis elegans. Genetics. 1979;93: 393–402.

70. Carmi I, Kopczynski JB, Meyer BJ. The nuclear hormone receptor SEX-1 is an X-chromosome signal that determines nematode sex. Nature. 1998;396: 168–173. doi:10.1038/24164

71. Farboud B, Novak CS, Nicoll M, Quiogue A, Meyer BJ. Dose-dependent action of the RNA binding protein FOX-1 to relay X-chromosome number and determine C. elegans sex. Black DL, Manley JL, Burge CB, editors. eLife. 2020;9: e62963. doi:10.7554/eLife.62963

72. Gladden JM, Farboud B, Meyer BJ. Revisiting the X:A signal that specifies Caenorhabditis elegans sexual fate. Genetics. 2007;177: 1639–1654. doi:10.1534/genetics.107.078071

73. Barakat TS, Gribnau J. X Chromosome Inactivation and Embryonic Stem Cells. Madame Curie Bioscience Database [Internet]. Landes Bioscience; 2013. Available: https://www.ncbi.nlm.nih.gov/books/NBK45037/

74. Brown CJ, Hendrich BD, Rupert JL, Lafrenière RG, Xing Y, Lawrence J, et al. The human XIST gene: analysis of a 17 kb inactive X-specific RNA that contains conserved repeats and is highly localized within the nucleus. Cell. 1992;71: 527–542. doi:10.1016/0092-8674(92)90520-m

75. Lyon MF. Gene Action in the X-chromosome of the Mouse (Mus musculus L.). Nature. 1961;190: 372–373. doi:10.1038/190372a0

76. Huynh KD, Lee JT. X-chromosome inactivation: a hypothesis linking ontogeny and phylogeny. Nat Rev Genet. 2005;6: 410–418. doi:10.1038/nrg1604

77. Barr ML, Bertram EG. A Morphological Distinction between Neurones of the Male and Female, and the Behaviour of the Nucleolar Satellite during Accelerated Nucleoprotein Synthesis. Nature. 1949;163: 676–677. doi:10.1038/163676a0

78. Yang L, Kirby JE, Sunwoo H, Lee JT. Female mice lacking Xist RNA show partial dosage compensation and survive to term. Genes Dev. 2016;30: 1747. doi:10.1101/gad.281162.116

79. Brockdorff N, McCabe M, Norris P, Cooper J, Swift S, Kay F. The Product of the Mouse Xist Gene Is a 15 kb Inactive X-Specific Transcript Containing No Consewed ORF and Located in the Nucleus.

80. Lee J, Davidow LS, Warshawsky D. Tsix, a gene antisense to Xist at the X-inactivation centre. Nat Genet. 1999;21: 400–404. doi:10.1038/7734

81. Plath K, Fang J, Mlynarczyk-Evans SK, Cao R, Worringer KA, Wang H, et al. Role of Histone H3 Lysine 27 Methylation in X Inactivation. Science. 2003;300: 131–135. doi:10.1126/science.1084274

82. Chu C, Zhang QC, da Rocha ST, Flynn RA, Bharadwaj M, Calabrese JM, et al. Systematic discovery of Xist RNA binding proteins. Cell. 2015;161: 404–416. doi:10.1016/j.cell.2015.03.025

83. McHugh CA, Chen C-K, Chow A, Surka CF, Tran C, McDonel P, et al. The Xist lncRNA interacts directly with SHARP to silence transcription through HDAC3. Nature. 2015;521: 232–236. doi:10.1038/nature14443

84. Malcore RM, Kalantry S. A Comparative Analysis of Mouse Imprinted and Random X-Chromosome Inactivation. Epigenomes. 2024;8: 8. doi:10.3390/epigenomes8010008

85. Żylicz JJ, Bousard A, Žumer K, Dossin F, Mohammad E, Da Rocha ST, et al. The Implication of Early Chromatin Changes in X Chromosome Inactivation. Cell. 2019;176: 182-197.e23. doi:10.1016/j.cell.2018.11.041

86. Chen C-K, Blanco M, Jackson C, Aznauryan E, Ollikainen N, Surka C, et al. Xist recruits the X chromosome to the nuclear lamina to enable chromosome-wide silencing. Science. 2016;354: 468–472. doi:10.1126/science.aae0047

87. Nesterova TB, Wei G, Coker H, Pintacuda G, Bowness JS, Zhang T, et al. Systematic allelic analysis defines the interplay of key pathways in X chromosome inactivation. Nat Commun. 2019;10: 3129. doi:10.1038/s41467-019-11171-3

88. Heard E, Rougeulle C, Arnaud D, Avner P, Allis CD, Spector DL. Methylation of Histone H3 at Lys-9 Is an Early Mark on the X Chromosome during X Inactivation. Cell. 2001;107: 727–738. doi:10.1016/S0092-8674(01)00598-0

89. Brinkman AB, Roelofsen T, Pennings SWC, Martens JHA, Jenuwein T, Stunnenberg HG. Histone modification patterns associated with the human X chromosome. EMBO Rep. 2006;7: 628–634. doi:10.1038/sj.embor.7400686

90. John C. Lucchesi, William G. Kelly, Barbara Panning. Chromatin Remodeling in Dosage Compensation. Annu Rev Genet.

91. Kelley RL, Meller VH, Gordadze PR, Roman G, Davis RL, Kuroda MI. Epigenetic spreading of the Drosophila dosage compensation complex from roX RNA genes into flanking chromatin. Cell. 1999;98: 513–522. doi:10.1016/s0092-8674(00)81979-0

92. Alekseyenko AA, Peng S, Larschan E, Gorchakov AA, Lee O-K, Kharchenko P, et al. A Sequence Motif within Chromatin Entry Sites Directs MSL Establishment on the Drosophila X Chromosome. Cell. 2008;134: 599–609. doi:10.1016/j.cell.2008.06.033

93. Shevelyov YY, Ulianov SV, Gelfand MS, Belyakin SN, Razin SV. Dosage Compensation in Drosophila: Its Canonical and Non-Canonical Mechanisms. Int J Mol Sci. 2022;23: 10976. doi:10.3390/ijms231810976

94. Akhtar A, Becker PB. Activation of transcription through histone H4 acetylation by MOF, an acetyltransferase essential for dosage compensation in Drosophila. Mol Cell. 2000;5: 367–375. doi:10.1016/s1097-2765(00)80431-1

95. Morra R, Yokoyama R, Ling H, Lucchesi JC. Role of the ATPase/helicase maleless (MLE) in the assembly, targeting, spreading and function of the male-specific lethal (MSL) complex of Drosophila. Epigenetics Chromatin. 2011;4: 6. doi:10.1186/1756-8935-4-6

96. Meller VH, Wu KH, Roman G, Kuroda MI, Davis RL. roX1 RNA Paints the X Chromosome of Male Drosophila and Is Regulated by the Dosage Compensation System. Cell. 1997;88: 445–457. doi:10.1016/S0092-8674(00)81885-1

97. Gelbart ME, Larschan E, Peng S, Park PJ, Kuroda MI. Drosophila MSL complex globally acetylates H4K16 on the male X chromosome for dosage compensation. Nat Struct Mol Biol. 2009;16: 825–832. doi:10.1038/nsmb.1644

98. Meyer BJ, Casson LP. Caenorhabditis elegans compensates for the difference in X chromosome dosage between the sexes by regulating transcript levels. Cell. 1986;47: 871–881. doi:10.1016/0092-8674(86)90802-0

99. Lau AC, Csankovszki G. Balancing up and downregulation of the C. elegans X chromosomes. Curr Opin Genet Dev. 2015;31: 50–56. doi:10.1016/j.gde.2015.04.001

100. Lau AC, Nabeshima K, Csankovszki G. The C. elegans dosage compensation complex mediates interphase X chromosome compaction. Epigenetics Chromatin. 2014;7: 31. doi:10.1186/1756-8935-7-31

101. Hirano T. Condensin-Based Chromosome Organization from Bacteria to Vertebrates. Cell. 2016;164: 847–857. doi:10.1016/j.cell.2016.01.033

102. Wood AJ, Severson AF, Meyer BJ. Condensin and cohesin complexity: the expanding repertoire of functions. Nat Rev Genet. 2010;11: 391–404. doi:10.1038/nrg2794

103. Volkov A, Mascarenhas J, Andrei-Selmer C, Ulrich HD, Graumann PL. A Prokaryotic Condensin/Cohesin-Like Complex Can Actively Compact Chromosomes from a Single Position on the Nucleoid and Binds to DNA as a Ring-Like Structure. Mol Cell Biol. 2003;23: 5638–5650. doi:10.1128/MCB.23.16.5638-5650.2003

104. Palou R, Dhanaraman T, Marrakchi R, Pascariu M, Tyers M, D'Amours D. Condensin ATPase motifs contribute differentially to the maintenance of chromosome morphology and genome stability. PLOS Biol. 2018;16: e2003980. doi:10.1371/journal.pbio.2003980

105. Ono T, Losada A, Hirano M, Myers MP, Neuwald AF, Hirano T. Differential Contributions of Condensin I and Condensin II to Mitotic Chromosome Architecture in Vertebrate Cells. Cell. 2003;115: 109–121. doi:10.1016/S0092-8674(03)00724-4

106. Csankovszki G, Collette K, Spahl K, Carey J, Snyder M, Petty E, et al. Three distinct condensin complexes control C. elegans chromosome dynamics. Curr Biol. 2009;19: 9–19. doi:10.1016/j.cub.2008.12.006

107. Hirano T. Condensins: organizing and segregating the genome. Curr Biol CB. 2005;15: R265-275. doi:10.1016/j.cub.2005.03.037

108. Cutts EE, Vannini A. Condensin complexes: understanding loop extrusion one conformational change at a time. Biochem Soc Trans. 2020;48: 2089–2100. doi:10.1042/BST20200241

109. Ganji M, Shaltiel IA, Bisht S, Kim E, Kalichava A, Haering CH, et al. Real-time imaging of DNA loop extrusion by condensin. Science. 2018;360: 102–105. doi:10.1126/science.aar7831

110. Gerlich D, Hirota T, Koch B, Peters J-M, Ellenberg J. Condensin I Stabilizes Chromosomes Mechanically through a Dynamic Interaction in Live Cells. Curr Biol. 2006;16: 333–344. doi:10.1016/j.cub.2005.12.040

111. Hirota T, Gerlich D, Koch B, Ellenberg J, Peters J-M. Distinct functions of condensin I and II in mitotic chromosome assembly. J Cell Sci. 2004;117: 6435–6445. doi:10.1242/jcs.01604

112. Tsai CJ, Mets DG, Albrecht MR, Nix P, Chan A, Meyer BJ. Meiotic crossover number and distribution are regulated by a dosage compensation protein that resembles a condensin subunit. Genes Dev. 2008;22: 194–211. doi:10.1101/gad.1618508

113. Lieb JD, Albrecht MR, Chuang PT, Meyer BJ. MIX-1: an essential component of the C. elegans mitotic machinery executes X chromosome dosage compensation. Cell. 1998;92: 265–277. doi:10.1016/s0092-8674(00)80920-4

114. Chuang PT, Albertson DG, Meyer BJ. DPY-27:a chromosome condensation protein homolog that regulates C. elegans dosage compensation through association with the X chromosome. Cell. 1994;79: 459–474. doi:10.1016/0092-8674(94)90255-0

115. Lieb JD, Capowski EE, Meneely P, Meyer BJ. DPY-26, a link between dosage compensation and meiotic chromosome segregation in the nematode. Science. 1996;274: 1732–1736. doi:10.1126/science.274.5293.1732

116. Plenefisch JD, DeLong L, Meyer BJ. Genes that implement the hermaphrodite mode of dosage compensation in Caenorhabditis elegans. Genetics. 1989;121: 57–76. doi:10.1093/genetics/121.1.57

117. Hsu DR, Meyer BJ. The Dpy-30 Gene Encodes an Essential Component of the Caenorhabditis Elegans Dosage Compensation Machinery. Genetics. 1994;137: 999–1018.

118. Yonker SA, Meyer BJ. Recruitment of C. elegans dosage compensation proteins for gene-specific versus chromosome-wide repression. Development. 2003;130: 6519–6532. doi:10.1242/dev.00886

119. Csankovszki G, McDonel P, Meyer BJ. Recruitment and spreading of the C. elegans dosage compensation complex along X chromosomes. Science. 2004;303: 1182–1185. doi:10.1126/science.1092938

120. Chu DS, Dawes HE, Lieb JD, Chan RC, Kuo AF, Meyer BJ. A molecular link between gene-specific and chromosome-wide transcriptional repression. Genes Dev. 2002;16: 796–805. doi:10.1101/gad.972702

121. Manser J, Wood WB, Perry MD. Extragenic suppressors of a dominant masculinizing her-1 mutation in C. elegans identify two new genes that affect sex determination in different ways. Genes N Y N 2000. 2002;34: 184–195. doi:10.1002/gene.10118

122. Nusbaum C, Meyer BJ. The Caenorhabditis Elegans Gene Sdc-2 Controls Sex Determination and Dosage Compensation in Xx Animals. Genetics. 1989;122: 579–593.

123. Villeneuve AM, Meyer BJ. The role of sdc-1 in the sex determination and dosage compensation decisions in Caenorhabditis elegans. Genetics. 1990;124: 91–114. doi:10.1093/genetics/124.1.91

124. Brejc K, Bian Q, Uzawa S, Wheeler BS, Anderson EC, King DS, et al. Dynamic Control of X Chromosome Conformation and Repression by a Histone H4K20 Demethylase. Cell. 2017;171: 85-102.e23. doi:10.1016/j.cell.2017.07.041

125. Hodgkin J. X chromosome dosage and gene expression in Caenorhabditis elegans: Two unusual dumpy genes. Mol Gen Genet. 1983;192: 452–458. doi:10.1007/BF00392190

126. Breimann L, Morao AK, Kim J, Sebastian Jimenez D, Maryn N, Bikkasani K, et al. The histone H4 lysine 20 demethylase DPY-21 regulates the dynamics of condensin DC binding. J Cell Sci. 2022;135: jcs258818. doi:10.1242/jcs.258818

127. Wells MB, Snyder MJ, Custer LM, Csankovszki G. Caenorhabditis elegans dosage compensation regulates histone H4 chromatin state on X chromosomes. Mol Cell Biol. 2012;32: 1710–1719. doi:10.1128/MCB.06546-11

128. Custer LM, Snyder MJ, Flegel K, Csankovszki G. The onset of C. elegans dosage compensation is linked to the loss of developmental plasticity. Dev Biol. 2014;385: 279–290. doi:10.1016/j.ydbio.2013.11.001

129. Terranova R, Pujol N, Fasano L, Djabali M. Characterisation of set-1, a conserved PR/SET domain gene in Caenorhabditis elegans. Gene. 2002;292: 33–41. doi:10.1016/S0378-1119(02)00671-6

130. Vielle A, Lang J, Dong Y, Ercan S, Kotwaliwale C, Rechtsteiner A, et al. H4K20me1 contributes to downregulation of X-linked genes for C. elegans

dosage compensation. PLoS Genet. 2012;8: e1002933.
doi:10.1371/journal.pgen.1002933

131. Kohlmaier A, Savarese F, Lachner M, Martens J, Jenuwein T, Wutz A. A
Chromosomal Memory Triggered by Xist Regulates Histone Methylation in X
Inactivation. PLOS Biol. 2004;2: e171. doi:10.1371/journal.pbio.0020171

132. Akhtar A, Gasser SM. The nuclear envelope and transcriptional control. Nat Rev
Genet. 2007;8: 507–517. doi:10.1038/nrg2122

133. Lau AC, Csankovszki G. Condensin-mediated chromosome organization and
gene regulation. Front Genet. 2014;5: 473. doi:10.3389/fgene.2014.00473

134. Mattout A, Pike BL, Towbin BD, Bank EM, Gonzalez-Sandoval A, Stadler MB, et
al. An EDMD mutation in C. elegans lamin blocks muscle-specific gene relocation
and compromises muscle integrity. Curr Biol. 2011;21: 1603–1614.
doi:10.1016/j.cub.2011.08.030

135. Ahringer J, Gasser SM. Repressive Chromatin in Caenorhabditis elegans:
Establishment, Composition, and Function. Genetics. 2018;208: 491–511.
doi:10.1534/genetics.117.300386

136. Snyder MJ, Lau AC, Brouhard EA, Davis MB, Jiang J, Sifuentes MH, et al.
Anchoring of Heterochromatin to the Nuclear Lamina Reinforces Dosage
Compensation-Mediated Gene Repression. PLoS Genet. 2016;12: e1006341.
doi:10.1371/journal.pgen.1006341

137. Peric-Hupkes D, Meuleman W, Pagie L, Bruggeman SWM, Solovei I, Brugman W,
et al. Molecular maps of the reorganization of genome-nuclear lamina interactions
during differentiation. Mol Cell. 2010;38: 603–613.
doi:10.1016/j.molcel.2010.03.016

138. Bian Q, Anderson EC, Yang Q, Meyer BJ. Histone H3K9 methylation promotes
formation of genome compartments in Caenorhabditis elegans via chromosome
compaction and perinuclear anchoring. Proc Natl Acad Sci U S A. 2020;117:
11459–11470. doi:10.1073/pnas.2002068117

139. Towbin BD, González-Aguilera C, Sack R, Gaidatzis D, Kalck V, Meister P, et al.
Step-wise methylation of histone H3K9 positions heterochromatin at the nuclear
periphery. Cell. 2012;150: 934–947. doi:10.1016/j.cell.2012.06.051

140. Gonzalez-Sandoval A, Towbin BD, Kalck V, Cabianca DS, Gaidatzis D, Hauer
MH, et al. Perinuclear Anchoring of H3K9-Methylated Chromatin Stabilizes
Induced Cell Fate in C. elegans Embryos. Cell. 2015;163: 1333–1347.
doi:10.1016/j.cell.2015.10.066

141. Ohno S. Sex Chromosomes and Sex-Linked Genes: Springer Berlin Heidelberg;
1967. doi:10.1007/978-3-642-88178-7

142. Kong M, Cutts EE, Pan D, Beuron F, Kaliyappan T, Xue C, et al. Human Condensin I and II Drive Extensive ATP-Dependent Compaction of Nucleosome-Bound DNA. Mol Cell. 2020;79: 99-114.e9. doi:10.1016/j.molcel.2020.04.026

143. Hirano T. Condensins: universal organizers of chromosomes with diverse functions. Genes Dev. 2012;26: 1659–1678. doi:10.1101/gad.194746.112

144. Mets DG, Meyer BJ. Condensins Regulate Meiotic DNA Break Distribution, thus Crossover Frequency, by Controlling Chromosome Structure. Cell. 2009;139: 73–86. doi:10.1016/j.cell.2009.07.035

145. Hirano T, Kobayashi R, Hirano M. Condensins, chromosome condensation protein complexes containing XCAP-C, XCAP-E and a Xenopus homolog of the Drosophila Barren protein. Cell. 1997;89: 511–521. doi:10.1016/s0092-8674(00)80233-0

146. Paul MR, Hochwagen A, Ercan S. Condensin action and compaction. Curr Genet. 2019;65: 407–415. doi:10.1007/s00294-018-0899-4

147. Hagstrom KA, Holmes VF, Cozzarelli NR, Meyer BJ. C. elegans condensin promotes mitotic chromosome architecture, centromere organization, and sister chromatid segregation during mitosis and meiosis. Genes Dev. 2002;16: 729–742. doi:10.1101/gad.968302

148. Pferdehirt RR, Meyer BJ. SUMOylation is essential for sex-specific assembly and function of the Caenorhabditis elegans dosage compensation complex on X chromosomes. Proc Natl Acad Sci. 2013;110: E3810–E3819. doi:10.1073/pnas.1315793110

149. Kruesi WS, Core LJ, Waters CT, Lis JT, Meyer BJ. Condensin controls recruitment of RNA polymerase II to achieve nematode X-chromosome dosage compensation. Elife. 2013;2: e00808. doi:10.7554/eLife.00808

150. Meyer BJ. Targeting X chromosomes for repression. Curr Opin Genet Dev. 2010;20: 179–189. doi:10.1016/j.gde.2010.03.008

151. Yuzyuk T, Fakhouri THI, Kiefer J, Mango SE. The polycomb complex protein mes-2/E(z) promotes the transition from developmental plasticity to differentiation in C. elegans embryos. Dev Cell. 2009;16: 699–710. doi:10.1016/j.devcel.2009.03.008

152. Sulston JE, Schierenberg E, White JG, Thomson JN. The embryonic cell lineage of the nematode Caenorhabditis elegans. Dev Biol. 1983;100: 64–119. doi:10.1016/0012-1606(83)90201-4

153. Cabianca DS, Muñoz-Jiménez C, Kalck V, Gaidatzis D, Padeken J, Seeber A, et al. Active chromatin marks drive spatial sequestration of heterochromatin in C. elegans nuclei. Nature. 2019;569: 734–739. doi:10.1038/s41586-019-1243-y

154. Hedgecock EM, White JG. Polyploid tissues in the nematode *Caenorhabditis elegans*. Dev Biol. 1985;107: 128–133. doi:10.1016/0012-1606(85)90381-1

155. Zhang L, Ward JD, Cheng Z, Dernburg AF. The auxin-inducible degradation (AID) system enables versatile conditional protein depletion in C. elegans. Development. 2015;142: 4374–4384. doi:10.1242/dev.129635

156. Kelly WG, Schaner CE, Dernburg AF, Lee M-H, Kim SK, Villeneuve AM, et al. X-chromosome silencing in the germline of C. elegans. Dev Camb Engl. 2002;129: 479–492.

157. Crittenden SL, Leonhard KA, Byrd DT, Kimble J. Cellular Analyses of the Mitotic Region in the Caenorhabditis elegans Adult Germ Line. Mol Biol Cell. 2006;17: 3051–3061. doi:10.1091/mbc.E06-03-0170

158. Schiksnis EC, Nicholson AL, Modena MS, Pule MN, Arribere JA, Pasquinelli AE. Auxin-independent depletion of degron-tagged proteins by TIR1. MicroPublication Biol. 2020: 10.17912/micropub.biology.000213. doi:10.17912/micropub.biology.000213

159. Natsume T, Kiyomitsu T, Saga Y, Kanemaki MT. Rapid Protein Depletion in Human Cells by Auxin-Inducible Degron Tagging with Short Homology Donors. Cell Rep. 2016;15: 210–218. doi:10.1016/j.celrep.2016.03.001

160. Martinez MA, Kinney BA, Medwig-Kinney TN, Ashley G, Ragle JM, Johnson L, et al. Rapid degradation of Caenorhabditis elegans proteins at single-cell resolution with a synthetic auxin. G3 Genes Genomes Genet. 2020;10: 267–280.

161. Samejima K, Booth DG, Ogawa H, Paulson JR, Xie L, Watson CA, et al. Functional analysis after rapid degradation of condensins and 3D-EM reveals chromatin volume is uncoupled from chromosome architecture in mitosis. J Cell Sci. 2018;131: jcs210187. doi:10.1242/jcs.210187

162. Hirano T, Mitchison TJ. A heterodimeric coiled-coil protein required for mitotic chromosome condensation in vitro. Cell. 1994;79: 449–458. doi:10.1016/0092-8674(94)90254-2

163. Houlard M, Godwin J, Metson J, Lee J, Hirano T, Nasmyth K. Condensin confers the longitudinal rigidity of chromosomes. Nat Cell Biol. 2015;17: 771–781. doi:10.1038/ncb3167

164. Piskadlo E, Tavares A, Oliveira RA. Metaphase chromosome structure is dynamically maintained by condensin I-directed DNA (de)catenation. eLife. 2017;6: e26120. doi:10.7554/eLife.26120

165. Zhiteneva A, Bonfiglio JJ, Makarov A, Colby T, Vagnarelli P, Schirmer EC, et al. Mitotic post-translational modifications of histones promote chromatin compaction in vitro. Open Biol. 2017;7: 170076. doi:10.1098/rsob.170076

166. Corvalan AZ, Coller HA. Methylation of histone 4's lysine 20: a critical analysis of the state of the field. Physiol Genomics. 2021;53: 22–32. doi:10.1152/physiolgenomics.00128.2020

167. Wilkins BJ, Rall NA, Ostwal Y, Kruitwagen T, Hiragami-Hamada K, Winkler M, et al. A cascade of histone modifications induces chromatin condensation in mitosis. Science. 2014;343: 77–80. doi:10.1126/science.1244508

168. Javasky E, Shamir I, Gandhi S, Egri S, Sandler O, Rothbart SB, et al. Study of mitotic chromatin supports a model of bookmarking by histone modifications and reveals nucleosome deposition patterns. Genome Res. 2018;28: 1455–1466. doi:10.1101/gr.230300.117

169. Methot SP, Padeken J, Brancati G, Zeller P, Delaney CE, Gaidatzis D, et al. H3K9me selectively blocks transcription factor activity and ensures differentiated tissue integrity. Nat Cell Biol. 2021;23: 1163–1175. doi:10.1038/s41556-021-00776-w

170. Csankovszki G, Panning B, Bates B, Pehrson JR, Jaenisch R. Conditional deletion of Xist disrupts histone macroH2A localization but not maintenance of X inactivation. Nat Genet. 1999;22: 323–324. doi:10.1038/11887

171. Csankovszki G, Nagy A, Jaenisch R. Synergism of Xist RNA, DNA methylation, and histone hypoacetylation in maintaining X chromosome inactivation. J Cell Biol. 2001;153: 773–783. doi:10.1083/jcb.153.4.773

172. Heard E, Disteche CM. Dosage compensation in mammals: fine-tuning the expression of the X chromosome. Genes Dev. 2006;20: 1848–1867. doi:10.1101/gad.1422906

173. Leonhardt H, Page AW, Weier HU, Bestor TH. A targeting sequence directs DNA methyltransferase to sites of DNA replication in mammalian nuclei. Cell. 1992;71: 865–873. doi:10.1016/0092-8674(92)90561-p

174. Audergon PNCB, Catania S, Kagansky A, Tong P, Shukla M, Pidoux AL, et al. Epigenetics. Restricted epigenetic inheritance of H3K9 methylation. Science. 2015;348: 132–135. doi:10.1126/science.1260638

175. Margueron R, Justin N, Ohno K, Sharpe ML, Son J, Drury III WJ, et al. Role of the polycomb protein EED in the propagation of repressive histone marks. Nature. 2009;461: 762–767. doi:10.1038/nature08398

176. Hansen KH, Bracken AP, Pasini D, Dietrich N, Gehani SS, Monrad A, et al. A model for transmission of the H3K27me3 epigenetic mark. Nat Cell Biol. 2008;10: 1291–1300. doi:10.1038/ncb1787

177. Liu W, Tanasa B, Tyurina OV, Zhou TY, Gassmann R, Liu WT, et al. PHF8 mediates histone H4 lysine 20 demethylation events involved in cell cycle progression. Nature. 2010;466: 508–512. doi:10.1038/nature09272

178. Li Q, Kaur A, Mallory B, Hariri S, Engebrecht J. Inducible degradation of dosage compensation protein DPY-27 facilitates isolation of *Caenorhabditis elegans* males for molecular and biochemical analyses. Ward J, editor. G3 GenesGenomesGenetics. 2022;12: jkac085. doi:10.1093/g3journal/jkac085

179. Brenner S. The genetics of Caenorhabditis elegans. Genetics. 1974;77: 71–94.

180. Zhang S. Cell isolation and culture. WormBook. 2013; 1–39. doi:10.1895/wormbook.1.157.1

181. Porta-de-la-Riva M, Fontrodona L, Villanueva A, Cerón J. Basic Caenorhabditis elegans Methods: Synchronization and Observation. J Vis Exp JoVE. 2012; 4019. doi:10.3791/4019

182. M9 Buffer for Worms. Cold Spring Harb Protoc. 2014;2014: pdb.rec081315. doi:10.1101/pdb.rec081315

183. Ashley GE, Duong T, Levenson MT, Martinez MAQ, Johnson LC, Hibshman JD, et al. An expanded auxin-inducible degron toolkit for *Caenorhabditis elegans*. Greenstein D, editor. Genetics. 2021;217: iyab006. doi:10.1093/genetics/iyab006

184. Nabeshima K, Mlynarczyk-Evans S, Villeneuve AM. Chromosome Painting Reveals Asynaptic Full Alignment of Homologs and HIM-8–Dependent Remodeling of X Chromosome Territories during Caenorhabditis elegans Meiosis. PLoS Genet. 2011;7: e1002231. doi:10.1371/journal.pgen.1002231

185. Ollion J, Cochennec J, Loll F, Escudé C, Boudier T. TANGO: a generic tool for high-throughput 3D image analysis for studying nuclear organization. Bioinforma Oxf Engl. 2013;29: 1840–1841. doi:10.1093/bioinformatics/btt276

186. Zhang S, Kuhn JR. Cell isolation and culture. WormBook: The Online Review of C elegans Biology [Internet]. WormBook; 2018. Available: https://www.ncbi.nlm.nih.gov/books/NBK153594/

187. Martin M. Cutadapt removes adapter sequences from high-throughput sequencing reads. EMBnet.journal. 2011;17: 10–12. doi:10.14806/ej.17.1.200

188. FastQC. 2015. Available: https://qubeshub.org/resources/fastqc

189. Patro R, Duggal G, Love MI, Irizarry RA, Kingsford C. Salmon provides fast and bias-aware quantification of transcript expression. Nat Methods. 2017;14: 417–419. doi:10.1038/nmeth.4197

190. Love MI, Huber W, Anders S. Moderated estimation of fold change and dispersion for RNA-seq data with DESeq2. Genome Biol. 2014;15: 550. doi:10.1186/s13059-014-0550-8

191. Torres EM, Williams BR, Amon A. Aneuploidy: cells losing their balance. Genetics. 2008;179: 737–746. doi:10.1534/genetics.108.090878

192. DPY-27:a chromosome condensation protein homolog that regulates C. elegans dosage compensation through association with the X chromosome - PubMed. [cited 13 Jan 2023]. Available: https://pubmed.ncbi.nlm.nih.gov/7954812/

193. Conte D, MacNeil LT, Walhout AJM, Mello CC. RNA Interference in Caenorhabditis Elegans. Curr Protoc Mol Biol. 2015;109: 26.3.1-26.330. doi:10.1002/0471142727.mb2603s109

194. Boeck ME, Huynh C, Gevirtzman L, Thompson OA, Wang G, Kasper DM, et al. The time-resolved transcriptome of C. elegans. Genome Res. 2016;26: 1441–1450. doi:10.1101/gr.202663.115

195. Jin F, Li Y, Dixon JR, Selvaraj S, Ye Z, Lee AY, et al. A high-resolution map of the three-dimensional chromatin interactome in human cells. Nature. 2013;503: 290–294. doi:10.1038/nature12644

196. Elliott AD. Confocal Microscopy: Principles and Modern Practices. Curr Protoc Cytom. 2020;92: e68. doi:10.1002/cpcy.68

197. Negishi T, Kitagawa S, Horii N, Tanaka Y, Haruta N, Sugimoto A, et al. The auxin-inducible degron 2 (AID2) system enables controlled protein knockdown during embryogenesis and development in Caenorhabditis elegans. Genetics. 2022;220: iyab218. doi:10.1093/genetics/iyab218

198. Bickmore WA, van Steensel B. Genome architecture: domain organization of interphase chromosomes. Cell. 2013;152: 1270–1284. doi:10.1016/j.cell.2013.02.001